2017

Optimisation of the isolation and identification of circulating melanoma cells

Anda-Gabriela Marsavela
Edith Cowan University

Edith Cowan University

Copyright Warning

Optimisation of the isolation and identification

of circulating melanoma cells

This thesis is presented in partial fulfilment of the degree of
Master of Science (Human Biology)

Anda-Gabriela Marsavela

Edith Cowan University
School of Medical and Health Sciences
2017

ABSTRACT

Although melanoma is largely curable when detected in its earliest stages, it can metastasise to other tissues, drastically reducing survival rates. The most recent therapies used to treat metastatic melanoma are effective long-term in only 11 to 33% of patients. Our ability to monitor treatment failure is limited. New prognostic markers are urgently required to allow monitoring of treatment response and disease progression.

Circulating tumour cells (CTCs) are released into the bloodstream by the tumours within a patient, this being a key step in melanoma spread. Since CTCs can be detected in the blood of metastatic melanoma patients, these cells can be used as a "liquid biopsy", providing critical insight into each person's melanoma biology.

Melanoma CTCs have been described as very heterogeneous, hindering their isolation via commonly used CTC capturing methods. To address this, microfluidic devices have been developed to isolate viable CTCs from blood, independently of their marker expression. This study aimed to determine the effectiveness of two different microfluidic devices (Slanted and A5) in recovering melanoma cell lines, and their potential use in the isolation of CTCs from the blood of metastatic melanoma patients. It also aimed to study additional cancer or melanoma specific markers to be used in immunostaining protocols for detection of CTCs after microfluidic enrichment.

The optimal isolation procedure was identified as two rounds of enrichment with the Slanted spiral device, after which we obtained a 3-log depletion of white blood cells and a recovery of over 60% when cells from two melanoma cell lines were spiked into blood samples from healthy volunteers. In addition, we optimised the detection of CTCs using four melanoma markers (gp100, Melan-A, s100 and MCSP) combined in a multimarker immunocytochemistry staining protocol. The optimised enrichment and detection procedures were validated in a cohort of ten metastatic melanoma patients. Results showed that 40% of the patients had one or more CTCs in their blood (1-4 CTCs/8 mL of blood).

Furthermore, three additional markers (Vimentin, RANK, and ABCB5) were trialled so as to increase detection of highly heterogeneous melanoma CTCs in samples that have been processed through the Slanted microfluidic device.

The improved enrichment and detection of CTCs in the blood of melanoma patients using the methods developed as part of this study will facilitate the molecular, genomic and functional characterisation of melanoma CTCs. This will ultimately improve our understanding of the biology of melanoma CTCs and their role in metastatic spread and treatment response.

ACKNOWLEDGEMENTS

STATEMENT OF CONTRIBUTION OF OTHERS

Gabriela Marsavela conducted the experiments, analysed the results and wrote the thesis. Michael Millward recruited patients into the study, supervised collection of blood samples and procurement of clinical data. Jamie Freeman assisted with optimisation of the multimarker immunostaining panel, aided with the development of the immunostaining processes and co-counted CTCs isolated from metastatic melanoma patients. Pauline Zaenker, Ashleigh McEvoy, and Danielle Bartlett have collected blood samples from healthy donors used in the study. Dr. Elin Gray, a co-supervisor of the project provided specific insight into protocols and methodologies. Dr. Carlos Aya-Bonilla, a co-supervisor, provided guidance with the experimental design of the process and the development of the protocols. Prof. Melanie Ziman, the principle supervisor of the project, provided guidance and supervision throughout all the study, and reviewed the writing of the thesis.

TABLE OF CONTENTS

INDEX OF FIGURES

INDEX OF TABLES

LIST OF TERMS

ACD: Adenocortical Dysplasia Homolog (Mouse)
AJCC: American Joint Commission on Cancer
ALM: Acral Lentiginous Melanoma
ASIP: Agouti Signaling Protein
BAP1: BRCA1 Associated Protein-1
BRAF: B-raf Proto-Oncogene, Serine/Threonine Kinase
CDH1: Epithelial Cadherin
CDH2: Non-epithelial Cadherin
CDK4: Cyclin-Dependent Kinase 4
CDKN2A: Cyclin-Dependent Kinase Inhibitor 2A
CM: Cutaneous Melanoma
CTCs: Circulating Tumour Cells
ctDNA: Circulating Tumour DNA
CTLA-4: Cytotoxic T-Lymphocyte Antigen 4
DAPI: 4', 6-diamidino-2-phenylindole
EGF: Epidermal Growth Factor
IL-2: Interleukin-2
KIT: V-Kit Hardy-Zuckerman 4 Feline Sarcoma Viral Oncogene Homolog
LDH: Lactate Dehydrogenase
LM/SNB: Lymphatic Mapping/Sentinel Node Biopsy
LMM: Lentigo Maligna Melanoma
MAPK: Mitogen Activated Protein Kinase
MC1R: Melanocortin 1 Receptor
MITF: Microphthalmia-Associated Transcription Factor
MRI: Magnetic Resonance Imaging
NK: Natural Killer
NRAS: Neuroblastoma RAS Viral (V-Ras) Oncogene Homolog
PET: Positron Emission Tomography
POT1: Protection of Telomeres 1
PTEN: Phosphatase and Tensin Homolog
SLN: Sentinel Lymph Node
SSM: Superficial Spreading Melanoma
TERF2IP: Telomeric Repeat Binding Factor 2, Interacting Protein
TERT: Telomerase Reverse Transcriptase
TP53: Tumour Protein P53
TYR: Tyrosinase
TYRP1: Tyrosinase-Related Protein 1
UV: Ultraviolet Radiation
WLE: Wide Local Excision
WNT5A: Wingless-Type MMTV Integration Site Family, Member 5A

1. INTRODUCTION

Melanoma is an aggressive cutaneous cancer responsible for the majority of skin cancer-related deaths and its incidence is increasing worldwide[1]. Generally, patients are considered cured after complete surgical resection of the primary tumour. Nevertheless, around 20% of patients will develop metastatic disease, which is extremely difficult to treat[2].

The use of targeted therapies and immunotherapies has improved the survival of these patients, but the prognosis is still poor due to the development of drug resistance to targeted therapies and low response rates to immunotherapies. Moreover, adverse side-effects of current immunotherapies restrict treatment efficacy in some cases[3]. Therefore, new biomarkers are urgently needed to allow personalised monitoring of the disease, with the aim to determine treatment response and recurrence at earlier stages. This will allow optimal selection of therapy that improves survival rates in patients.

Circulating tumour cells (CTCs) appear in the peripheral blood from primary or metastatic solid tumours as the first step in tumour metastasis. Cancer cells enter the bloodstream and travel to distant organs where they may initiate development of a new tumour.

During the last decade, the quantification of CTCs has been described in the literature, as a prognostic marker in various tumours such as breast, prostate, colorectal cancer, and melanoma[4-9]. The high heterogeneity of the tumour and the very low concentration of CTCs in peripheral blood (1-10 cells per 10 mL), has made the isolation and quantification of CTCs a difficult challenge[10]. The most widely used methods of enrichment rely on antibody capture of CTCs. More recently, physical properties of the CTCs have been used to improve the isolation, and currently innovative strategies are being developed with the aim of improving the capture and detection of these rare cells.

Microfluidic devices can integrate biological processes into microstructures that handle nano- and pico-litre volumes. This technology is becoming popular because of its ability to isolate label-free and viable intact CTCs based on their physical properties, such as cell size. In addition to this, these devices have several advantages in the isolation of CTCs, which make them promising platforms for implementation in clinical settings. The main

advantages include low cost, and high-throughput enrichment of CTCs from other cells. Successful isolation of CTCs from lung and breast cancer patients by physical size, using a microfluidic device, was reported by Warkiani *et al*.[11, 12]. The detection of CTCs in the blood of these patients at different therapy stages has been shown to be a potential prognostic marker of treatment efficacy and patient survival.

In this study, microfluidic devices[11, 12] have been used, for the first time, to enumerate CTCs from melanoma patients. Although there are still challenges to be resolved, the improvement of CTC isolation and detection procedures will ultimately assist in the understanding of CTC biology, the metastatic process, development of a personalised guide to treatment efficacy and early prediction of treatment resistance.

2. LITERATURE REVIEW

2.1 Cutaneous Melanoma

The skin, which is the largest organ in the body, protects us from UV light, injuries and infections, among other important functions[13]. The main layers of the skin are the inner dermal layer and the outer epidermal layer. The dermis contains three different types of skin cells: squamous cells, basal cells, and melanocytes. Melanocytes are located in the basal layer of the epidermis and are responsible for melanin pigment production (Figure 1).
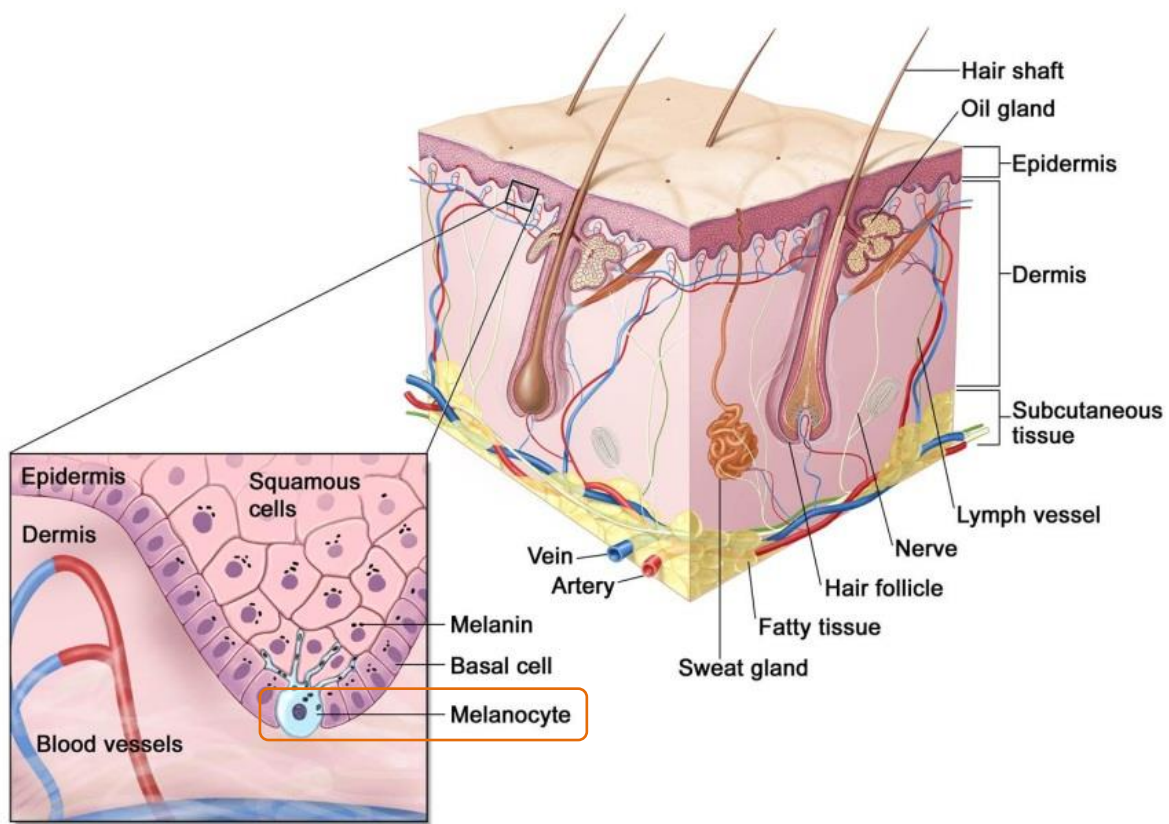
Figure 1. Representation of normal skin anatomy. Melanocytes are present in the basal layer of the epidermis[14].

Cutaneous Melanoma (CM) is a highly aggressive skin tumour originating from the neoplastic transformation of melanocytes. Melanoma occurs principally in the skin; however, it may also develop in the conjunctiva and uvea of the eye (uveal melanoma), on various mucosal membranes with pigmented tissues, such as the gastrointestinal tract, oral or genital membranes, meninges, and in internal organs, such as in the central nervous system[15].

2.1.1 Epidemiology

Cutaneous melanoma is the most serious form of skin cancer, being responsible for 80% of skin cancer deaths, even though it represents <5% of all dermatological cancers[16]. The incidence of this aggressive type of cancer is increasing worldwide. New Zealand together with Australia are the countries with the highest incidence of melanoma (Figure 2)[17]. In Australia, melanoma was the 4th most commonly diagnosed cancer in 2014 and it is estimated that 12,960 new cases of melanoma skin cancer were diagnosed in 2015[18].

A male predominance has been observed after the age of 44 years and in the age group of 20-24 years a female predominance exists in Australia for melanoma over other types of cancer[19]. The location of the tumour varies with age, being on the trunk or extremities more commonly in younger ages, but on head and neck locations in advanced ages[20].
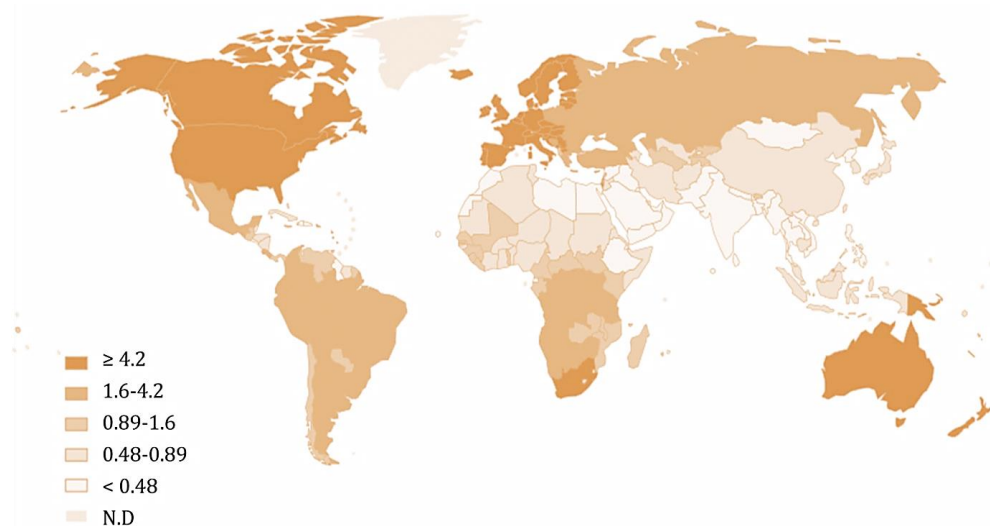
Figure 2. Incidence rate of melanoma per 100,000 inhabitants in 2012. Australia has the second highest incidence worldwide (34.90), behind New Zealand (35.84) followed distantly by Switzerland (20.30)[21].

2.1.2 Aetiology

The first connection between melanoma and the risk factor, UV irradiation, was made by Henry Lancaster[22]. Nowadays, we know that sun exposure or artificial tanning is the major known environmental factor associated with cutaneous melanoma, since significant mutations have been identified as having direct UVB-induced origin[23-26]. Melanoma has the highest prevalence of C>T transition mutations, and this is driven by UV exposure, resulting in the biggest median number of somatic mutations across all human cancer types[27].

Trends in melanoma incidence show that Caucasian race, male gender, and older age are characteristics associated with an increased risk of developing melanoma[28]. Also, fair-skinned individuals with red or blond hair and many freckles are more likely to suffer from the disease[29, 30]. Having a higher number of moles, also increases the risk of developing melanoma[31]. Other host factors, such as a personal history of melanoma or non-melanoma tumours, including other cancers, can increase the risk of developing melanoma[32, 33]. Moreover, a weak immune system or having a disease that weakens the immune system, increases the cancer risk, with a higher incidence of cutaneous melanoma in patients after organ transplantation due to medical immunosuppression[34].

Genetic factors are also involved in melanoma development. About 10% of all melanomas are estimated to be developed due to hereditary susceptibility[35]. Since William Norris[36] first suggested that melanomas have a hereditary component, the knowledge of melanoma genetics has advanced significantly. It is now known that having a family history of melanoma increases the risk 1.74 times compared with a negative family history of the disease[37]. Inherited genetic risk factors can be classified by their penetrance and prevalence[38].

Rare high penetrance genetic mutations are present in *CDKN2A* and *CDK4* genes and prevail in familial melanoma. Both genes are involved in cell-cycle and melanocyte senescence. As an example, the *CDKN2A* gene located on chromosome 9p21.3, encodes for two proteins, p14ARF and p16INK, which control cell cycle entry at the G1 checkpoint and stabilise p53 expression[39]. Low penetrance mutations present in the general population, also referred to as single nucleotide polymorphisms (SNPs), have been detected in genes involved in hair and skin pigmentation, such as *MC1R*, *ASIP*, *TYR* and *TYRP1*[40-43]. Nevertheless, *BAP1*, *POT1*, *ACD*, *TERF2IP*, and *TERT* are also considered melanoma high penetrance inherited risk genes[44].

There are also non-inherited gene mutations that increase the risk of melanoma. Mutations in *TP53* tumour suppressor gene mutations caused by UV radiation are present in melanoma[45]. Both sporadic and continuing or chronic UV light exposures are linked to the pathogenesis of melanoma and produce extensive although, different mutational profiles[23, 27]. However, more research is needed to better understand the genetics of somatic and hereditary melanoma.

2.1.3 Diagnosis

The first step in melanoma diagnosis is the visual characterisation of suspicious lesions. A nevus (or mole) is a visual delimited zone of chronic lesion found in the skin or mucosa[46]. Even though a nevus is considered benign, more than 50% of malignant melanomas arise from pre-existing nevi[47]. The principal visual identification of a nevus which would suggest a malignant change is established by the "ABCDE criteria". Visual characteristics of a transformed mole comprise: *A*symmetry, a *B*order that is irregular, *C*olour that is uneven, a *D*iameter longer than 6 millimetres and, a shape, size or colour that is *E*volving (Figure 3). Other early signs of a malignant change could be itching, ulceration or bleeding. By contrast, nodular melanomas do not follow these criteria. They have their own "EFG criteria". The lesion is *E*levated above the surrounding skin, the nodule is *F*irm to the touch and *G*rowing in size.
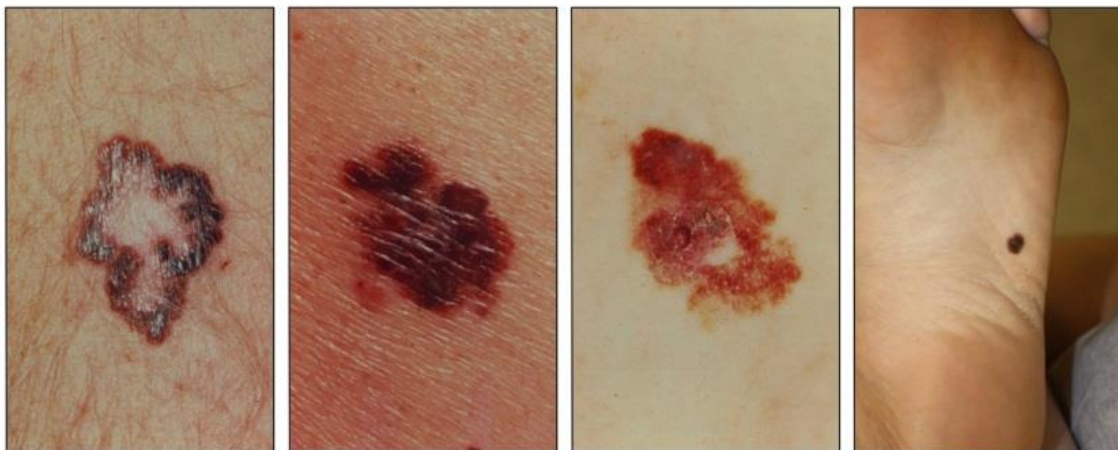
Figure 3. Melanomas with characteristic asymmetry, border irregularity, colour variation and large diameter[48].

Total body photography is used to assist with the diagnosis of melanoma[49]. Dermoscopy is an important tool that can aid in differentiating melanoma from other types of carcinoma or benign lesions[50]. Some of the diagnostic techniques available for better identification of skin cancer include: multispectral imaging, automated diagnosis, confocal scanning laser microscopy, ultrasound imaging, magnetic resonance imaging, and optical coherence tomography.

A histological study of a biopsy of a lesion is needed to diagnose malignancy. The histopathological criteria of melanoma are based on the characteristics of the lesion such as the extent and penetrance of the tumour or the mitotic rate of the cells in the lesion.

The discovery of histologic markers that uniquely identify melanocytes in melanoma has aided melanoma diagnosis. The most commonly used markers are S-100 calcium binding protein[51], MART-1/Melan-A[52], and HMB-45[53, 54]. However, new potential immunohistochemical markers such as SOX-10[55] or MC1R[56,57] have been identified to assist in the classification of melanocytic tumours. Nowadays, a combination of multiple positive histologic markers and histopathological criteria provides the most reliable method of diagnosis.

2.1.4 Staging of melanoma

To determine the treatment and the prognosis of a patient with melanoma, staging of the biopsied material is needed. The American Joint Commission on Cancer (AJCC) updated the melanoma classifications in 2009[58] using the most significant prognostic values as shown in Table 1.

The clinical staging of melanoma is based on the clinical and radiological examination of the regional lymph nodes and the micro-staging of the primary excised melanoma. Patients are classified into five main groups. In patients with stage 0 (*in situ* melanoma), melanoma is confined to the epidermis and has not invaded deeper skin layers. Patients with clinical stages I and II, have no evidence of metastases. Stage III patients have evidence of regional and lymph metastases and stage IV melanoma patients have been diagnosed with one or more distant metastases[59]. Pathological staging includes micro-staging of the primary melanoma and pathological information about the regional lymph nodes after partial or complete lymphadenectomy. Both clinical and pathological staging are important in melanoma diagnosis for correct decisions.

The TNM classification is used to stage patients based on the extent of the primary tumour (T), the presence or not and the extent of regional lymph node metastases (N), and the presence or absence of distant metastases (M)[60]. The T category is further characterised by defining the presence in the primary tumour of ulceration, mitotic rate, and tumour thickness as defined by Breslow[61]. Breslow's thickness is measured from the top of the granular layer of the epidermis or from the base of the ulcer to the deepest dermal invasive cell if the surface is ulcerated. This factor is still the most powerful predictor of survival[62, 63]. The mitotic rate within the tumour is the average number of mitoses per millimetre squared and is also a significant prognostic factor[64]. Level of

invasion as defined by Clark *et al.*[65] has been supplanted and is less commonly used for defining melanoma stages. The N category defines the number of micro or macro-metastatic nodes determined by standard immunohistochemical staining against melanoma markers. The presence of intralymphatic metastasis, including the presence or absence of satellites or in-transit metastases, is also taken into consideration in this category. Regional nodal metastasis is defined as a disease confined to one nodal basin, while patients with distant nodal metastases will be classified as having M stage disease[60]. The M category defines the presence of distant metastases in the skin, subcutaneous tissue, or distant lymph nodes or organs. In addition, elevated serum lactate dehydrogenase (LDH) is an independent significant predictor of survival outcome among patients with distant metastases and has been included in this staging category[66].

Table 1. Classification of the pathological stage and the main features related to melanoma progression[58].

Pathologic Stage	TNM	Breslow's Thickness (mm)	Ulceration	No. Positive Nodes	Nodal Type	Distant Metastasis	Survival (%) 5 years	Survival (%) 10 years
0	Tis	-	No	0	-	-	99+	99+
IA	T1a	1	No	0	-	-	95.3	87.9
IB	T1b	1	Yes/Level IV, V	0	-	-	90.9	83.1
	T2a	1.01-2.0	No	0	-	-	89.0	79.2
IIA	T2b	1.01-2.0	Yes	0	-	-	77.4	64.4
	T3a	2.01-4.0	No	0	-	-	78.7	63.8
IIB	T3b	2.01-4.0	Yes	0	-	-	63.0	50.8
	T4a	>4.0	No	0	-	-	67.4	53.9
IIC	T4b	>4.0	Yes	0	-	-	45.1	32.3
IIIA	N1a	Any	No	1	Micro	-	69.5	63.0
	N2a	Any	No	2-3	Micro	-	63.3	56.9
IIIB	N1a	Any	Yes	1	Micro	-	52.8	37.8
	N2a	Any	Yes	2-3	Micro	-	49.6	35.9
	N1b	Any	No	1	Macro	-	59.0	47.7
	N2b	Any	No	2-3	Macro	-	46.3	39.2
IIIC	N1b	Any	Yes	1	Macro	-	29.0	24.4
	N2b	Any	Yes	2-3	Macro	-	24.0	15.0
	N3	Any	Any	4	Micro Macro	-	26.7	18.4
IV	M1a	Any	Any	Any	Any	Skin	18.8	15.7
	M1b	Any	Any	Any	Any	Lung	6.7	2.5
	M1c	Any	Any	Any	Any	Other Visceral	9.5	6.0

Cutaneous melanoma can be subdivided into several subtypes, based on common anatomical locations and different patterns of growth[67]. Superficial spreading melanoma (SSM) is the most frequent, followed by nodular melanoma, acral lentiginous melanoma (ALM) and lentigo maligna melanoma (LMM)[59].

2.1.5 Genetic and histopathological changes in melanoma development

Melanocytes progress to a malignant phenotype through several steps, in a process known as melanomagenesis[68] (Figure 4).

Both genetic predisposition and exposure to environmental agents are risk factors for melanoma development. However, the critical factor that takes place during this malignant transformation is the progressive accumulation of mutations in genes that target important pathways of cell proliferation, differentiation, and cell death (Table S1 and Figure S1)[69], until finally, melanoma cancer cells acquire the ability to initiate and sustain angiogenesis.
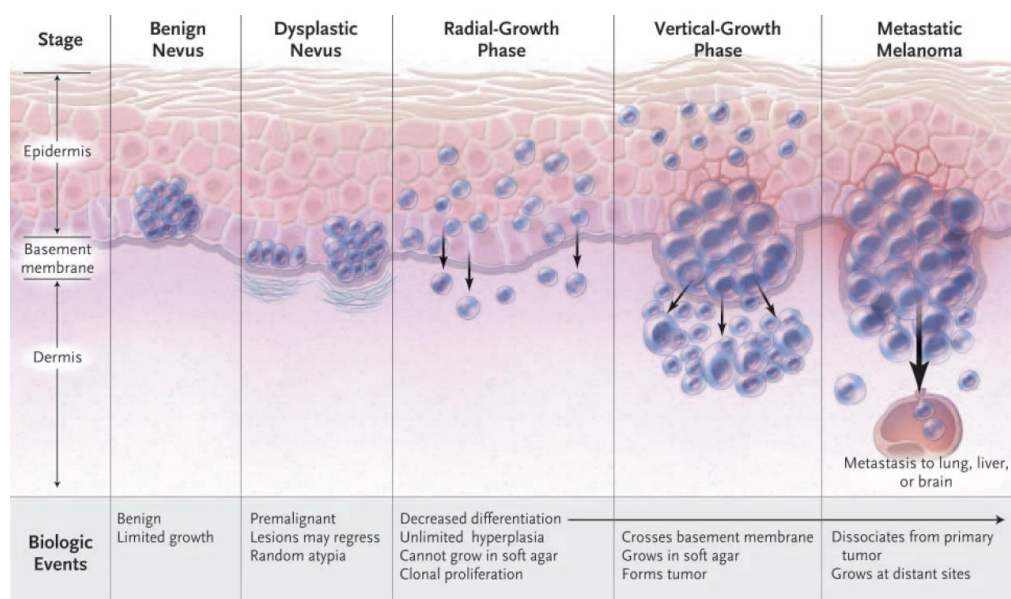
Figure 4. Biologic events that take place in melanoma progression. The benign nevus commences a dysplastic transformation, through radial and vertical growth until the metastatic phenotype arises[2].

The Ras/Raf/MEK/ERK mitogen-activated protein kinase (MAPK) signal transduction pathway is one of the most important pathways in the origin and progression of melanoma. BRAF is a member of the Raf family of serine-threonine kinases, along with ARAF and CRAF (also called RAF1). Mutations in the *BRAF* gene have been described in 40-60%[70, 71] of all melanoma cases. Among mutations in the *BRAF* gene, 80% of the

mutations result in the substitution of glutamic acid (E) for valine (V) in codon 600, known as the *BRAF V600E* mutation; about 16% of mutations in this gene result in a lysine (K) substitution at the same *BRAF V600K* codon, and 3% result in an aspartic acid (D) or arginine (R) substitution that produces a *V600D/R* codon[72]. These last two mutant forms of *BRAF* tend to be present in melanomas arising in older patients[73]. All of these mutations occur as early events in melanomagenesis and result in a mutant protein that is constitutively active in the cell without the need for activation signals. The consequence is uncontrolled proliferation and resistance to apoptosis. Nevertheless, the presence of *BRAF* mutations in 80% of benign nevi suggests that mutational activation of the MAPK pathway is a critical step in melanocytic transformation, but alone is insufficient for melanoma tumourigenesis[74].

Mutations in the *NRAS* gene are present in approximately 15 to 20% of all cutaneous melanomas[75]. Tumours that carry *NRAS* mutations represent a distinct subpopulation, since *BRAF* and *NRAS* mutations generally occur mutually exclusively[76, 77]. Together, *NRAS* and *BRAF* mutations are present in about 70% of the most common types of melanoma[78]. In addition to these mutations, melanomas (mostly acral melanomas) may carry mutations that activate the KIT receptor protein tyrosine kinase. The *KIT* gene is located on the long (q) arm of chromosome 4. Most *KIT* mutations are located in exon 11, which encodes for the juxtamembrane domain, and in exon 13, which encodes for a kinase domain[79].

2.1.6 Treatment and prognosis

The standard treatment for *in situ* and primary melanoma is wide local excision (WLE) of the skin and subcutaneous tissues around the melanoma. Removing the melanoma from the skin by surgery offers the best chance for a complete cure, and this treatment alone is usually successful in patients categorised as stage 0, I and stage II (71% of all patients[59]). Most patients do not need either radiotherapy or chemotherapy, since the tumour is still localised and metastasis has not been diagnosed. Nevertheless, greater tumour thickness is associated with an increased risk of local recurrence[80]. WLE is the treatment of choice in local recurrences, with consideration given to adjuvant therapy in some situations[59], since there is a risk of systematic or regional metastasis.

A sentinel lymph node biopsy is a recommended test for stage II patients with thicker tumours, to see whether a small number of melanoma cells have spread to the nearest lymph nodes[81]. If this procedure has positive results, the patient will be diagnosed with melanoma stage III. Since patients with positive lymph nodes are at high risk for systemic dissemination, a therapeutic lymph node dissection may be considered.
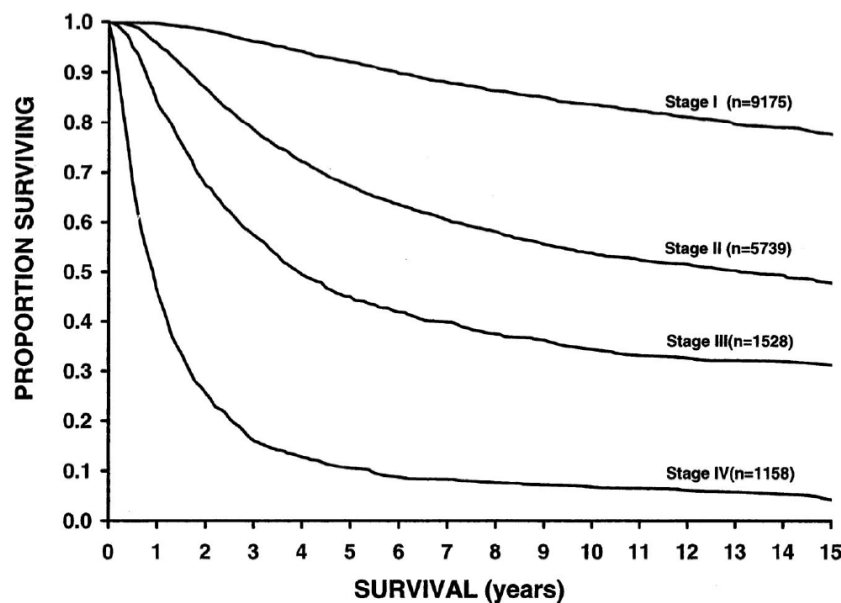
Figure 5. Survival rates for patients with melanoma stages I through IV[59].

In summary, in regards to prognosis, the main clinical and histopathologic predictors of outcome are Breslow's thickness, the presence of ulceration, the sentinel lymph node (SLN) status[58] and the presence of distant metastases. Patients diagnosed with different stages have large differences in their survival rates (Figure 5). Unfortunately, for patients diagnosed with stage III and IV melanoma, the overall 5 and 10 years survival rates are drastically reduced relative to those with stages I or II (Table 1).

2.2 Metastatic Melanoma

Approximately 20% of all melanoma patients develop metastases within the first 2 years of diagnosis[2]. The typical sites of metastatic disease are the lungs, brain, skin, bone and liver[82]. Despite remarkable advances in the treatment of patients with metastatic spread, only 20% show long lasting responses (>2 years) to current treatments[83, 84].

The metastatic process starts with the vertical growth-phase of tumour development when melanoma cells penetrate the basement membrane, reaching the adjacent dermis

containing blood vessels and lymph, through which they then spread to form metastases at a distant location[85]. Modifications in surface protein expression profiles allow the detachment of melanoma cells from the primary tumour and provide the ability to metastasise[2]. The most important change in cell surface proteins is the loss of E-cadherin/CDH1 and the expression of N-cadherin/CDH2. This transition triggers alterations in cell adhesion properties[86]. N-cadherin assists metastatic spread by allowing melanoma cells to interact with endothelial cells present in the stroma, which also express N-cadherin and this interaction increases the survival and migration of melanoma cells[87]. These alterations indicate the radial-growth phase to vertical-growth phase transition which is associated with changes in expression of metastasis initiation genes that allow these tumour cells to migrate and enter blood vessels (intravasation) (Figure 4)[88, 89].

In the next metastatic step, tumour cells can extravasate into distal tissues due to their low E-cadherin expression levels. Their entry can also be mediated by Rac activation[90]. When Rac is activated, the melanoma cells can changes shape and pass between adjacent cells, assisted by matrix metalloproteinases, which destroy integrins[91].

Metastasis progression genes allow melanoma cells to spread to distant organs. These cells are predominantly apoptotic and necrotic with a relatively short survival time in the blood of patients with several types of cancer. Immune cells present in blood can prevent almost all these cells from producing a secondary colony, except the most proficient[92]. These tumour cells, released from the primary tumour, extravasate into distant tissues where they finally develop a secondary tumour when the microenvironment is adequate (Figure 6). The extravasated cells are commonly found in clusters, covered by immunologically active cells, such as monocytes or leukocytes, and platelets that may play a critical role in CTC survival/destruction[93,94].

Once melanoma cells arrive at target tissues, cancer cells commence new organ colonisation and it is thought that, due to their neural crest origin, melanocytes retain some embryonic plasticity, contributing to their high metastatic potential[95]. The short latency of metastatic relapse suggests the existence of multi-organ metastatic competency in the malignant cells[96]. Nonetheless, metastatic disease can occur even 10 years after an initial primary lesion[97].

Despite the new advances in understanding metastasis in cancer, the pathways that melanoma cells use to metastasise are still unclear. Therefore, studies involving melanoma cells that invade and colonise new organs and tissues will unmask the cellular and molecular mechanisms underlying the metastasis of melanoma tumours.

Currently, available tools to predict or detect metastatic spread in melanoma are relatively insensitive, which results in late detection of metastatic disease, significantly decreasing prognosis and survival. If patients with residual disease that might require treatment post-surgery were able to be identified earlier, treatment may be more effective when disease burden is lower[4, 98].
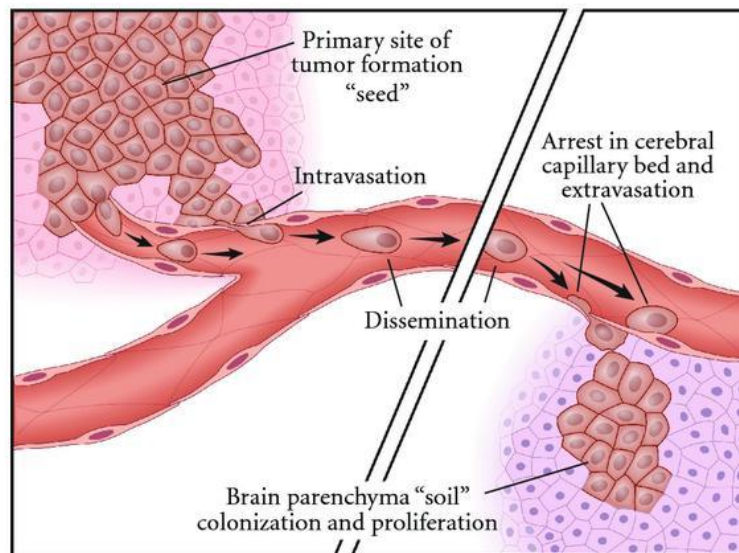
Figure 6. Melanoma metastatic process. Metastatic tumour cells detach from the primary site and penetrate the adjacent parenchyma to reach the blood vessels, adhering to secondary sites such as the brain, forming new colonies[99].

2.2.1 Progression

Metastatic melanoma can be classified into local recurrence, in transit metastasis, nodal metastasis and distal metastasis, based on the location of metastases.

Local recurrence is defined as a recurrence of melanoma within 2 cm of the surgical scar of a primary melanoma[100]. This recurrence can result either from extension of the primary melanoma, or from the spread via lymphatic or haematogenous vessels[101]. In transit metastasis is defined as melanoma deposits within the lymphatic vessels located more than 2 cm from the site of the primary melanoma. Nodal metastasis involves the

spread of tumour cells into the lymph nodes. Haematogenous spread of metastatic melanoma results in development of distal metastasis[82].

A variety of sophisticated imaging techniques are used to follow and evaluate patients with melanoma, including chest radiographs, regional nodal ultrasound imaging, computerised tomography (CT) scans, positron emission tomography (PET), PET/CT scans, and brain/spine and hepatic magnetic resonance imaging (MRI) to detect nodal disease and distal metastases[59, 102]. However, such technologies are relatively insensitive and unable to detect micrometastases[59]. There is therefore, a special need for sensitive methods that detect serological markers in patients likely to develop distant metastases and new biomarkers are being studied[103, 104]. At present the AJCC staging system only includes LDH blood levels as a prognostic marker for patients with stage IV disease[62], and a more sensitive marker of residual disease is required.

2.2.2 Treatment and prognosis

The choice of therapy for the management of metastatic melanoma depends on the number of lesions, their anatomical location, and their size. The aims of treatment for metastatic melanoma are to control the melanoma and to relieve any symptoms, with curable intentions. Treatments that may be offered include surgery, radiotherapy, targeted therapies, chemotherapy, immunotherapy and diverse clinical trials of these and other new drugs individually or in combination are underway.

New combinatorial drug development using targeted therapy and immunotherapy have revolutionised the clinical management of melanoma patients, improving the quality of life and the length of survival of patients with stage III or stage IV melanoma[105-107]. Nowadays, targeted therapies and immunotherapies are within the standard treatment choices for metastatic melanoma in Australia and several other countries[108].

Targeted Therapy

Since the discovery of activating mutations in the *BRAF* oncogene in approximately 50% of melanomas[70], there has been notable progress in the development of targeted therapies for unresectable and metastatic melanoma. The American Food and Drug Administration (FDA) has now approved the use of *BRAF* inhibitors vemurafenib and dabrafenib routinely[109] for *BRAF* positive melanoma. These targeted treatments act as a

direct inhibitor of BRAF, which is constitutively active due to the presence of mutant copies of the *BRAF* gene and thus activates the MAPK pathway regulating tumour growth gene[70].

More recently, MEK inhibitors such as trametinib are administrated in combination with BRAF inhibitors[110]. Current clinical trials are testing different combinations of dabrafenib or vemurafenib with MEK inhibitor drugs as trametinib or cobimetinib[111], respectively.

Mutations in *NRAS* lead to up-regulation of heterogeneous effector pathways, thus making drug development more difficult and no standard drug is currently available for patients that carry *NRAS* mutations. However, new drugs are under investigation in pre-clinical and clinical trials for NRAS inhibition as well as for alternative BRAF or c-kit mutations[3, 112].

Targeted therapy is effective in most patients. Unfortunately, despite the impressive initial tumour shrinkage, targeted therapy treatment responses are relatively short-lived and acquired resistance occurs in a high proportion of cases[109, 113]. Another disadvantage of this type of therapy is that significant toxicities are associated with BRAF inhibitors[114] and with combination therapies[112, 115].

Immunotherapy

Immunotherapy is a promising cancer therapy that aims to strengthen anti-tumour response in patients with stages III or IV malignant melanoma. In 2011, the FDA approved the use of immune checkpoint inhibitor, ipilimumab for unresectable or metastatic melanoma. This antibody binds to cytotoxic T-lymphocyte antigen 4 (CTLA-4) on tumour cells and blocks its activity, allowing immune cells to target the melanoma cells. Unfortunately, the patient response rate is low (11.9%) and immune-related adverse effects are severe and common[116].

Alternate immune attenuating checkpoints have been studied and the interaction between programmed death-1 factor (PD-1) with its ligand (PD-L1) on diverse cells, such as, antigen presenting cells (APC) or tumour cells, is now routinely targeted for the treatment of metastatic melanoma[107, 117]. Pembrolizumab and nivolumab are anti-PD-1 antibodies approved by FDA for the treatment of advanced melanoma in BRAF negative melanomas or after the failure of previous treatments[118, 119]. Anti-PD-1 blockade

antibodies are now available as first line therapy in *BRAF*-mutant negative melanoma patients. The response rate of melanoma patients to nivolumab, and pembrolizumab are 43.7% and 33.7% respectively[106, 120]. Also, new immune checkpoints inhibitors as well as the combination of current immune therapies, such as ipilimumab/nivolumab or pembrolimumab/ipilimumab are being trialled[121-123].

Biomarkers

Current therapeutic options for late stage disease are more effective when the disease is treated in patients with a lower disease burden[124, 125]. Consequently, melanoma must be treated at earlier stages to maximise the chances of patient survival. Thus, the ability to identify signs of melanoma progression prior to overt metastatic disease would be a valuable clinical tool. The rapidly evolving clinical landscape of melanoma therapy urgently requires the discovery and the development of reliable and accurate biomarkers that assist in early detection, diagnosis, staging, prognosis as well as prediction, and monitoring of treatment response. Also, biomarkers could improve the process of drug development and response prediction[126].

Biomarkers are classified as serum or tissue-specific biomarkers. Several serum biomarkers have been shown to have prognostic relevance in melanoma. One such marker routinely used is the enzyme lactate dehydrogenase (LDH) which has been shown to have prognostic value in later disease stages, and is incorporated in TNM classification[127]. However the sensitivity of this marker is reduced during progression[128]. Tyrosine and vascular endothelial growth factor (VEGF) were initially reported to have prognostic value[129, 130]. Subsequent studies could not confirm these findings and no prognostic value is attributed to them. Other diagnostic and prognostic serum biomarkers are osteopontin[131], YKL-40 glycoprotein[132], melanoma-inhibitory activity (MIA) protein[133], s100 family protein[134] and interleukin-8 (IL-8)[135]. However, none of these are commonly utilised in clinical settings.

Tissue specific biomarkers for melanoma are molecules that are over-expressed in melanoma lesions. Cyclooxygenase-2 (COX-2) is an essential protein in catabolic metabolism. This protein is induced in tumour cells and a correlation between COX-2 over-expression and Breslow thickness has been found in primary tumours[136]. Cell adhesion molecules and matrix metalloproteinases also play an important role in tumour

progression[85]. Chondroitin sulphate proteoglycan 4 (CSPG4/HMW-MAA/MCSP) is over-expressed in over 80% of all melanomas and recent studies indicate that the protein is potentially valuable as a marker of response to treatment or progression[137]. Currently, different immune molecules associated with tumour inflammation, such as Galectin-3 may be used to monitor treatment response in melanoma patients[138]. The prognostic utility of novel melanoma biomarkers, such as ctDNA, exosomes, or miRNA have been evaluated with promising results, although none have yet been clinically utilised. Although ctDNA measurements have been utilised in early detection of melanoma and in monitoring treatment response, there is a need to find additional biomarkers that can aid in measuring the disease load and treatment responses. Therefore, the need for melanoma biomarkers with the ability to provide information early during treatment are of critical importance when the patient is undergoing systemic treatment.

For patients with advanced melanoma as well as those with localised disease, the analysis of circulating tumour cells (CTCs) may provide a novel biomarker to guide therapeutic decisions. Detailed molecular characterisation of melanoma cells circulating in the bloodstream may yield new insights into the process of melanoma metastasis[139].

2.3 Circulating tumour cells (CTCs)

During the last decade, circulating tumour cells (CTCs) have received extensive attention as new biomarkers. On average, 20 new publications were published each week in 2013 under the key phrase "circulating tumour cell"[10], and the number of publications has continued to increase since then.

The presence of tumour cells circulating in the blood of cancer patients was first reported by Thomas Ashworth in 1869[140]. It was observed that these cells were identical to the cancer cells found in the tumour, leading to the idea that these cells relate directly to neoplastic development and tumour metastases. The first detection of CTCs was made by B. Smith[141] when technologies had evolved to permit the study of these rare cells.

Circulating tumour cells (CTCs) are cancer cells which detach from primary or metastatic sites, enter the peripheral blood stream, and may develop into a secondary tumour at distant sites due to their capacity to enter and exit the bloodstream (Figure 7)[82, 142, 143]. However, only a small fraction of CTCs survive, since they have to escape from immune

system attack and survive in stressful ambient conditions without cell-matrix interaction[9]. CTCs have shown stem-like properties, which might facilitate initiation of metastatic lesions[144, 145]. Interestingly, these cells can enter into a state of clinical cancer dormancy, where, after dissemination, cell division processes may stop and the cell may persist in a quiescent state, sometimes for more than 10 years[146]. The amount of time involved in the dormancy process varies among different kinds of cancers, being generally relatively short in melanoma (1-2 years)[82], although this may vary. CTCs show malignant features[147] not present in healthy cells, and may have less genomic alterations than primary tumour cells, suggesting that the dissemination may happen in earlier stages of the disease[148].
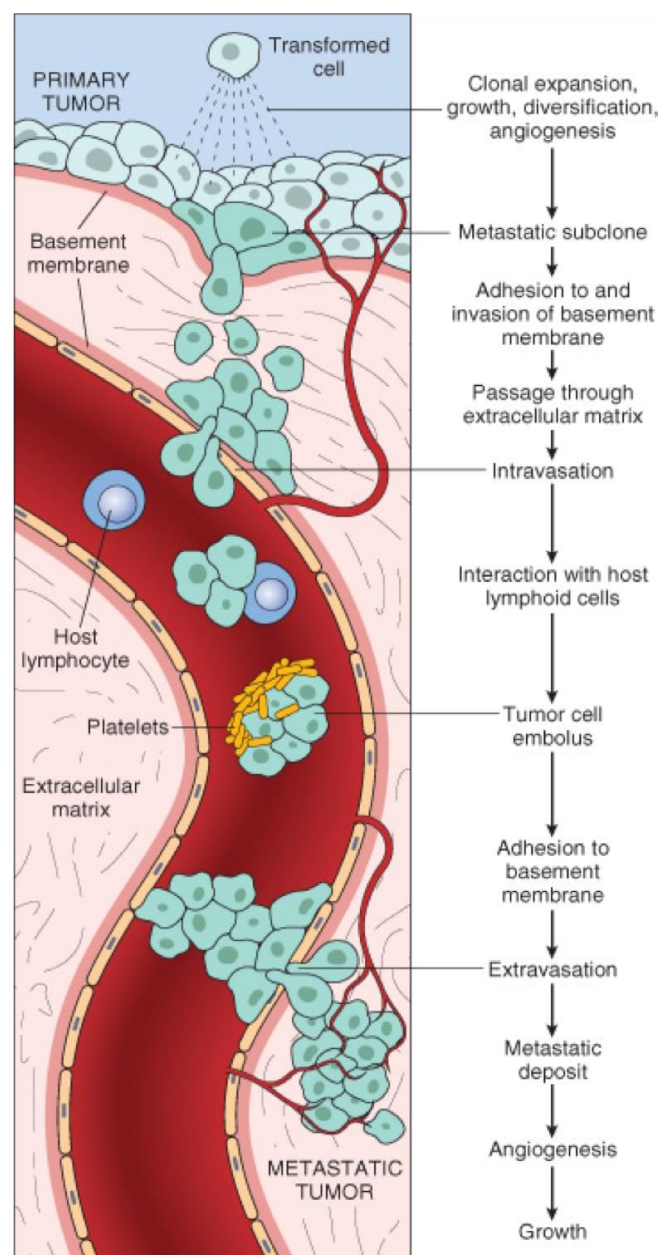
Figure 7. Metastatic cascade[149].

2.3.1 Biomarker value of CTCs

Circulating tumour cells are derived from the primary and metastatic tumours and their study provides significant information about the biology and development of the tumour. Since these cells can be isolated from blood using relatively non-invasive approaches, their presence in peripheral blood can serve as a "liquid biopsy". As an independent prognostic marker, the number of CTCs before, during and after therapy administration has been shown to be an indication of the length of progression free survival (PFS) and of overall survival (OS) in various cancers[8, 9, 150].

The utility of CTCs as biomarkers for the prognosis and in the monitoring of response to anticancer therapies has been widely reported for several types of solid cancers. In breast cancer, CTCs have indicated prognostic value[151, 152]. Several studies in ovarian cancer have shown the utility of CTCs in disease monitoring[153, 154] with elevated numbers of CTCs indicating an unfavourable prognosis[155]. Similar results have been found in other cancer types such as prostate[6], lung[156], colorectal[157], and hepatocellular carcinoma[158]. Several of these studies have used the CellSearch® system (Veridex LCC), the only FDA-approved CTC enumeration test, which exploits CTCs as a new parameter for estimating prognosis and monitoring treatment success in metastatic breast, colorectal, and prostate cancer[159-161].

2.3.2 Biomarker value of CTCs in melanoma

While additional studies are required to further characterise melanoma CTCs and confirm their clinical utility as a biomarker of treatment response, monitoring the levels of CTCs before and during melanoma treatment has been shown to be informative with respect to prognosis and therapy response in melanoma patients.

RT-PCR has been widely used to detect mRNA transcripts associated with melanoma in blood. Reid *et al.*, examined whole blood RNA from 230 melanoma patients and showed that the presence of MLANA and ABCB5 transcripts was associated with disease recurrence and the expression of MCAM was significantly more common in patients with a negative treatment outcome[162]. Also, the presence of multiple melanoma markers in patient blood significantly correlated with their AJCC stage[163]; the detection of more than

one marker at baseline and at any time during treatment administration was a negative prognostic factor for disease-free survival (DFS) and for overall survival (OS)[164].

Several studies using immunomagnetic bead-based isolation techniques have also shown that the number of melanoma CTCs is higher in the blood of patients with advanced disease[4, 165-167]. The number of CTCs was also shown to be associated with treatment failure and shorter median OS if ≥ 2 CTCs are found per 7.5 mL during the time that patients are receiving treatment[168, 169]. By contrast, a low CTC count at baseline (< 2 CTCs) or a decrease in CTCs after treatment initiation was associated with response to treatments and longer progression free survival (PFS) rates[98].

More recently, Gray *et al*, showed that the presence of CTCs was associated with PFS[170]. Interestingly, early-stage patients were generally positive for a single marker compared to late-stage patients who had larger numbers of CTCs expressing a variety of markers. Remarkably the differential pharmacodynamic response of CTC subtypes to treatment was evident in patients treated with BRAF inhibitors (n=16), since the proportion of CTCs expressing RANK were significantly increased after therapy. In addition, patients with more than 5 RANK+ CTCs in 4 mL of blood had significantly lower PFS than those with less than 5 or no RANK expressing CTCs[170]. Similarly, a preliminary study showed that the presence of CTCs expressing PD-L1 was associated with response to anti-PD1 blockade[171]. Thus, prognostic utility might be found not by using total CTCs counts but by studying specific subpopulations of CTCs.

New experiments with patient-derived xenografts (PDX) are providing new information that can inform treatment decisions for each patient. Alternately, where tumours are inaccessible, CTC-derived xenografts or *in vitro* growth of CTCs may provide a powerful option for testing of drug efficacy in a patient's cells. Girotti *et al*, showed that CTC-derived xenografts (CDX) established from advanced stage patients could aid in monitoring and predicting patient responses to treatments. In fact, they have been successful in generating CDXs in 6 out of 21 cases (28.6%)[172]. While the isolation of only a few CTCs capable of developing xenografts may underestimate the tumour heterogeneity, these are excellent first steps to addressing several of the issues surrounding the clinical benefit of CTC characterisation, including the fact that CTCs that develop xenografts are capable of seeding metastases and therefore harbor significant

information about the metastatic process. Additionally, further studies characterising CTC subpopulations prior to injecting them into mice will provide crucial information about CTC phenotypes that are most likely to develop CDXs.

2.4 Methods for the isolation and detection of melanoma CTCs

The enrichment and detection of CTCs from melanoma patients is extremely challenging, mainly due to the limited amount of sample available and the very low concentration of these cells in the peripheral blood, roughly 1 CTC in 10^6 normal blood cells. In addition, for melanoma, the difficulties are magnified because common CTC markers, such as EpCAM, used in CTC enrichment of epithelial cancers, are not commonly expressed by melanoma CTCs, since melanocytes originate from the neural crest and not the epithelium[173]. In fact, melanomas CTCs are a very heterogeneous population of cells[4, 170, 174], yet current techniques used to enrich melanoma cells from blood, commonly do not consider this fact.

Assays used for CTC identification and characterisation (Figure 8) usually require a combination of enrichment and detection procedures that aim firstly to increase the concentration of CTCs in a background of white blood cells and secondly, to enable easier detection and characterisation of single cells. Despite the actual advances in CTC isolation and detection technologies, the enrichment of pure CTCs from patient blood remains the most challenging step to date.
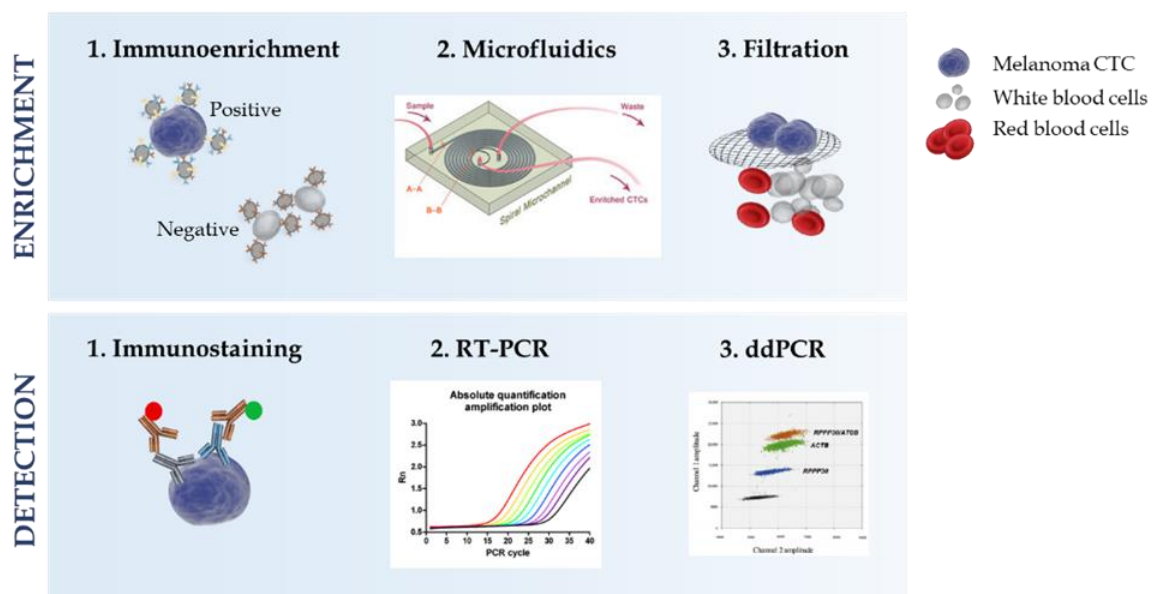
Figure 8. Melanoma CTC isolation and detection technologies.

2.4.1 Isolation techniques in melanoma

Isolation technologies take advantage of the biological and physical properties of the CTCs. Biological properties, such as cell surface protein expression, can be useful characteristics for the isolation of tumour cells from peripheral blood of cancer patients. On the other hand, cell size, density, total electric charges, and deformability are now the main physical characteristics used in CTC enrichment[175, 176]. Thus, CTC isolation assays can be grouped into label-dependent and label-independent methods[177], each method of enrichment having different advantages and disadvantages (Table 2). These methods are detailed below.

Table 2. Advantages and disadvantages of the label-dependent and label-independent isolation methods.

	Label-dependent methods*	Label-free methods
Advantages	Lower WBC Background	Do not rely on the expression of surface markers for CTC isolation
	Most commonly used	Integrity of the membrane not affected
	The only FDA-approved method for isolation of CTCs uses this technology	Viability of the cell is maintained
		More heterogeneous population of CTCs is isolated
		High recovery efficiency
		Huge heterogeneity in the population of CTCs isolated
Disadvantages	Low heterogeneity in the population of CTCs isolated	Not widely used in CTCs isolation. More study is needed
	Alteration of membrane integrity	Higher WBC Background
	Viability of CTCs is affected	
	Only CTCs expressing the targeted biomarker are isolated	

*Excluding Negative Immunomagnetic Enrichment

Label-dependent methods

Despite the demonstrated heterogeneity of melanoma CTCs[170, 174, 178], methods for capture and enrichment of melanoma CTCs have to date relied predominantly on the expression of one or two known cell surface markers. For example, immunomagnetic enrichment using magnetic beads coupled with antibodies against known melanoma-specific antigens have been developed to enrich CTCs (positive selection). Alternate

methods that deplete white blood cells using beads targeting common leukocyte (CD45 or CD34) antigens (negative selection) have also been widely used[168, 169, 179, 180].

The CellSearch™ system (Veridex LCC) is the only FDA-approved CTC enumeration test. This platform involves immunomagnetic bead capture of CTCs followed by cancer-specific marker staining for CTC detection. For breast, prostate and colorectal cancer, EpCAM is used to capture CTCs followed by staining with cytokeratin[150, 181-183]. For melanoma, however, a different CellSearch™ kit was developed that firstly captures CTCs expressing melanoma cell adhesion molecule (MCAM) from whole blood and secondly detects CTCs by immunostaining with anti-MCSP (melanoma-associated chondroitin sulphate proteoglycan). This kit also immunostains CD45 and CD34 positive cells to exclude leukocytes and endothelial cells. Khoja and colleagues[168] used this melanoma specific CellSearch™ kit to detect CTCs in 101 metastatic melanoma patients, and found 0-36 CTCs/7.5 mL of blood at baseline prior to treatment, with 60% of patients having no CTCs and 40% of patients with at least one detectable CTC. Similarly, Rao *et al.*, found 0 to 8,042 CTCs/7.5 mL of blood in 44 melanoma patients: 23% of the patients had two or more CTCs[169].

The need to better capture all melanoma CTCs has driven the development of multiplex assays where beads linked to cocktails of antibodies against both cancer-related markers and melanoma-specific cell surface antigens are used.

Freeman and colleagues[4] found that using a combination of MCSP, MCAM, ATP-binding cassette sub-family B member 5 (ABCB5), and cluster of differentiation 271 (CD271) targeting antibodies captured a significantly higher number of melanoma CTCs in metastatic melanoma patients than did the use of MCSP or MCAM alone. This finding demonstrated, for the first time, the high diversity of melanoma CTCs and improved the sensitivity of bead-based CTC enrichment compared with experiments that target single markers. Moreover, when using a combination of all of these labelled beads, stage I-II (n=10) and stage III-IV (n=13) patients showed significantly higher numbers of CTCs than controls (n=15). More than 1 CTC/mL of blood was detected in 73.9% of patients (range: 0-2.5 CTCs/1 mL of blood). Despite the improvements in sensitivity produced by using a cocktail of antibodies for CTC capture, spiking experiments revealed that immunomagnetic enrichment still has low capture efficiency (34%)[4].

In order to improve capture efficiency, a device has been developed more recently that uses micro-vortices generated by herringbone-shaped grooves to direct cells toward surface channels coated with a combination of antibodies targeting melanoma-specific antigens. One study using the herringbone-chip (HB-chip) technology with a combination of 12 antibodies against melanoma cell surface epitopes detected CTCs by immunostaining in 79% of patients (8 CTCs/2.5 mL) from a total of 41 metastatic melanoma patients at various stages of melanoma treatment[165].

To avoid capture bias, other methods use negative selection procedures, which capture leukocytes with anti-CD45 antibody coated beads followed by depletion of white blood cells using magnetic separation. Systems such as EasySep™ or RosetteSep™ use this approach. Fusi *et al.* using the EasySep™ method and detecting CTCs as cells expressing gp100 and MLANA (melanoma antigen recognized by T cells 1) by flow cytometry, found 87.5% of 32 metastatic melanoma patients had CTCs with a median of 53 CTCs/10 mL of blood[184]. Using RosetteSep™, Girotti *et al.* successfully enriched CTCs and injected them into NSG mice to generate CDX models[172]. While the authors have not provided CTC quantities used to generate the models, it is likely that relatively large numbers of cells were isolated for successful tumour uptake.

Although negative selection is advantageous for removing cells that do not express the most common melanoma markers, the purity of CTCs obtained in the enriched fraction is low, hampering the quantification of CTCs as well as limiting downstream analysis of the detected CTCs for prognosis. In fact, a spiking experiment comparing the recovery and purity of CD45 depletion, with positive enrichment, or a combination of both methods, showed that the greatest recovery was found by using negative selection (58% recovery rate). However, the greatest purity of the CTC fraction was obtained by using the combination method (background reduced from 3×10^7 to 1.5×10^3 of WBCs)[179].

The targeting and capturing of CTCs using protein-based enrichment approaches as is most commonly performed, typically do not allow capturing all CTCs present within a patient and furthermore, the harsh conditions of the isolation techniques may alter the integrity and viability of CTCs[185, 186], and hence, they are highly critical in functional studies. Methods that isolate CTCs with high purity, integrity and viability are urgently needed to determine the real biomarker potential of CTCs in prognosis and in the

prediction of therapeutic responses in metastatic melanoma patients. Thus, the development of label-free enrichment technologies is a promising alternative for the successful isolation of melanoma CTCs.

Label-free methods

To further improve CTC capture, alternative techniques have been developed more recently, that exploit the larger cell size of melanoma CTCs compared to the remaining white blood cells. Although it has been shown that melanoma CTCs can have a diverse range of cell sizes[185], most of the CTCs are thought to be larger (10-20 μm) than other blood components, such as RBCs (6-8 μm), leukocytes (7-12 μm) or platelets (2-3 μm).

Taking advantage of this perceived difference in cell size, the "enrichment by size of epithelial tumour cells" (ISET®) technique was developed in 2000[187]. The ISET® system uses polycarbonate filters with 8 μm diameter circular pores for CTC enrichment and detection of cells trapped in filters as CTCs involves immunohistochemical staining and PCR-based genetic analyses. De Giorgi *et al.* detected CTCs in 29% of patients with primary invasive melanoma and in 62.5% of metastatic melanoma patients using this microfiltration system followed by positive detection by real-time RT-PCR for tyrosinase transcripts. Experiments assessing the sensitivity of this assay showed that ISET® had a limit of detection of 1 CTC/mL of blood[188]. However, challengingly, this approach was also found to isolate benign circulating nevus cells[189], suggesting that the molecular analysis of tyrosinase mRNA by RT-PCR-based systems, cannot reliably distinguish between benign nevus cells and melanoma cells.

Nevertheless, when using the same ISET enrichment technique, with CTCs defined by positive immunohistochemistry expression of s100 and negative expression for CD45 or CD144 (leucocyte and endothelial cell markers, respectively), 57% of 90 metastatic melanoma patients had detectable CTCs (1-44 CTCs/mL of blood)[174].

The OncoQuick® system is another size-based technique that incorporates a filter for size-based separation of CTCs which is used in conjunction with density-based centrifugation[190]. Spiking experiments showed a ≥60% recovery rate when assessed by qPCR amplification of cytokeratin 8 (KRT8) and 18 (KRT18) RNAs, for 4, 20, 100 and 500 spiked SkMel28 cells. When the OncoQuick® was used for isolation of CTCs from

melanoma patients, and target RNA transcript levels (MLANA, MIF, TYR, and MITF) were then quantified by qPCR, results showed that about 1/3 of patients expressed elevated levels of MIF and MLANA transcripts, in comparison with healthy controls ($p < 0.0001$ and $p < 0.001$, respectively)[191].

Microfluidics

Microfluidic devices control microliter to milliliter volumes in micro-channels of 1 μm to 1000 μm in size. In such conditions, the concentrations of particles/cells can be effectively controlled, since the flow is strictly laminar[192, 193].

At the beginning of the 21st century and the arrival of nanotechnology, many microfluidic components that work with nanoliter volumes were developed for use in biological studies[194-196]. Since then, the field of microfluidics has evolved rapidly, allowing the manipulation of DNA, RNA, proteins and mammalian cells, as well as single cell assays for disease diagnosis and prognosis, amongst several other applications[193]. At present, microfluidics are valuable for cancer cell investigations due to their high sensitivity, high throughput, low material consumption, low cost and improved spatial-temporal control. Microfluidic devices are now proving very useful for isolating CTCs from the blood of patients with different cancer types.

To date very few studies have utilised microfluidic devices to isolate CTCs from melanoma patients. The more recently developed CTC-iChip (Figure 9) separates cells based on size selection using deterministic lateral displacement and inertial focusing followed by negative depletion in a magnetophoresis. Using this chip, CTCs from melanoma patients were successfully enriched and detected as positive by staining for the melanoma antigen recognized by T cells 1 (MART-1)[185].

Previous studies identified that CTCs exist as circulating tumour microemboli (CTM) or CTC clusters in the blood of melanoma patients, raising the idea that cells enter the bloodstream via collective cell migration, allowing them to survive shear stress and anoikis forces[93, 174]. Recently, the Cluster-Chip (Figure 9) was developed particularly to isolate CTC clusters[178]. The Cluster-Chip captures CTC clusters of two or more cells directly from 4 mL of blood, independently of cell tumour-specific marker expression. This microchip technology relies on the strength of the cluster union as well as on their

behaviour when a flow speed is applied through a set of triangular pillars. Captured CTC clusters were identified and detected by immunofluorescence staining in 30% (~0.15 CTCs/mL) of 20 tested metastatic melanoma patients. Interestingly, no correlation was found between the number of CTC clusters isolated using the Cluster-Chip and the number of single CTCs isolated using CTC-iChip (n=19)[178].
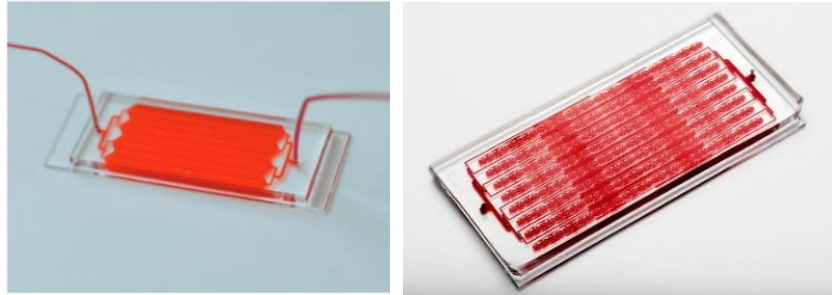
Figure 9. The CTC-iCHIP (left) and Cluster-Chip (right) microfluidic CTC devices[178, 185].

Two new spiral microfluidic devices (A5 and Slanted) that allow CTC enrichment based on Dean Drag forces and the inertial microfluidic phenomenon, have been developed for CTC isolation[11, 12]. This separation technology is termed Dean Flow Fractionation (DFF), and allows a size-based separation using hydrodynamic forces and Dean Drag forces acting on cells within a laminar flow due to the curvilinear geometry of the microchannels. The Drag equation calculates the force of drag experienced by an object due to movement through a fully enclosing fluid. The microenvironment created by these forces causes different sized particles to travel at different speeds in the liquid phases with the result that each particle acquires different lateral positions and exhibits different degrees of focusing inside the chip, allowing a successful size-based separation. Cells are affected differently by these forces depending on their size, allowing separation through two different outlets (see Figure 11). Since the size of most of the CTCs are thought to be larger (10-20 μm)[12, 197] than that of other blood components, the DFF-based method appears suitable for separation of these cell types.

CTC isolation using spiral microfluidic devices that use Dean drag forces[198] to separate tumour cells on the basis of their size[11, 12, 199] were tested in this study for the isolation of melanoma CTCs. The big advantage of this method over label-based isolation techniques is that it isolates all CTCs regardless of their cell surface proteins. Moreover, there is no manipulation of cells, which can affect their viability, as well as downstream analyses[185, 186].

The Slanted microfluidic device

The Slanted spiral microfluidic device relies on inertial microfluidic forces and Dean Drag forces to separate CTCs from blood cells. This device contains 8-looped spiral microchannels with one inlet for the sample and two outlets, one inner outlet for collection of the CTC-enriched cellular fraction (CTC outlet) and one outer outlet for collection of unwanted blood cells (waste outlet) (Figure 10). The operating principle of this chip allows large CTCs to stay near the inner channel wall and to be collected from the inner cell outlet of the chip.

The trapezoidal geometry of the channel cross-section[200] increases the resolution of the separation due to its influence on the formation of Dean vortex cores in the outer walls. This design is ideally effective when isolating particles with large diameter and low abundance from smaller and abundant particles. Accordingly, the enrichment of low-abundant CTCs from other blood components is a satisfactory condition for this design. This Slanted microchip has been shown to efficiently capture cancer cells from blood cells when using cell lines (MCF-7, T24, and MDA-MB-231) spiked into whole blood. The results showed an isolation efficiency of ~85%, with a viability of captured cells of >90%[11]. High purity was also achieved (400-680 WBCs per mL; ~4 log depletion of WBCs).

Waste Outlet   *CTC Outlet*   *Sample Inlet*
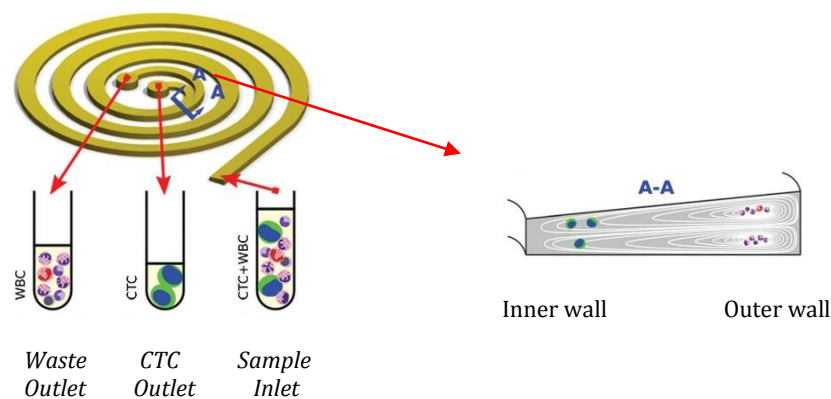
Figure 10. Slanted microchip operating principles for CTC isolation. One inlet for the sample and two outlets for the enriched cells (CTC outlet) and for the other blood components (waste outlet). The trapezoidal section is represented as A-A[11].

Validation of this isolating principle has been performed in clinical samples. Five patients with metastatic breast cancer (MBC) and 5 patients with non-small cell lung cancer

(NSCLC) were studied, as well as 5 healthy controls. All cancer patients had detectable CTCs (6-57 CTCs mL^{-1} for MBC and 3-125 CTCs mL^{-1} for NSCLC)[11].

A5 microfluidic device

The A5 chip also relies on Dean Flow Fractionation (DFF) forces to isolate CTCs from blood. Due to the presence of Dean Forces and inertial lift forces in the curvilinear channels of the device, a more efficient, high resolution size-based separation is achieved[12] (see Table 3). The microchip consists of 2 inlet and 2 outlet spiral microchannels of ~10 cm in length. The design of the chip allows larger CTCs to focus their position inside the channel and be collected through the inner CTC output, while smaller blood components, less affected by the Drag forces, are removed via the outer outlet. The blood sample is pumped into the sample inlet, and a sheath fluid is pumped into the sheath inlet at a higher flow rate. Once the sample is inserted into the device, the separation process is initiated, with the cells taking different positions inside the channels, allowing their separation into the outlet portals (Figure 11).

The efficiency of this DFF device was validated using cancer cell lines cells spiked into whole blood. Three different cell lines (MCF-7, HeLa, and MDA-MB-231) were tested and a cell recovery of ~85% was achieved using spiked cancer cells. Also, a 2000 fold leukocyte reduction and a CTC/leukocyte purity of ~10% was achieved from ~2X dilution of whole blood with saline buffer.

To test the efficacy of this device to isolate CTCs from blood, 20 metastatic lung cancer patients and 20 healthy controls were tested and CTCs were successfully detected in all cancer patients (5-88 CTCs/mL)[12]. The enrichment of CTCs from lung cancer patients demonstrated the high-throughput capability and high-sensitivity separation of CTCs using this device.

Moreover, the label-free procedure and the purity of the output sample, allows a downstream analysis of the live retrieved cells, which include RNAseq, single-cell next generation sequencing (NGS), quantitative-PCR (q-PCR), FISH or immunofluorescence staining.
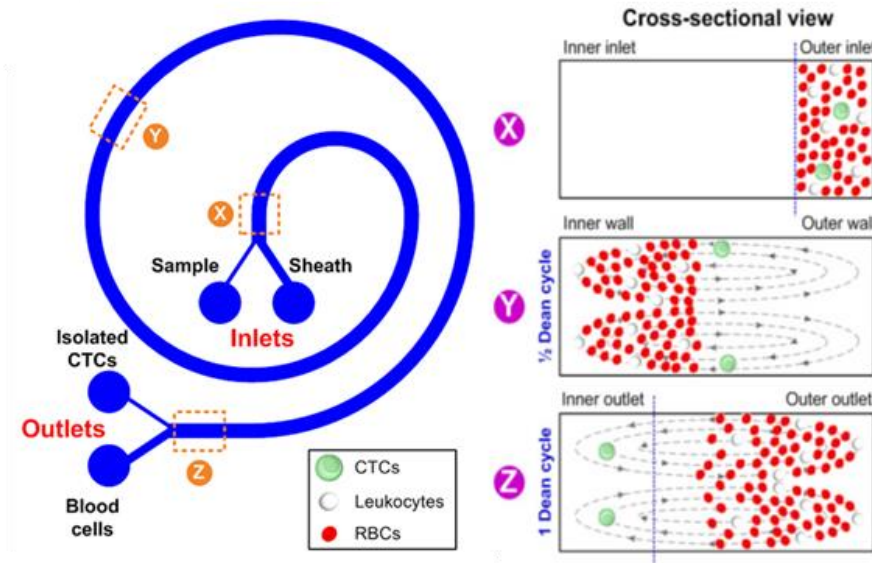
Figure 11. Optical image of the A5 spiral microfluidic device used in capturing CTCs. Two inlets for the sample and the sheath flow, and two outlets for the enriched cells (CTC outlet) and for the other blood components (waste outlet)[12].

Recently, a multiplexed version of the A5 chip, that combines three spiral circuits in the same chip[199], has shown better detection of CTCs from breast and lung cancers than those detected with the FDA-approved CellSearch® method. CTCs were detected in 100% of the cancer patient samples (n=56), while CellSearch® only detected CTCs in 80% of the samples[201]. Furthermore, lower numbers of CTCs were obtained using the CellSearch® system[201]. The major advantage of the A5 chip compared to the CellSearch® method, is the capability of it to be used in different cancers, of both epithelial and non-epithelial origin, since this approach does not require initial cell surface biomarker selection.

Table 3. Main characteristics of the two microfluidic devices used in this project.

		Slanted chip	*A5 chip*
Characteristics	Number of inlets	1	2
	Number of outlets	2	2
	Viability test	Yes (>90%)**	Yes (>98%)**
	Processing time	1.1 min per 1 mL blood	20 min per 1 mL blood
	Flow rates	1700 µL min⁻¹ sample inlet	750 µL min⁻¹ sheath inlet 100 µL min⁻¹ sample inlet
	Sample concentration	0.5x	0.5x
	Purity	~4 log depletion of WBCs	~3 log depletion of WBCs*
	Recovery rates	> 85%**	>85%**

*From whole blood. **Using cell lines.

In this thesis, the ability of these two novel microfluidic chips to isolate melanoma cells and CTCs from metastatic melanoma patients was tested for the first time. Three different settings were studied, namely: single Slanted (1X Slanted), single A5 and double Slanted (2X Slanted).

2.4.2 Detection techniques

While the above techniques are utilised to isolate/enrich CTCs, optimisation of methods for the visualisation of the isolated CTCs is also required. A few methods that detect melanoma CTCs in whole blood from patients, without an enrichment step, have been reported. For example, Ruiz *et al.* describes the use of the Epic Sciences platform to detect intact melanoma CTCs. Erythrocyte lysis was followed by nuclear size analysis and immunocytochemical identification of melanoma CTCs using a panel of seven anti-MCSP monoclonal antibodies. Micromanipulation was performed to isolate single CTCs for whole genome amplification and copy number variation (CNV) analyses. This method detected 1-250 CTCs in 8 mL of blood (0.5 to 371.5 CTCs/mL of blood) from 22 of 40 metastatic melanoma patients (55%). Interestingly, CNV analyses revealed deletions of *CDKN2A* and *PTEN*, and amplifications of *TERT*, *BRAF*, *KRAS* and *MDM2* genes among others[202].

Currently, CTCs present in the enriched fraction are studied and detected by methods that assess their morphology and/or protein expression using immunocytochemistry (ICC) or flow cytometry. These techniques stain the cells with a cocktail of antibodies against cell surface or intracellular markers associated with melanocyte biology or melanoma pathogenesis[4, 170, 203, 204]. Cells are considered tumour cells if positively fluorescently stained for melanocytic markers, melanoma or tumour-specific markers, and for the nuclear dye (DAPI or Hoechst 33342), but negative for the common leukocyte antigen CD45 (a marker present only in leukocytes and not in tumour-derived CTCs). Using multicolour image analysis with a fluorescence microscope, CTCs are thus identified as melanocyte/melanoma markers^{+}/CD45^{-}/DAPI^{+} cells (Figure 12).

In addition, molecular approaches that detect RNA or DNA from enriched melanoma CTCs, by quantitative real-time PCR (qRT-PCR)[205] or droplet digital PCR (ddPCR)[206] respectively, have been used for CTC detection and more detailed CTC characterisation.

New methods based on the presence of elevated telomerase activity are being trialled for CTC detection[207].
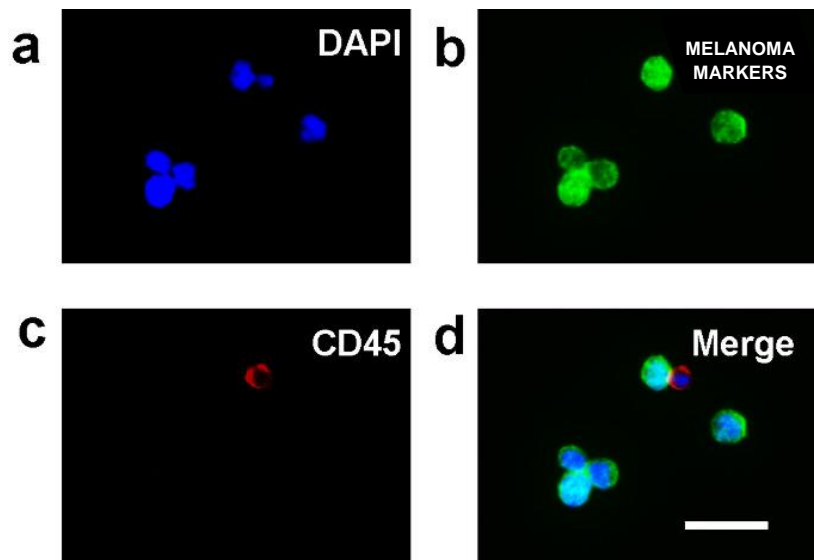
Figure 12. Immunofluorescent CTC staining.

Gray *et al.* has recently developed a flow-cytometry multimarker approach to detect and analyse CTCs for the presence of melanoma-associated markers, such as MCSP and MCAM, in combination with melanoma stem cell markers, such as ABCB5, RANK (receptor activator of NF-κβ) and CD271[170]. Using this approach we provided for the first time, a detailed insight into the diversity of melanoma CTCs, and showed that the prognostic utility of melanoma CTCs may not rely on the total count of CTCs but on the CTC subpopulations circulating within an individual. This study indicated that a high number of melanoma CTCs express melanoma-initiating or stem cell markers (ABCB5 and RANK) while only a very low number of CTCs express melanoma markers MCSP and MCAM[170]. Importantly, this study also observed that the common expression of these melanoma-initiating markers by melanoma CTCs did not correlate with the expression of these markers in patient-matched tumours, where a rare frequency of melanoma tumour cells positive for these markers was observed. This finding provides evidence supporting the hypothesis that CTCs, at least in in melanoma, are derived from rare subpopulations present in the tumour, which might have the ability to seed new metastases, and not from the bulk melanoma cells shaping the tumour[170].

In summary, the use of microfluidic devices to isolate highly heterogeneous melanoma CTCs independently of their marker expression could be beneficial. Additionally, the

application of multimarker immunostaining protocols for the detection of CTCs in the enriched fraction is of vital importance. Table 4 shows eight of the most common tumour and melanoma-specific markers used in immunological detection of melanoma.

Table 4. Markers commonly used in immunological detection procedures in melanoma.

Marker	Name or encoding gene	References	Cellular location
gp100	Also known as premelanosome protein (**PMEL**), silver locus protein homolog (**SILV**), **ME20**, or **Pmel17**.	208	Cytosol
MART1	*Melanoma antigen recognized by T cells* 1. Also known as **Melan-A protein**.	52, 209, 210	Cytosol
s100	Different types encoded by the **s100b**(**number**) genes.	51, 210	Cytosol
MCSP	*Melanoma chondroitin sulphate proteoglycan*. Also known as chondroitin sulfate proteoglycan 4 (**CSPG4**) or neuron-glial antigen 2 (**NG2**).	169, 203, 211	Membrane
Vimentin	This protein is a type III intermediate filament expressed in mesenchymal cells, encoded by the VIM gene.	212-214	Cytosol
RANK	*Receptor activator of nuclear factor κβ*. Also known as **TRANCE Receptor** or **TNFRSF11A.**	4, 170, 215	Membrane
ABCB5	*ATP-binding cassette sub-family B member 5*. Also known as **P-glycoprotein ABCB5**.	4, 170, 216	Membrane

In this study, we developed and optimised a protocol for improved staining of CTCs that utilises three internal markers (gp100, MART1/Melan-A, and s100) and one cell surface marker (MCSP) to identify CTCs isolated from patient blood using the microfluidic devices. Lastly, based on Gray *et al.* findings which show a high number of melanoma CTCs express the melanoma-initiating or stem cell markers, we have incorporated ABCB5[217], RANK[170] and Vimentin[213] into our panel, to improve the detection and characterisation of CTCs after spiral microfluidic enrichment in future studies.

3. THEORETICAL FRAMEWORK

New biomarkers are required for the early detection of disease progression and therapeutic response in metastatic melanoma patients. Circulating tumour cells (CTCs) have been shown to be a useful biomarker of cancer development and for therapeutic response guidance[16, 218, 219]. However, isolation of melanoma CTCs is very challenging because of the low quantities of CTCs in blood and the heterogeneity of cell surface markers expressed by melanoma CTCs[10, 170, 174]. These challenges have limited the utility of CTCs as biomarkers in patients with metastatic melanoma.

Microfluidic chips can successfully isolate CTCs with high integrity from different cancer types[11, 199, 201], with few used in melanoma to date[178, 220]. The ability of microfluidic devices to isolate label-free and viable CTCs with high efficiency and low cost has prompted their use in this study for isolation of heterogeneous melanoma CTCs[170].

The detection of CTCs using melanoma-specific markers has previously indicated the extreme heterogeneity of these cells[170, 174, 220]. To better understand their biology and the differential response of heterogeneous CTCs to treatment, immunostaining protocols that combine multiple cancer, melanocyte and melanoma-specific markers are developed and optimised here to assist with detection of diverse CTC subpopulations isolated from metastatic melanoma patients using a label free device[4, 170].

The optimisation of live and label-free CTC isolation procedures using available microfluidic devices as well as the optimisation of approaches for the detection of a broad spectrum of CTC subtypes from metastatic melanoma patients is of importance for the study of melanoma progression and therapeutic efficacy.

The overall aim of this study was to determine the effectiveness of the isolation of melanoma cell lines using three microfluidic approaches (1X Slanted[11], A5[12] and 2X Slanted), and the potential for these devices to be utilised for the isolation of pure CTCs from the blood of metastatic melanoma patients. Furthermore, the study aimed to assess additional cellular markers to be used in immunostaining that can improve the detection of CTCs isolated from melanoma patients using microfluidic devices. The implementation of this label-free method in isolating CTCs will facilitate downstream functional studies as well as phenotypic and genomic characterisation of melanoma CTCs.

3.1 Hypothesis

Spiral microfluidic devices allow the isolation of circulating melanoma cancer cells (CTCs) from the blood of metastatic patients.

3.2 Aims

1. _To measure the efficiency of three spiral microfluidic approaches to isolate differently sized melanoma cell lines spiked into healthy control blood._

In order to determine for the first time the ability of the spiral microfluidic devices to isolate melanoma cells, spiking experiments were performed to compare the recovery rates after processing through single Slanted (1X Slanted), single A5 and double Slanted (2X Slanted). The recovery efficiency and purity were analysed for each method.

2. _To detect CTCs from metastatic melanoma patients enriched by the 2X Slanted device, using an optimised immunostaining protocol._

After enrichment through the 2X Slanted device, protocols for detection of CTCs from patient samples, such as cytospin conditions and immunostaining were optimised. Blood samples from 10 metastatic melanoma patients were then analysed for the presence of CTCs after enrichment using the 2X Slanted microfluidic device, followed by the revised immunostaining protocol. In addition, 3 healthy volunteers were used as negative controls.

3. _To test additional cellular markers that can be used in immunostaining assays for optimisation of detection and phenotypic characterisation of heterogeneous melanoma CTCs._

In order to further improve the detection of CTCs, three additional cancer stem-cell and tumour markers were tested, Vimentin, RANK, and ABCB5. To assess their ability to improve CTC detection, the expression of these markers was assessed by immunocytochemistry in three melanoma cell lines, either alone or when spiked into blood from healthy volunteers.

4. METHODS AND MATERIALS

4.1 Aim 1. To measure the efficiency of three spiral microfluidic approaches to isolate differently sized melanoma cell lines spiked into healthy control blood.

4.1.1 Experimental Design and Methods

Figure 13 illustrates the key steps followed in the preparation and processing of the samples in order to determine the efficiency of different spiral microfluidic approaches to isolate spiked melanoma cells with different cell sizes spiked into blood samples from healthy donors. For this, three microfluidic approaches were used: single Slanted (1X Slanted), single A5 and double Slanted (2X Slanted), by which the sample is processed twice through the Slanted device. The last setting was tested with the aim of improving WBC depletion rates.
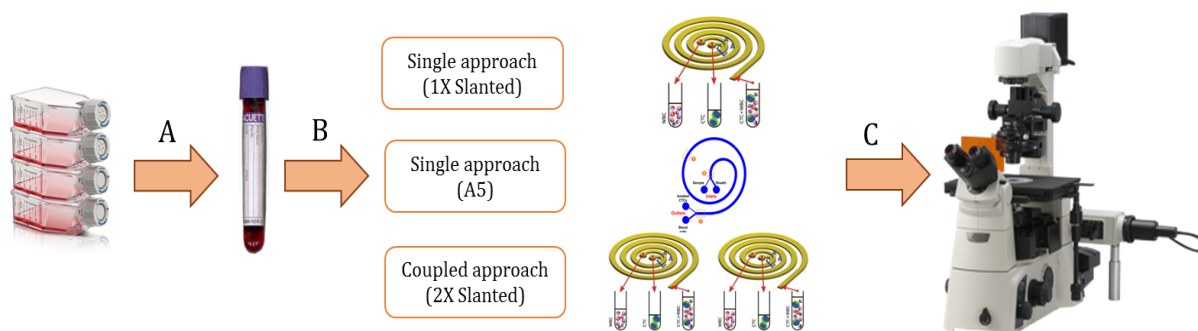
Figure 13. Overview of the methodology of sample preparation and processing. Firstly, the spiking of melanoma cells into healthy blood samples was completed (A) prior to processing the blood using three different approaches (B). Finally, the recovery analysis (C) determined the recovery rates for each spiral microfluidic approach by counting total red labelled cells recovered in the enriched fraction.

Cell lines and cell culture

Two melanoma cell lines (A2058 and SKMEL5) obtained from the American Type Culture Collection (ATCC, USA) were used in spiking experiments. Previous studies in our research laboratory have identified melanoma cell lines A2058 and SKMEL5, as the cell lines with the smallest and largest cell size respectively, from a panel of six melanoma cell lines (Figure 14).
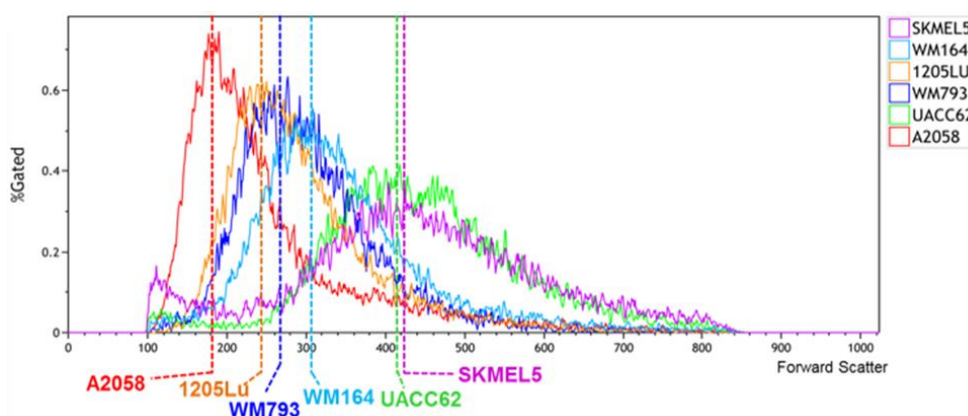
Figure 14. Melanoma cell line heterogeneity in size determined by flow cytometry.

Cells lines were cultured in high-glucose Dulbecco's modified Eagle's medium (DMEM) (Thermo Fisher Scientific, USA) supplemented with 10% foetal bovine serum (FBS) (Invitrogen, USA). The cultures were maintained at 37 °C in a humidified atmosphere containing 5% (v/v) CO_2 until 80% confluence. Cell lines were passaged every 72 hours as per ATCC guidelines. Sub-confluent monolayers were dissociated using 5mM Ethylenediaminetetraacetic acid (EDTA) in DMEM. Viability and cell counts of cell cultures at every passage were determined using a Vi-CELL XR cell counter (Beckman Coulter, USA). Only cell cultures with a viability higher than 80% were used in subsequent experiments.

CellTracker™ labelling

For the counting and detection of recovered cells after processing melanoma spiked blood samples through the three microfluidic approaches, melanoma cell cultures were firstly stained with CellTracker™ Red CMTPX dye (Thermo Fisher Scientific, USA), which passes freely through cell membranes into cells, and stains all cells similarly. For the CellTracker™ staining, A2058 and SKMEL5 cell cultures were washed twice with PBS (137 mM NaCl, 10 mM Phosphate, 2.7 mM KCl, pH of 7.4) after removing the culture media followed by incubation in 2 mL of DMEM, containing 2 μL of CellTracker™ dye (1μM) for 45 min at 37 °C in a humidified atmosphere containing 5% (v/v) CO_2. After incubation, the staining media was removed and two washes with a PBS solution were performed. Cells were dissociated using a 5mM EDTA in DMEM solution for 5 minutes and 2 mL of 10% FBS/DMEM media was added to inhibit dissociation activity. After this, the cells in suspension were ready for spiking purposes. Staining of cells was confirmed under an inverted fluorescent microscope (Eclipse Ti-E, Nikon®, Japan).

Blood collection

For all experiments, healthy donors provided signed consent forms, previously approved by the Human Research Ethics Committees at ECU (No.11543). The blood was drawn by phlebotomists into Vacutainer tubes containing EDTA anticoagulant (Becton-Dickinson, USA), after discarding the first 2 mL to avoid epithelial contamination.

Spiking experiments

For spiking experiments, in order to mimic the low numbers of CTCs commonly present in melanoma patients, 50 x CellTracker-stained melanoma cells derived from either A2058 or SKMEL5 cell cultures were manually counted and picked with a pipette under the microscope and collected cells were spiked into 8 mL of blood, in triplicate experiments. Then, red blood cells were lysed using red blood cell (RBC) lysis buffer (140 mM NH_4Cl, 17 mM Tris, pH 7.65) at a 1:10 vol/vol ratio for 5 min at room temperature with continuous gentle mixing. The lysed RBCs were removed after centrifugation at 300 g for 10 min, and the nucleated cell fraction was washed twice with 20 mL of PBS before resuspension into 16 mL (0.5X concentration) of a PBS solution containing 0.5% bovine serum albumin (0.5% BSA-PBS) to prevent non-specific adsorption and bubble formation during processing. Nucleated cells from blood were processed through the spiral microfluidic devices using the three microfluidic approaches: single Slanted (1X Slanted), single A5 and double Slanted (2X Slanted).

Determination of the recovery rate of melanoma cells spiked into blood and isolated using the microfluidic devices

Prior to sample processing, the biochips were washed with ethanol 70% and PBS before being primed with PBS/0.5% BSA using a syringe pump (PHD 2000, Harvard Apparatus, USA) for around 2 min at a flow rate of 1 mL min^{-1} for each solution. For isolation of melanoma cells, the processed blood samples containing spiked melanoma cells were placed in a 20 mL syringe (20 mL Luer-Lok, BD™, USA) and pumped through the device using a syringe pump connected to the microchannel device with flexible Tygon® tubing (Cole-Parmer, USA) (Figure 15).
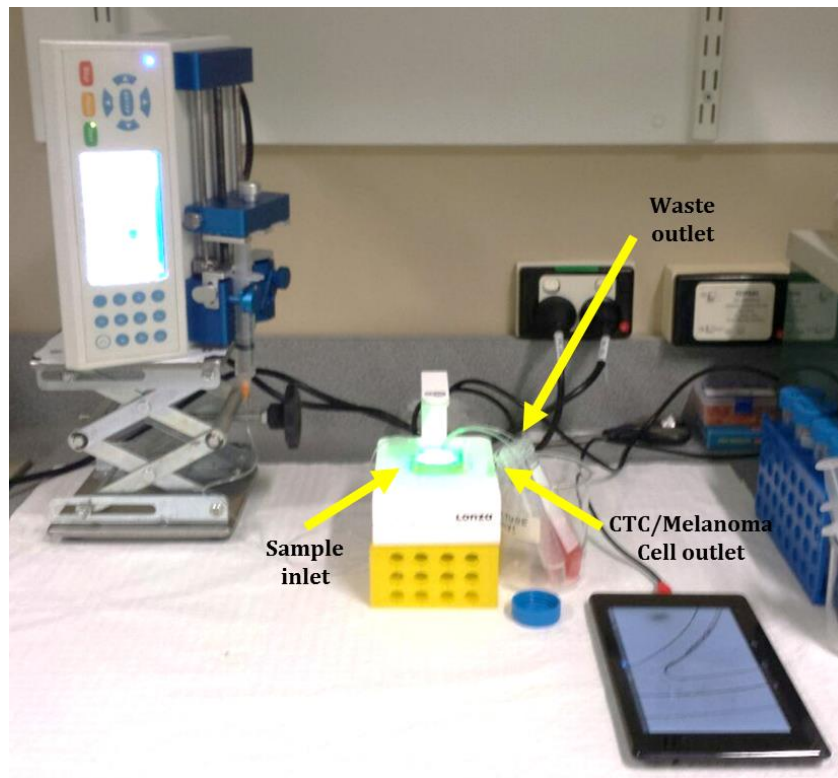
Figure 15. The workstation setup for melanoma cell or CTC separation. The blood after erythrolysis is pumped through the microfluidic device using a syringe pump.

As recommended in literature[11, 199], the flow rate for the input flow of the Slanted chip was 1700 µL min^{-1}. For the A5 spiral microfluidic device, a flow rate of 750 µL min^{-1} was used for the sheath inlet and 100 µL min^{-1} for the blood inlet. 0.5% BSA in PBS buffer was used for the sheath inlet in the experiments with the A5 microfluidic device[11, 221].

After processing the sample through 1X Slanted, A5 alone, or 2X Slanted, cells were collected from two outlets: one containing the recovered melanoma cells (CTC outlet) and the other containing the remaining white blood cells (waste outlet) (Figure 10 and 11). For the 2X Slanted approach, the CTC outlet sample, retrieved after processing through Slanted the first time, was resuspended in 6 mL of 0.5% BSA/PBS, changed into a syringe and pumped directly into the inlet of the Slanted chip using the conditions mentioned previously.

In order to determine the recovery rates, the cellular fraction from the CTC outlet was evaluated and counted for each experiment. For this, cells in the CTC fraction were separated from the supernatant by centrifugation at 500 g for 5 min. The cell pellet was resuspended and transferred to a 12-well plate (Greiner Bio-One, Austria). Using the NIS-Elements High Content Analysis software, version 4.2 using an inverted fluorescent

microscope (Eclipse Ti-E, Nikon®, Japan), cells were identified individually by studying both their morphology, and their CellTracker™ staining pattern to allow their correct identification as a spiked melanoma cell. A TRITC filter with set excitation and emission (Ex/Em) wavelengths of 555/607 nm, was used for red fluorescence identification.

The recovery rate for each experiment was determined as the number of red-labelled cells recovered, divided by the number of spiked cells per experiment.

Determination of the purity of the enriched fraction

In order to determine the purity of the recovered fraction, 8 mL of blood from healthy donors was run in triplicate through 1X Slanted, A5 and 2X Slanted, counting the WBC content with a Neubauer chamber (Hawksley, England), before and after the microfluidic isolation. For this, 10μL of a previous dilution of the enriched fraction containing the isolated melanoma cells, mixed 1:1 in Trypan Blue (Sigma, USA) was placed in the chamber. Total cells present in the four main corner squares were counted. Sample concentration was calculated as:

$$\frac{number\ of\ cells\ x\ 10^4\ x\ dilution\ factor}{number\ of\ squares} =\ total\ cells/mL$$

For the 2X Slanted approach, WBCs content was determined before, after one round and after two rounds. WBCs counts were log10 transformed and depletion rates were calculated by comparing the total number of cells after microfluidic processing to the initial WBC count.

Statistical analysis

To test whether the data was approximately normally distributed, a Shapiro-Wilk's test was used (p>0.05). One-way ANOVA was used to determine if it exists an overall difference between the groups analysed and Tukey post-hoc analysis was used to determine if the efficiency of the Slanted device to deplete WBCs from the total after 2X Slanted enrichment of control samples in particular, was significant. These analyses were performed using Microsoft Excel, SPSS Statistical software (version 22.0) and GraphPad Prism (version 5.0). Statistical significance was reached with a P <0.05.

4.2 Aim 2. To detect CTCs from metastatic melanoma patients enriched by the 2X Slanted device, using an optimised immunostaining protocol.

4.2.1 Experimental design and Methods

In order to confirm that the 2X Slanted method was able to isolate CTCs from metastatic melanoma patients, an optimised multimarker immunostaining assay was developed that included melanocyte/melanoma-specific cell surface markers and intracellular markers. To ensure that the majority of melanoma CTCs isolated by this device were successfully transferred onto glass slides for further immunostaining detection, the cytospin and immunostaining processes were optimised prior to processing of blood samples from metastatic melanoma patients. The steps followed for the enrichment and detection of melanoma CTCs from the blood of metastatic melanoma patients are indicated in the schematic below (Figure 16).
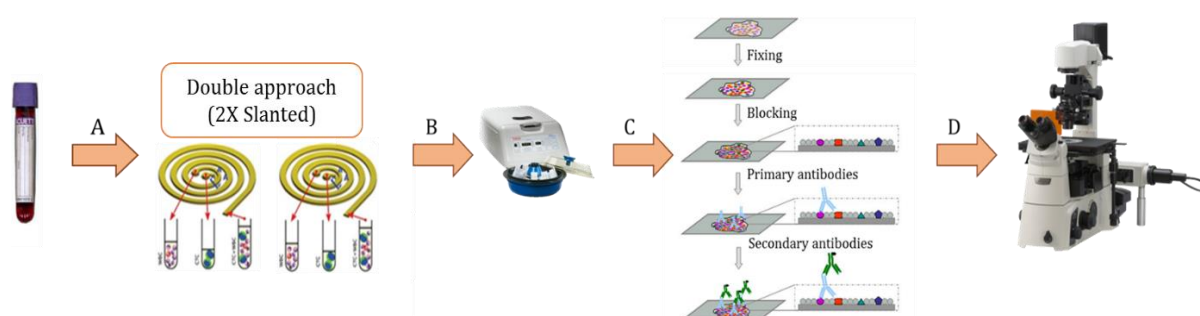
Figure 16. Flowchart of CTC enrichment and detection procedures. The processed blood from the melanoma patients was run through the 2X Slanted microfluidic device for CTC enrichment (A). The CTC output from the microfluidic enrichment was transferred onto slides by centrifugation (B) for optimisation of the subsequent immunostaining process (C). Finally, the CTCs were identified using an automated fluorescence microscope (D).

Cell lines and cell culture

A2058 melanoma cell line was used in the cytospin and staining optimisation processes. This melanoma cell line was obtained from the American Type Culture Collection (ATCC, USA).

WBCs isolation from healthy volunteers

Healthy donors provided signed consent forms, previously approved by the Human Research Ethics Committees at ECU (No.11543). The blood was drawn by phlebotomists

into Vacutainer tubes containing EDTA anticoagulant (Becton-Dickinson, USA), after discarding the first 2 mL to avoid epithelial contamination.

Then, red blood cells were lysed using red blood cell (RBC) lysis buffer at a 1:10 vol/vol ratio for 5 min at room temperature with continuous gentle mixing. The lysed RBCs were removed after centrifugation at 300 g for 10 min and the nucleated cell fraction was washed twice with 20 mL of PBS before resuspension into 10 mL PBS. Cells were then counted using a Vi-CELL XR cell counter (Beckman Coulter, USA) before proceeding with the spiking experiments.

Cytospin optimisation

In order to confirm that the cells enriched by the 2X Slanted device are entirely transferred onto glass slides, the ability of the cytospin to improve recovery of spiked cells was tested. For this, and for the following protocol described in section 4.1.1, 50 cells from the melanoma cell line A2058 were stained with CellTracker™ and mixed with approximately 5×10^3 WBCs isolated from a healthy control. The cells were pelleted and carefully resuspended in a fixing solution of 4% PFA for 10 min at room temperature. Thereafter, cells were transferred into a cytofunnel (Shandon™ Single Cytofunnel™ with Brown Filter Cards, Thermo Fisher Scientific, USA) precoated with PBS supplemented with 0.5% BSA (0.5% BSA /PBS), after washing the tube. Cells were cytospun onto glass slides (Cytospin™ 4, Thermo Fisher Scientific, USA; Figure 17) for 5 min, at medium acceleration, and different centrifugation speeds: 1000, 1300, 1600, and 2000 rpm to identify the optimal centrifugation speed required. Finally, cells were stained with DAPI (4',6-diamidino-2-phenylindole) and mounted using ProLong® Gold Antifade Mountant with DAPI reagent (Thermo Fisher Scientific, USA). The slides were stored at 4°C until analysis by microscopy. Slides were scanned using an automated inverted fluorescent microscope (Eclipse Ti-E, Nikon®, Japan; Figure 18), and analysed using the NIS-Elements High Content Analysis software, version 4.2. In order to be qualified as a spiked A2058 cell, the cell needed to have a positive signal for the nuclear DAPI staining and also be positive for the CellTracker™ Red dye. The speed that offered the best recovery, was tested in triplicate in order to ensure consistency.

In order to study the recovery rate after microfluidic enrichment followed by the cytospin, 50 x A2058 CellTracker™ cells were spiked in triplicate experiments into 8 mL

of whole blood from healthy donors. After treating the blood plus melanoma cells with lysis buffer and processing the sample through the 2X Slanted device as explained in section 4.1.1, the enriched fraction was cytospun using the speed 2000 rpm as this provided the highest recoveries without affecting the cell morphology. The number of recovered cells in each sample was analysed as described in the previous paragraph.

Figure 17. Cytospin 4® centrifuge used in transferring cells onto slides.

Optimising the detection of cells processed through the microfluidic device

Previous studies in our laboratory have described three melanocyte/melanoma-specific markers highly expressed in melanoma cell lines. These markers (gp100, Melan-A, s100, and MCSP) were previously utilised in a multimarker approach to identify melanoma CTCs after immunomagnetic enrichment. In order to test the effectiveness of this multimarker immunostaining approach in detecting melanoma cells processed through the cytospin, 50 x A2058 cells and approximately $5x10^3$ WBCs isolated from healthy blood were mixed, pelleted and carefully resuspended in 4% PFA for 10 min at room temperature. Then, cells were cytospun as previously detailed (Cytospin™ 4, Thermo Fisher Scientific, USA; Figure 17) for 5 min, at medium acceleration, and 2000 rpm. Cells were again fixed with 4% PFA for 10 mins and incubated in a blocking buffer containing 10% NDS, 3% BSA and 0.2% Triton X-100 (Sigma-Aldrich, USA) in PBS (10%NDS/3%BSA/0.2%TX-PBS) for 15 mins. Cells were then incubated in blocking buffer for 1 hour at room temperature, containing the multimarker panel:

- Three internal markers (referred in this document as 'MEL-staining'): anti-gp100 antibody (clone EPR4864, Abcam), anti-Melan-A/MART1 antibody (clone EP1422Y, Abcam), and anti-s100 (EP1576Y, Abcam).
- One surface marker: anti-MCSP antibody conjugated to Alexa Fluor® 647 dye (MCSP-647; clone 9.2.27, BD Pharmingen).
- One leukocyte-specific marker: anti-CD45 antibody conjugated to Phycoerythrin (CD45-PE; clone HI30, BD Pharmingen).
- (See Table 6 for antibody dilution information).

After incubation, cells were washed three times with 0.2% TX-PBS solution, and incubated in blocking buffer with a secondary donkey anti-rabbit IgG antibody conjugated to Alexa Fluor® 488 dye (R488; Abcam) for internal marker staining. Finally, cells were stained with DAPI and mounted using ProLong® Gold Antifade Mountant with DAPI reagent (Thermo Fisher Scientific, USA). Once immunostaining was completed, slides were stored at 4°C.

Slides were scanned using an automated inverted fluorescent microscope (Eclipse Ti-E, Nikon®, Japan; Figure 18), and analysed using the NIS-Elements High Content Analysis software, version 4.2.

Internal markers ('MEL- staining') were identified using a FITC filter with set excitation and emission (Ex/Em) wavelengths of 470/535 nm with an exposure time of 700 ms. The signal produced by the cell membrane MCSP-647 dye was identified using a Cy5 filter (Ex/Em = 640/720 nm) with an exposure time of 1 s. On the other side, CD45-PE stained leukocytes were identified using a TRITC filter (Ex/Em = 555/607 nm) with an exposure time of 500 ms. Nuclear staining was identified with a DAPI filter (Ex/Em = 395/460 nm) with an exposure time of 200 ms.

In order to be qualified as A2058 melanoma cell, the cell needed to have positive expression for the nuclear DAPI staining and also be positive for either the internal melanoma markers ('MEL-staining') or MSCP staining, but negative for the CD45 leukocyte-specific marker.

Furthermore, the recovery rate of the whole process (Slanted enrichment, cytospin and immunostaining) was studied by spiking 50 cells in triplicate experiments into 8 mL of

blood from healthy donors. After treating whole blood with RBC lysis buffer and processing the sample through the 2X Slanted device as explained in section 4.1.1, the enriched fraction was cytospun and stained, as described in the above paragraph.

Patients and blood collection

Blood from 10 metastatic melanoma patients, collected prior to clinical treatment with targeted inhibitors or immunotherapies, was included in this study (Table 5). Healthy volunteers and melanoma patients signed consent forms previously approved by the Human Research Ethics Committees at ECU (No.11543) and Sir Charles Gairdner Hospital (SCGH, No. 2013-246). The blood was drawn by phlebotomists into one 8 mL Vacutainer tube containing EDTA anticoagulant (Becton-Dickinson, USA), after discarding the first 2 mL to avoid epithelial contamination.

Table 5. Demographic information of metastatic melanoma patients.

PATIENTS' CHARACTERISTICS		
	n	*% of total*
Total patients enrolled		
	10	
Age at enrolment (years)		
Median	68	
Range	46 - 78	
Gender		
Male	6	60%
Female	4	40%

CTC enrichment using the 2X Slanted enrichment

An EDTA tube containing 8 mL of blood from a total of 10 metastatic melanoma patients and healthy volunteers was used for analysis. Blood samples were processed, within 24 hours after collection. Whole blood was treated with RBC lysis buffer and washed twice with 20 mL of PBS before resuspension in 16 mL (0.5X concentration) of 0.5% BSA/PBS. Once the blood had been processed and resuspended into PBS/0.5% BSA, the 16 mL nucleated fraction derived from 8 mL of blood was processed through the Slanted using a flow rate of 1700 μL min^{-1}. The cellular fraction of the CTC outlet from the first round was resuspended in 6 mL of 0.5% BSA/PBS solution and processed again through the same Slanted device using an input flow rate of 1700 μL min^{-1}.

CTC detection from the enriched fraction

The cells recovered in the CTC outlet after processing the sample twice through the Slanted microfluidic device, were immediately pelleted and fixed by 10 min incubation with 4% PFA. After that, cells were cytospun (Cytospin™ 4, Thermo Fisher Scientific) onto glass slides at 2000 rpm for 5 mins at medium acceleration. Cells were again fixed with 4% PFA for 10 mins and incubated in a blocking buffer (10%NDS/3%BSA/0.2%TX-PBS) for 15 mins. Cells were then incubated in blocking buffer for 1 hour at room temperature, containing the multimarker panel:

- Three internal markers ('MEL-staining'): anti-gp100 antibody (clone EPR4864, Abcam), anti-Melan-A/MART1 antibody (clone EP1422Y, Abcam), and anti-s100 (EP1576Y, Abcam).
- One surface marker: anti-MCSP antibody conjugated to Alexa Fluor® 647 dye (MCSP-647; clone 9.2.27, BD Pharmingen).
- One leukocyte-specific marker: anti-CD45 antibody conjugated to Phycoerythrin (CD45-PE; clone HI30, BD Pharmingen).
- (See Table 6 for antibody dilution information).

After incubation, cells were washed three times with 0.2% TX-PBS solution, and incubated in blocking buffer with a secondary donkey anti-rabbit IgG antibody conjugated to Alexa Fluor® 488 dye (R488; Abcam) for the internal markers staining. Finally, cells were stained with DAPI and mounted using ProLong® Gold Antifade Mountant with DAPI reagent (Thermo Fisher Scientific, USA). Once immunostaining was completed, slides were stored at 4°C.

Slides were scanned using an automated inverted fluorescent microscope (Eclipse Ti-E, Nikon®, Japan; Figure 18), and analysed using the NIS-Elements High Content Analysis software, version 4.2 using the same fluorescent filters and exposure times as indicated above.
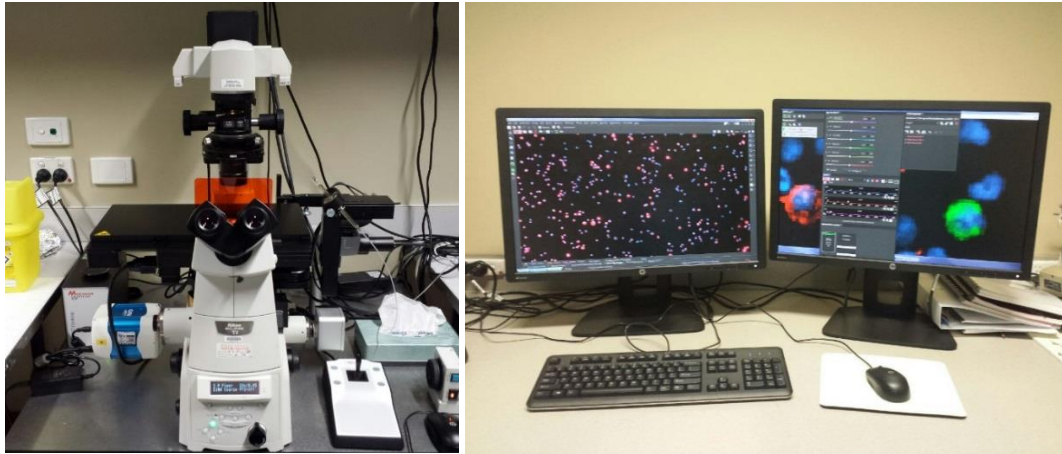
Figure 18. Eclipse Ti-E, Nikon® fluorescent automated microscope and software used in CTC quantification and analysis.

Additionally, cell sizes were also measured with this software. Background subtraction parameters for each marker derived from the immunostaining of A2058 melanoma cells spiked into WBC fractions, were stringently applied to all stained slides of CTC samples from patients. For this, the fluorescent intensity cut-offs applied in the analysis were: 2000 LUTs for FITC filter, 300 LUTs for Cy5 filter, 2000 LUTs for TRITC filter, and 1500 LUTs for DAPI filter.

In order to be identified as a CTC, the cell needed to have positive expression for nuclear DAPI staining and also be positive for either the internal melanoma markers ('MEL-staining') or MSCP staining, but negative for the CD45 leukocyte-specific marker.

Table 6. Antibody information (Aim 2).

Antibody	Antigen Location	Vendor	Dilution used	Notes
gp100	Cytosol	Abcam Clone EPR4864	1/50	Included in the Multimarker Panel
MART1	Cytosol	Abcam Clone EP1422Y	1/50	Included in the Multimarker Panel
S-100	Cytosol	Abcam Clone EP1576Y	1/500	Included in the Multimarker Panel
MCSP-AF647	Membrane	BD Pharmingen™ Clone 9.2.27	1/200	Included in the Multimarker Panel
CD45-PE	Membrane	BD Pharmingen™ Clone HI30	1/20	Leukocyte-specific antibody
Donkey anti-rabbit-R488	n/a	Abcam ab150065	1/500	Anti-rabbit Secondary Polyclonal Ab

Determination of the purity of the enriched fraction

In order to determine the purity of the recovered fraction after using the 2X Slanted approach, WBC content was determined in five patients, before and after one round of enrichment by counting cells in a Neubauer chamber (Hawksley, England). For this, 10µL of a previous dilution of the enriched fraction containing the isolated melanoma cells were mixed 1:1 in Trypan Blue (Sigma, USA) was placed in the chamber. Total cells present in the four main corner squares were counted. Sample concentration was calculated as:

$$\frac{number\ of\ cells\ x\ 10^4\ x\ dilution\ factor}{number\ of\ squares} = total\ cells/mL$$

After the second round of enrichment, WBC count was performed on the immunostained slides using an inverted fluorescent microscope equipped with the NIS-Elements High Content Analysis software, version 4.2. This software allows identification and quantification of single DAPI stained circular profiles with a set maximum area of 350 µm². WBCs counts were log10 transformed and depletion rates were calculated by comparing the total number of cells after microfluidic processing to the initial WBC count.

Statistical analysis

To test whether the data was approximately normally distributed, a Shapiro-Wilk's test ($p>0.05$) was used. One-way ANOVA was used to determine if it exists an overall difference between the groups analysed and Tukey post-hoc analysis was used to determine if the efficiency of the Slanted device to deplete WBCs from the total after 2X Slanted enrichment of melanoma patient samples in particular, was significant. These analyses were performed using Microsoft Excel, SPSS Statistical software (version 22.0) and GraphPad Prism (version 5.0). Statistical significance was reached with a $P <0.05$.

4.3 Aim 3. To test additional cellular markers that can be used in immunostaining assays for optimisation of detection and phenotypic characterisation of heterogeneous melanoma CTCs.

4.3.1 Experimental design and Methods

Figure 19 shows the main steps followed in order to determine melanoma markers are expressed in melanoma cells and potentially expressed by CTCs from melanoma patients.
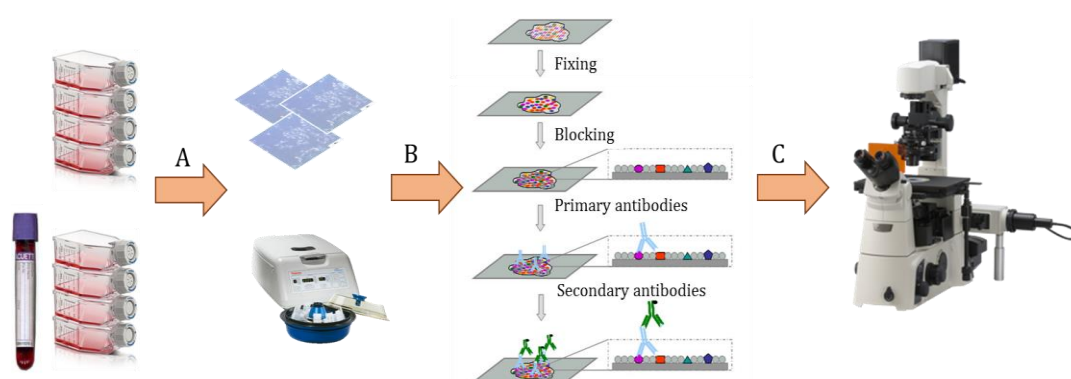
Figure 19. Overview of the process for all staining experiments. Melanoma cells were either seeded on coverslips or mixed with WBCs and cytospun onto glass slides (A). The cells were stained with the chosen biomarkers by immunocytochemistry (B). Finally, automated fluorescence scanning allowed the analysis of the immunostained cells with different markers (C).

Immunocytochemical staining of additional melanoma cell markers most commonly expressed in melanoma cell line cells for optimal melanoma cell/CTC detection

The optimisation of the immunostaining protocol by the addition of supplementary melanocyte/melanoma markers to the staining protocol for detection of an increased number of melanoma cells was completed using cells derived from melanoma cell lines. The expression of three additional markers (Vimentin, RANK and ABCB5) was assessed in A2058, WM164 and SKMEL5 melanoma cell lines in order to identify additional markers expressed in all or in the majority of the melanoma cells derived from cell lines, so as to best identify additional markers that can be used to stain and identify heterogeneous melanoma cells.

Firstly, the optimal concentration of the antibodies was assessed by determining the concentration that provided optimal staining with minimal background staining using A2058 cells cytospun and stained on cover slips. The optimal concentration was then used to stain another two cell lines to confirm the expression pattern of the marker in multiple melanoma cell lines.

Cell lines and cell culture

SKMEL5, A2058 and WM164 melanoma cell lines were used. The melanoma cell line WM164 was kindly provided by Professor Meenhard Herlyn from The Wistar Institute (Philadelphia, USA) and A2058 and SKMEL5 melanoma cell lines were obtained from the American Type Culture Collection (ATCC, USA) (Figure 20).
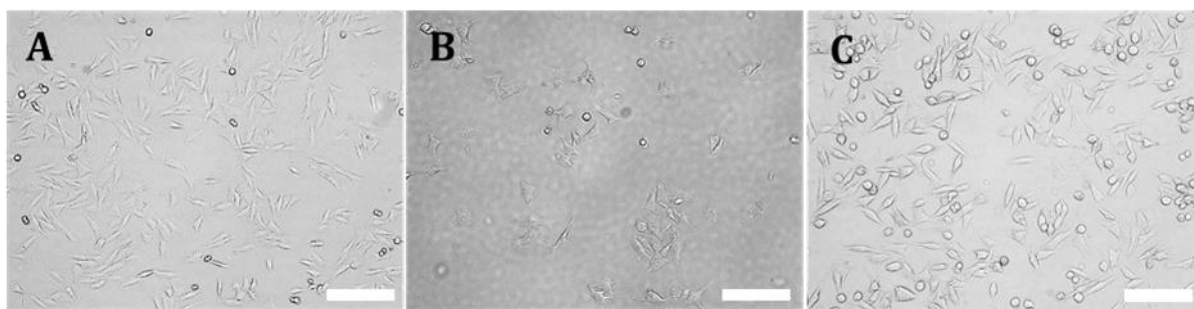
Figure 20. Microscopic bright field caption of A2058 cells (A), WM164 cells (B), and SKMEL5 cells (C) in culture. All images taken at 10x magnification. Scale Bar: 200 μm.

Cells were seeded on sterile square glass cover slips in 12-well cell culture plates (Greiner Bio-One, Austria) and incubated for 24 hours in high-glucose DMEM (Invitrogen, USA) supplemented with 10% FBS (Invitrogen, USA) and maintained at 37 °C in a humidified atmosphere containing 5% (v/v) CO_2.

WBCs isolation from healthy volunteers

Healthy donors provided signed consent forms, previously approved by the Human Research Ethics Committees at ECU (No.11543). The blood was drawn by phlebotomists into Vacutainer tubes containing EDTA anticoagulant (Becton-Dickinson, USA), after discarding the first 2 mL to avoid epithelial contamination.

Red blood cells were lysed using red blood cell (RBC) lysis buffer at a 1:10 vol/vol ratio for 5 min at room temperature with continuous gentle mixing. The lysed RBCs were removed after centrifugation at 300 g for 10 min and the nucleated cell fraction was washed twice with 20 mL of PBS before resuspension into 10 mL PBS. Cells were then counted using a Vi-CELL XR cell counter (Beckman Coulter, USA) before proceeding with the spiking experiments.

Immunofluorescent staining of the melanoma cell lines

Attached cells were washed with PBS and fixed with 4% paraformaldehyde (PFA) for 10 minutes at room temperature and then washed 3 times with PBS. Cell surface and intracellular markers were stained using different immunostaining protocols, as described below.

RANK cell surface marker was stained by incubating the cells with anti-RANK mouse antibody (clone 80704, R&D Systems) diluted in 3% BSA/PBS for one hour at room temperature. Antibody dilutions of 1/20, 1/50, and 1/100 were tested.

Subsequently, melanoma cells were washed 3 times with PBS and incubated with a secondary donkey anti-mouse IgG polyclonal antibody conjugated to Alexa Fluor® 488 dye (M488; Abcam) diluted 1/500 in 3%BSA/PBS and kept for 15 min at room temperature in the dark.

Intracellular markers were stained after permeabilising the cells with 0.2% TX-PBS for 10 min subsequent to fixing of the cells with 4% PFA solution for 10 min. Cells were then incubated with primary antibodies diluted in 3% BSA/0.2%TX-PBS solution for one hour at room temperature:

- Anti-Vimentin antibody conjugated to Alexa Fluor® 647 dye (VIM-647; clone V9, Abcam) was tested using dilutions of 1/1000, 1/2000, and 1/5000.
- Anti-ABCB5 mouse antibody (clone 5H3C6, Abcam) was tested using 1/20, 1/50, and 1/100 dilutions.

For the ABCB5 marker, melanoma cells were washed 3 times with 0.2%TX-PBS and incubated with a donkey anti-mouse IgG polyclonal antibody conjugated to Alexa Fluor® 488 dye (M488; Abcam) diluted 1/500 in 3% BSA/0.2%TX-PBS and kept for 15 min at room temperature in the dark (See Table 7).

Lastly, after the melanoma cells were stained for either cell surface or intracellular markers and secondary antibodies, cells were mounted with Prolong® Gold antifade reagent with DAPI mounting media (Thermo Fisher Scientific, USA) for nuclear staining and preservation of the cells. The slides were kept at 4 °C until their analysis was performed.

Slides stained with RANK and ABCB5 were scanned using a fluorescence microscope (BX51, OLYMPUS, Japan) with a FITC and DAPI filter. Negative controls that involve incubating the sample with secondary antibodies only were performed for each marker and in each cell line in order to detect the background level of expression. The expression analysis was performed using the DPController software, version 3.3.1.292 and background subtraction was performed for each marker and cell line by adjusting the

intensities and exposures as per matched negative controls. On the other hand, slides stained with Vimentin were scanned using an automated inverted fluorescent microscope (Eclipse Ti-E, Nikon®, Japan; Figure 18), and analysed.

Negative controls that involve incubating the sample with an isotype matched antibody labelled with Alexa Fluor® 647 dye at the same concentration as the Vimentin antibody were performed for each cell line in order to detect any background non-specific signal. Background subtraction was performed for each cell line and marker Using the NIS-Elements High Content Analysis software, version 4.2 using the Cy5 filter to identify the marker staining and the DAPI filter for nuclear recognition, background subtraction parameters were adjusted for each marker by altering the fluorescent intensity cut-offs (LUTs) as per matched negative controls. After background subtraction, signal for each fluorescent dye was also adjusted to enhance the staining for each marker.

Table 7. Antibody information (Aim 3).

Antibody	Antigen Location	Vendor	Dilutions tested	Dilution used	Notes
RANK	Membrane	R&D Systems Clone 80704	1/20 1/50 1/100	1/20	Additional Ab tested
Vimentin-AF647	Cytosol	Abcam Clone V9	1/1000 1/2000 1/5000	1/1000	Additional Ab tested
ABCB5	Internal Membrane	Abcam Clone 5H3C6	1/20 1/50 1/100	1/20	Additional Ab tested
ABCB5	External Membrane	1D12 n/a (donated)	1/550 1/275 1/100	1/275	Tested for TSA
MCSP	Membrane	BD Pharmingen™ 554275	n/a	1/500	Positive control for TSA
CD45-PE	Membrane	BD Pharmingen™ Clone HI30	n/a	1/20	Leukocyte-specific antibody
Donkey anti-mouse-AF488	n/a	Abcam Ab150109	n/a	1/500	Secondary Polyclonal Ab

TSA: Tyramide Signal Amplification

Optimised immunofluorescent staining of A2058 melanoma cells spiked into WBCs

The specificity of the selected markers was next assessed by determining their expression patterns when A2058 melanoma cell line cells were spiked into WBCs isolated from the blood of healthy donors. This was required to ensure that the WBCs did not express the melanoma markers and to ensure that the staining remained optimal when melanoma cells were spiked into WBCs.

For this, melanoma cells of the A2058 cell line were spiked into WBCs from healthy volunteers. Spiking and whole blood RBCs lysis were performed as previously described in section 4.1.1. Approximately $5x10^3$ A2058 melanoma cells and 10^5 WBCs were mixed, pelleted and fixed by resuspending them in 2% PFA for 10 min. Then, cells were transferred onto glass slides using the Cytospin 4® centrifuge (Thermo Fisher Scientific, USA; Figure 17) for 5 min, at 2000 rpm with medium acceleration. Attached cells were then fixed again with 4% PFA for 10 min and washed twice with PBS in a coupling jar.

After the cells were cytospun and fixed onto glass slides, cells were blocked with a blocking buffer containing 10% normal donkey serum (NDS), 3% bovine serum albumin (BSA) diluted in PBS or in 0.2% TX-PBS for internal markers staining. Subsequently, cells were incubated with different antibodies at their optimal dilutions (Vimentin: 1/1000; RANK: 1/20 and ABCB5: 1/20), in blocking buffer for one hour at room temperature. Then, cells were washed 3 times with PBS or 0.2% TX-PBS (for intracellular markers) and incubated for 15 min at room temperature in the dark with a donkey anti-mouse IgG polyclonal antibody conjugated to Alexa Fluor® 488 dye (M488; Abcam) diluted 1/500 in blocking buffer. In addition, a leucocyte marker, anti-CD45 antibody conjugated to Phycoerythrin (PE) (CD45-PE; clone HI30, BD Pharmingen) was used to specifically stain the leucocytes at 1/20 dilution. After washing again 3 times with PBS or 0.2% TX-PBS (for intracellular markers), cells were mounted with Prolong® Gold antifade reagent with DAPI mounting media (Thermo Fisher Scientific, USA) for nuclear staining and preservation of the cells.

The slides were kept at 4 °C until their analysis was performed. Slides were scanned using an automated inverted fluorescent microscope (Eclipse Ti-E, Nikon®, Japan). Marker expression patterns were analysed using the NIS-Elements High Content Analysis software, version 4.2.

RANK and ABCB5 markers were identified using a FITC filter with set excitation and emission (Ex/Em) wavelengths of 470/535 nm with an exposure time of 700 ms. The signal produced by VIM-647 expression was identified using a Cy5 filter (Ex/Em = 640/720 nm) with an exposure time of 1 s. On the other side, CD45-PE stained leukocytes were identified using a TRITC filter (Ex/Em = 555/607 nm) with an exposure time of 500

ms. Nuclear staining was identified with a DAPI filter (Ex/Em = 395/460 nm) with an exposure time of 200 ms.

In order to be counted as appropriately stained, the cell needed to have positive expression for the nuclear DAPI staining and also be positive for the melanoma marker tested (Vimentin, RANK or ABCB5), but negative for the CD45 leukocyte-specific marker.

Background subtraction parameters were adjusted for each marker by altering the fluorescent intensity cut-offs (LUTs). After background subtraction, signal for each fluorescent dye was also adjusted to enhance the staining for each marker.

Tyramide Signal Amplification (TSA)

In order to further enhance signal of markers that were weakly/intermittently expressed in melanoma cell lines, such as ABCB5, a tyramide signal amplification (TSA) methodology was tested (Figure 21).
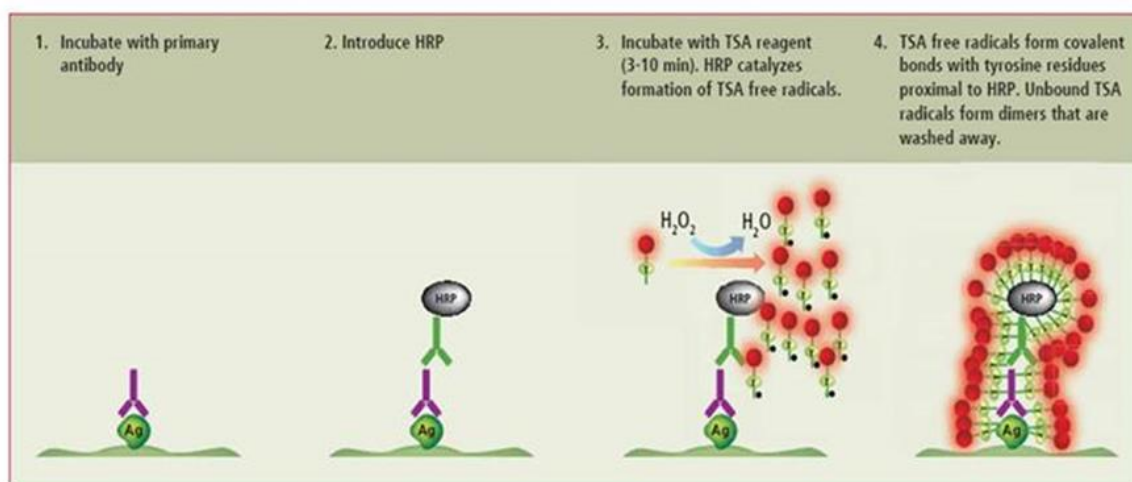
Figure 21. Tyramide Signal Amplification principle.

Since ABCB5 marker is commonly expressed on CTCs[170], and the ABCB5 staining protocol trialled above produced weak and suboptimal staining, we utilised a Tyramide Siganl Amplification (TSA) protocol to amplify the immunohistochemical staining signal of ABCB5. To interrogate, for the first time, the ability of this method to increase the signal of ABCB5 staining, an anti-ABCB5 antibody that binds to an epitope of the ABCB5 protein that is located in the external membrane of the cell was used, as this was identified previously as being commonly expressed on melanoma CTCs[170].

For this, A2058 cells were seeded on sterile square glass cover slips in 12-well cell culture plates (Greiner Bio-One, Austria) and incubated for 24 hours in DMEM (Invitrogen, USA) supplemented with 10% foetal bovine serum (FBS) (Invitrogen, USA) and maintained at 37 °C in a humidified atmosphere containing 5% (v/v) CO_2.

Attached cells were washed with PBS and fixed with 4% paraformaldehyde (PFA) for 10 minutes at room temperature and then washed 3 times with PBS. Cells were then blocked with a TBS blocking buffer (0.1 M Tris-HCl, 0.15 M NaCl, pH 7.5) supplemented with 3% BSA at room temperature for 15 min. Anti-ABCB5 mouse antibody (Clone 1D12) was then incubated for 1 hour at room temperature, diluted 1/275 in blocking buffer and the slides were washed three times in TBS-Tween washing buffer (0.1 M Tris-HCl, 0.15 M NaCl, pH 7.5, 0.05% Tween-20) for 5 min each under continuous shaking were performed. Incubation with anti-mouse antibody labelled with horseradish peroxidase (HRP; Perkin Elmer, USA) diluted 1/1000 in blocking buffer was performed for 30 min at room temperature. After washing again with washing buffer, the sample was incubated in TSA Plus Working Solution (Fluorescein; Perkin Elmer, USA) for 5 min. The sample was once again washed three times for 5 min each in continuous shaking before mounting with Prolong® Gold antifade reagent with DAPI mounting media (Thermo Fisher Scientific, USA) for nuclear staining and preservation of the cells. For this experiment, anti-MCSP antibody diluted 1/500 (BD Pharmingen) was included as a positive control since MCSP is highly expressed in the A2058 melanoma cell line[4]. Additionally, a negative control that involved incubating the sample with the secondary antibody only was performed in order to detect the background level of expression.

In order to test the specificity of the staining, A2058 melanoma cells were spiked into WBCs from healthy donors as detailed in section 4.1.1, processed and stained. For this, cells cytospun onto slides were fixed for 10 min with 4% PFA and washed three times with PBS. In order to quench the endogenous peroxidase activity of the blood cells, an incubation in 0.3% H_2O_2 in PBS for 20 min was performed. After washing again with PBS, cells were incubated for 1 hour at room temperature with anti-ABCB5 mouse antibody (Clone 1D12), diluted 1/275 in blocking buffer and washed three times in TBS-Tween washing buffer (0.1 M Tris-HCl, 0.15 M NaCl, pH 7.5, 0.05% Tween-20) for 5 min each under continuous shaking. Incubation with anti-mouse antibody labelled with horseradish peroxidase (HRP; Perkin Elmer, USA) diluted 1/1000 in blocking buffer was

performed for 30 min at room temperature. After washing again with washing buffer, the sample was incubated in TSA Plus Working Solution (Fluorescein; Perkin Elmer, USA) for 5 min. The sample was once again washed three times for 5 min each in continuous shaking before incubating the sample with a leucocyte marker, anti-CD45 antibody conjugated to Phycoerythrin (PE) (CD45-PE; clone HI30, BD Pharmingen at 1/20 dilution) to specifically stain the leucocytes. After washing again with washing buffer, cells were mounted with Prolong® Gold antifade reagent with DAPI mounting media (Thermo Fisher Scientific, USA) for nuclear staining and preservation of the cells. Additionally, anti-MCSP antibody diluted 1/500 (BD Pharmingen) was included as a positive control. Additionally, a negative control of mouse IgG1 isotype antibody (clone MOPC-21; Abcam, USA) alone was used to detect the any background non-specific signal.

Slides were kept at 4 °C until their analysis was performed. Slides were scanned using an automated inverted fluorescent microscope (Eclipse Ti-E, Nikon®, Japan), and analysed using the NIS-Elements High Content Analysis software, version 4.2 to measure the marker expression patterns. This software was used to scan across the slide using a FITC filter with set excitation and emission (Ex/Em) wavelengths of 470/535 nm with an exposure time of 100 ms or 700 ms to identify ABCB5 and MCSP expression; TRITC filter (Ex/Em = 555/607 nm) with an exposure time of 500 ms was used for the recognition of CD45-PE stained leukocytes; and nuclear staining was identified with a DAPI filter (Ex/Em = 395/460 nm) with an exposure time of 200 ms. In order to subtract the background expression, fluorescent intensity cut-offs were applied and adjusted for each marker, matching the negative controls values.

5. RESULTS

5.1 Aim 1. To measure the efficiency of three spiral microfluidic approaches to isolate differently sized melanoma cell lines spiked into healthy control blood.

5.1.1 Recovery rates using microfluidic devices

To assess the capacity of the spiral microfluidic devices to enrich and recover melanoma cells, 50 x CellTracker labelled cells from two cell lines, with different cell sizes (A2058 and SKMEL5), were spiked into 8 mL of blood donated by healthy volunteers and processed through 1X Slanted, A5 and 2X Slanted spiral microfluidic approaches.

As observed in Figure 22, the lowest recovery rate for both cell lines was found after processing the sample through the A5 chip, with an average of 33%. Conversely, the use of 1X Slanted provided the highest average recovery rate of more than 70% regardless of the cell size. The 2X Slanted enrichment caused an average recovery rate of 73.3% when spiking the small A2058 cells, and 56% when the larger SKMEL5 cells were spiked.

Interestingly, the average recovery rates for SKMEL5 cells were lower than for A2058 cells regardless of the enrichment approach used.
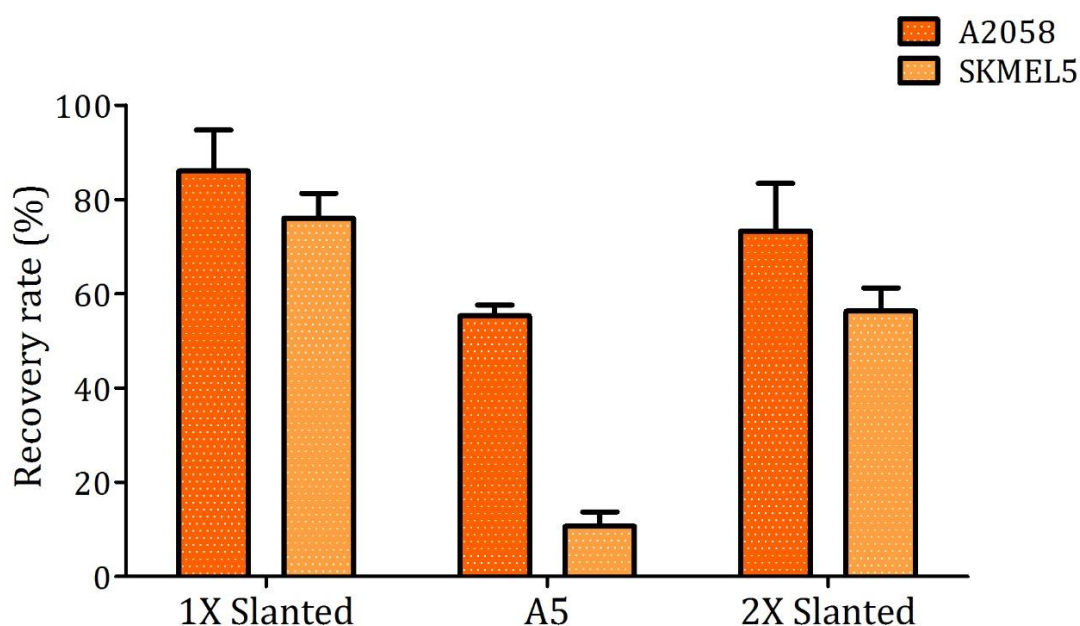
Figure 22. Recovery rates from the three enrichment procedures using 50 x spiked cells from two different cell lines with different cell sizes. Experiments were performed in triplicate using blood samples from healthy donors (n=3).

5.1.2 Purity analysis

To evaluate the purity of the enriched fractions, WBCs were counted in the sample prior to and after processing through the microfluidic chips.

Results showed that by running the sample through the 1X Slanted device, a 2 log reduction in WBCs was achieved (mean: 9.0×10^4; range: $0.56\text{-}1.45 \times 10^5$) relative to the initial WBC count (mean: 1.2×10^7; range: $0.8\text{-}1.62 \times 10^7$). Similarly, using the A5 device a 2 log reduction was achieved (mean: 4.3×10^5; range: $2.15\text{-}5.45 \times 10^5$) relative to the initial WBC count (mean: 1.6×10^7; range: $1.54\text{-}1.80 \times 10^7$) (Figure 23).

The need to achieve a higher purity in the enriched fraction, led us to add a second round of enrichment through the Slanted chip, referred to as double Slanted enrichment (2X Slanted). This approach offered the highest purity achieving a 3 log reduction in WBC counts (mean: 1.8×10^4; range: 6750-38250) relative to the initial amount of WBCs (mean: 1.4×10^7; range: $1.2\text{-}1.7 \times 10^7$) (Figure 23). Two rounds of enrichment through the Slanted, showed a significant depletion in WBCs in the enriched fraction (P<0.0001). In addition, these results show that after 1X Slanted, the recovery of A2058 melanoma cells drops to 86% and the WBC background results in 73.4% from the total. Although after 2X Slanted, the recovery of A2058 melanoma cells drops to 73%, the WBC background represents only 14.7% from the total, confirming the ability of this chip to reduce the WBC background without drastically impacting the recovery rates. Overall, the 2X Slanted protocol provided the best balance between recovery and WBC background reduction needed to implement downstream applications.
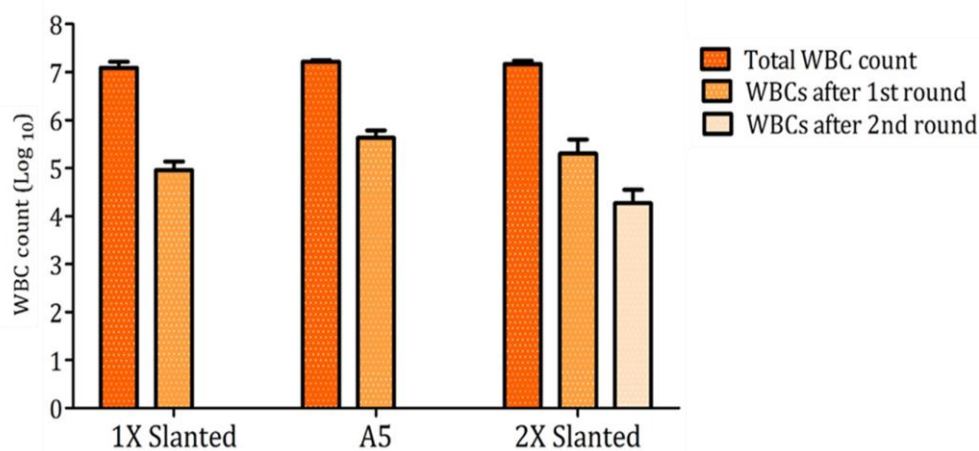
Figure 23. WBC counts in the blood of healthy donors (n=3) before and after one or two rounds of enrichment. Each experiment was performed in triplicate using blood samples from healthy donors (n=3). 2X Slanted enrichment showed significant depletion in the WBC count (p<0.0001).

5.2 Aim 2. To detect CTCs from metastatic melanoma patients enriched by the 2X Slanted device, using an optimised immunostaining protocol.

5.2.1 Cytospin optimisation

In order to confirm that the majority of melanoma cells are transferred onto glass slides using the cytospin centrifuge, 50 x A2058 cells stained with CellTracker™ and WBCs from healthy volunteers were cytospun at four different speeds. The majority of spiked cells were recovered when 2,000 rpm was used. To ensure consistency, this speed was tested in triplicate, and an average recovery rate of 94% was achieved (Figure 24).
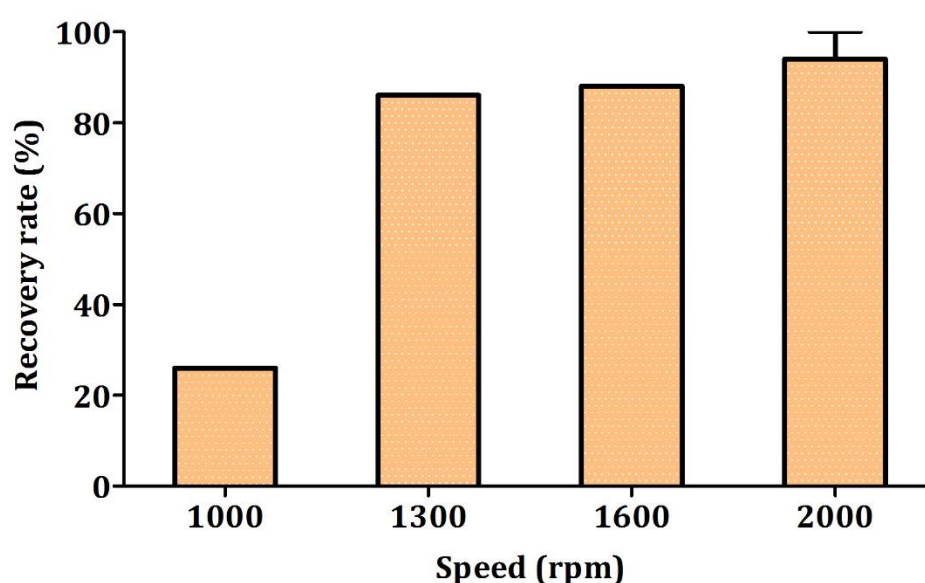
Figure 24. Recovery rates of 50 x A2058 cells labelled with CellTracker after centrifuging them at different speeds with the Cytospin centrifuge. 2000 rpm speed was tested in triplicate.

Finally, 50 x A2058 cells stained with Celltracker™, were spiked in triplicate into 8 mL of blood from healthy volunteers, RBCs were lysed, and the sample was processed twice through the 2X Slanted device prior to cytospinning the sample onto glass slides using a speed of 2000 rpm. Results showed an average overall (microfluidics plus cytospin) recovery rate of 58% spiked cells (Figure 25).

5.2.2 Staining optimisation

To ensure that the multimarker immunoassay, previously described in section 4.2.1, is effective in detecting melanoma cells that have been transferred onto glass slides using the cytospin centrifuge, 50 x A2058 cells were spiked in approximately 10^4 WBCs and cytospun at 2,000 rpm and stained with the multimarker panel in triplicate. Markers

included MCSP, a melanoma cell surface specific marker, together with a mixture of internal melanocytic markers, gp100 (glycoprotein 100), Melan-A, and s100 ('MEL-staining') in order to ensure detection of the majority of melanoma cells. Results showed an average recovery rate of 92% (Figure 25).

When the same experiment, using 50 x A2058 cells spiked into healthy blood was performed by conducting the entire process (2X Slanted processing, cytospin and multimarker immunostaining), the overall average recovery rate was 52% (ranging from 48 to 56%; Figure 25). Thus, the entire process of 2X Slanted resulted in a decrease in the number of recovered melanoma cells.
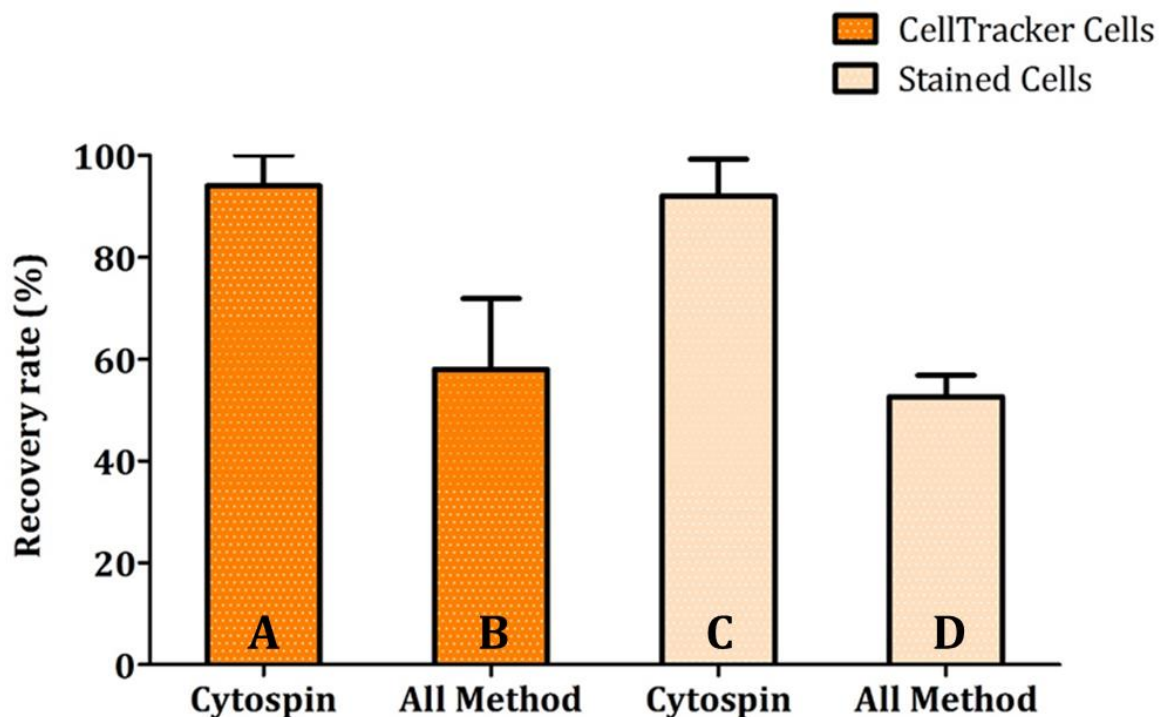
Figure 25. Recovery rates of 50 A2058 cells **A)** Stained with CellTracker® and directly transferred onto glass slides using Cytospin, **B)** Stained with Cell Tracker®, spiked into blood, processed through the 2X Slanted device and transferred onto glass slides using the Cytospin, **C)** Directly transferred onto glass slides using Cytospin and stained using the melanoma associated markers, and **D)** Spiked into blood, processed using the 2X Slanted device and transferred onto glass slides using the Cytospin prior to staining with the melanoma associated markers.

Interestingly, although the A2058 spiked cells are thought to be identical as they arise from a cell line, they showed different patterns of staining (Figure 26) in multiple experiments, with some cells being stained for only the internal set of markers (Figure 26, CELL 1), other cells for only the MCSP surface marker (Figure 26, CELL 2) and some cells were stained for both internal and surface markers (Figure 26, CELL 3).
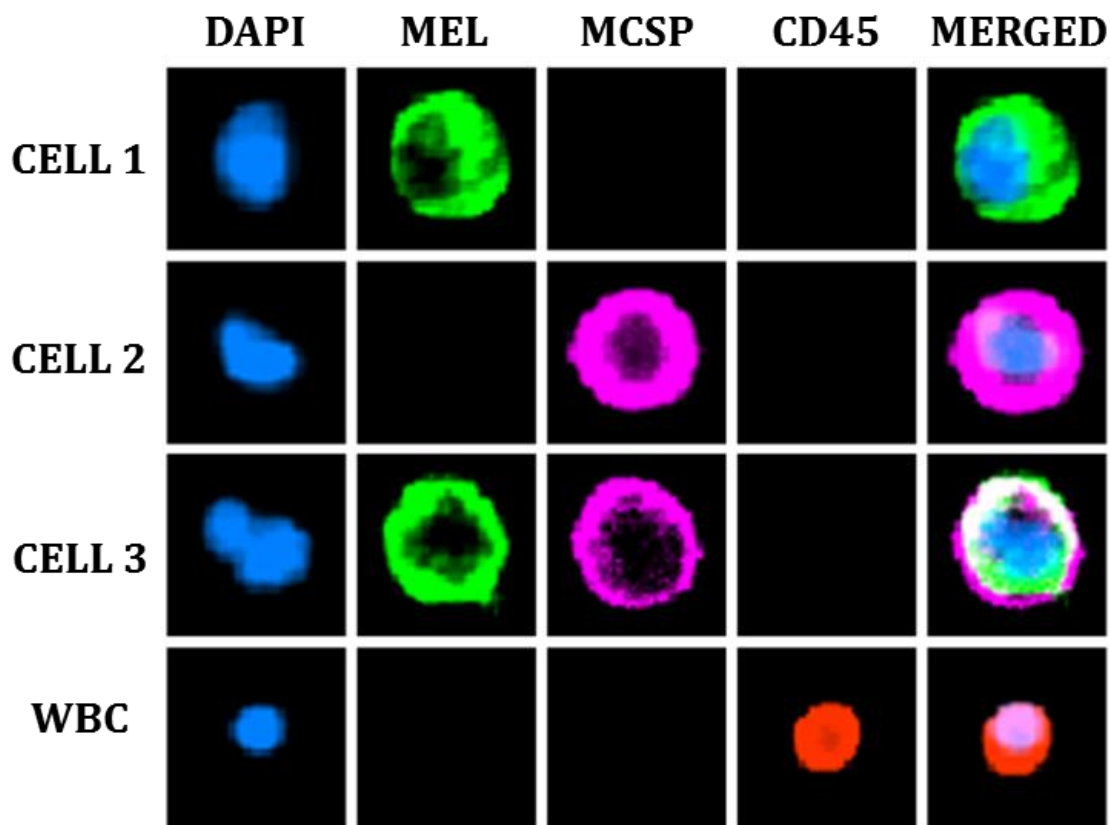
Figure 26. Microscopic images showing the differential expression of intracellular and cell surface markers in A2058 cells stained after 2X Slanted microfluidic enrichment. The immunostaining used to detect melanoma cells uses a combination of intracellular markers – 'MEL staining'- (gp100, MLANA and s100; AF488 -FITC- Shown here as green), and a surface marker (MCSP; AF467 -Cy5- Shown here as purple). DAPI (UV- Shown here as blue) was used as a nuclear stain and CD45 (PE-TRITC- Shown here as red) as a leukocyte-specific marker.

Results show that the majority of the detected cells were positive for internal and external markers (55%), more than a third expressed only the MCSP surface marker (39%) and only 6% of the detected cells were positive for the internal markers only. This results showed that combining numerous markers in the detection of these heterogeneous cells increases our ability to detect them. The use of different emission wavelengths to identify the different markers, with the internal markers (FITC) and cell surface markers (Alexa Fluor® 647) allowed the detection of this marker diversity.

5.2.3 CTCs isolated from the blood of melanoma patients

The above results showed the ability of the multimarker panel used in immunostaining to successfully detect melanoma cells that have been enriched with the 2X Slanted microfluidic device. In order to validate this enrichment (Aim 1) and detection procedure, blood samples from 10 metastatic melanoma patients were analysed. A total of 8 mL of

blood was treated with lysis buffer in order to deplete red blood cells. Then, the sample was processed through the Slanted microfluidic device using the 2X Slanted approach, the recovered cell fraction was cytospun and then immunostained with the multimarker panel described above.

True CTCs were identified by positive staining for intracellular markers ('MEL staining') or cell membrane MCSP as well as negative staining for the leukocyte-specific marker CD45 (Figure 27).

Using these enrichment and detection procedures, CTCs were effectively detected in the blood of 4 patients (40%). Two patients had 1 CTC (CELL 1 and 2), one patient had 3 CTCs (CELL 3-5) and the other was found with 4 CTCs (CELL 6-9) in 8 mL of blood (Figure 27). Interestingly, all detected CTCs were positive only for the combination of intracellular markers ('MEL staining' -gp100, Melan-A, and s100-) and no CTC expressing the cell membrane marker MCSP was found in any of these patients. Size analyses confirmed that CTCs were larger than the majority of white blood cells, exhibiting an average cell size of 19 μm (range: 13–24 μm), while WBC cell sizes were on average 10 μm (range: 8–12 μm). All detected CTCs were presented as single cells and no clusters of CTC cells were detected (Figure 27).

In addition, blood samples from three healthy controls were processed using the same protocol. The immunostaining of these samples showed that no CTCs were detected in the healthy control blood samples analysed.

5.2.4 Purity analysis of metastatic melanoma patients samples

To assess the purity of the enriched fractions when isolating cells from patients, WBC counts were completed before and after processing 8 mL of blood from five metastatic melanoma patients once and twice through the Slanted microfluidic device. As illustrated in Figure 28, a 2-3 log reduction in WBCs compared to the initial WBC count of 3.5×10^7 (range: 2.36×10^7 - 4.94×10^7) was achieved, after the first round of Slanted, 7.7×10^5 WBCs (range: 2.45×10^5 - 4.65×10^5) and after 2X Slanted, 8.7×10^4 WBCs (range: 46,532 – 123,203). A second round of enrichment significantly depleted the WBCs (p<0.0001) in patient samples even though the initial amount of WBCs was higher in patients than in healthy controls.
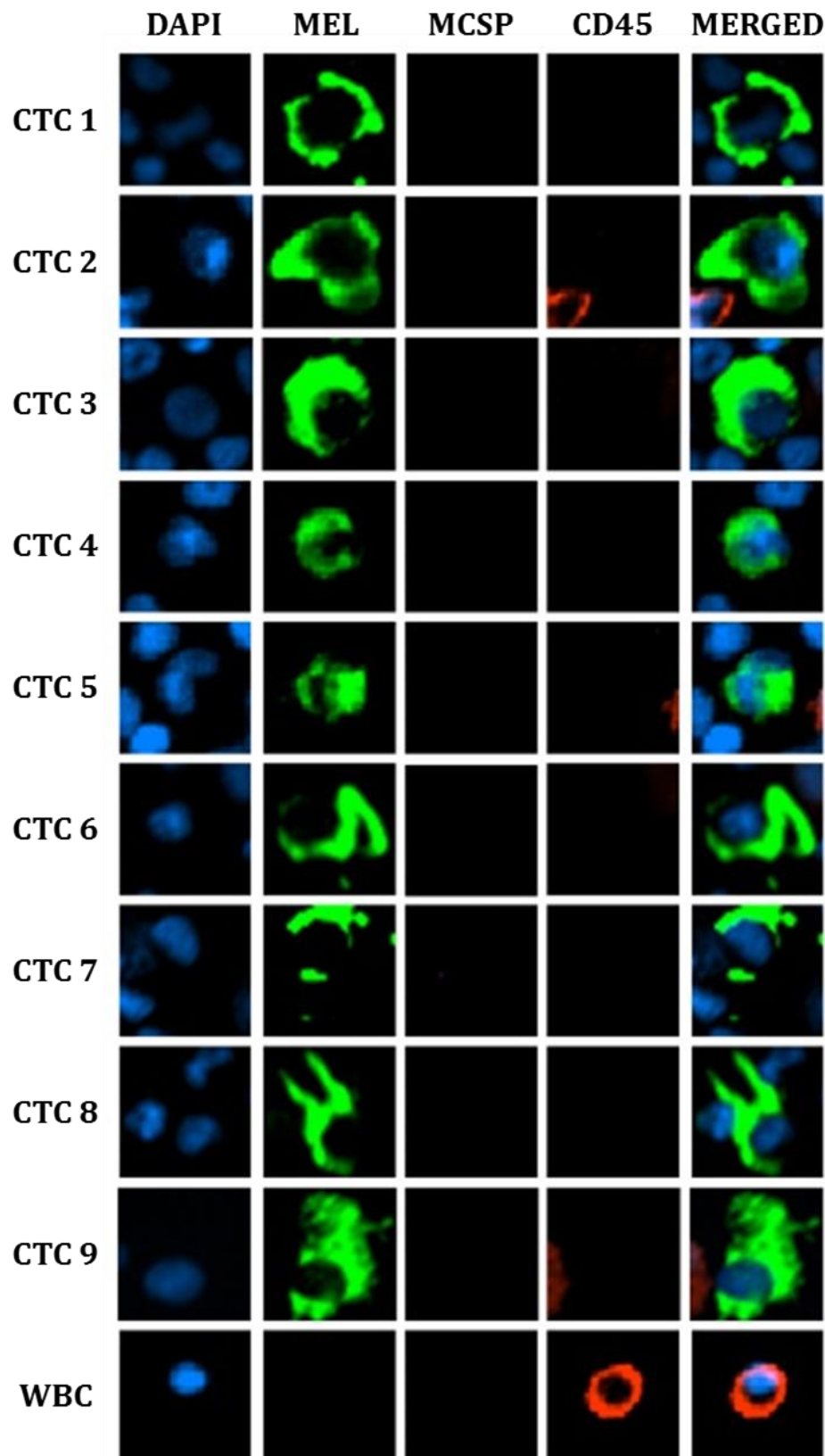
Figure 27. Expression pattern of intracellular and cell surface markers in CTCs isolated from metastatic melanoma patients. The immunostaining used a combination of intracellular markers -'MEL staining'- (gp100, MLANA and s100; AF488 -FITC- Shown here as green), and a surface marker (MCSP; AF647 -Cy5- Shown here as purple). DAPI (UV- Shown here as blue) was used as a nuclear stain and CD45 (PE -TRITC- Shown here as red) as a leukocyte-specific marker.
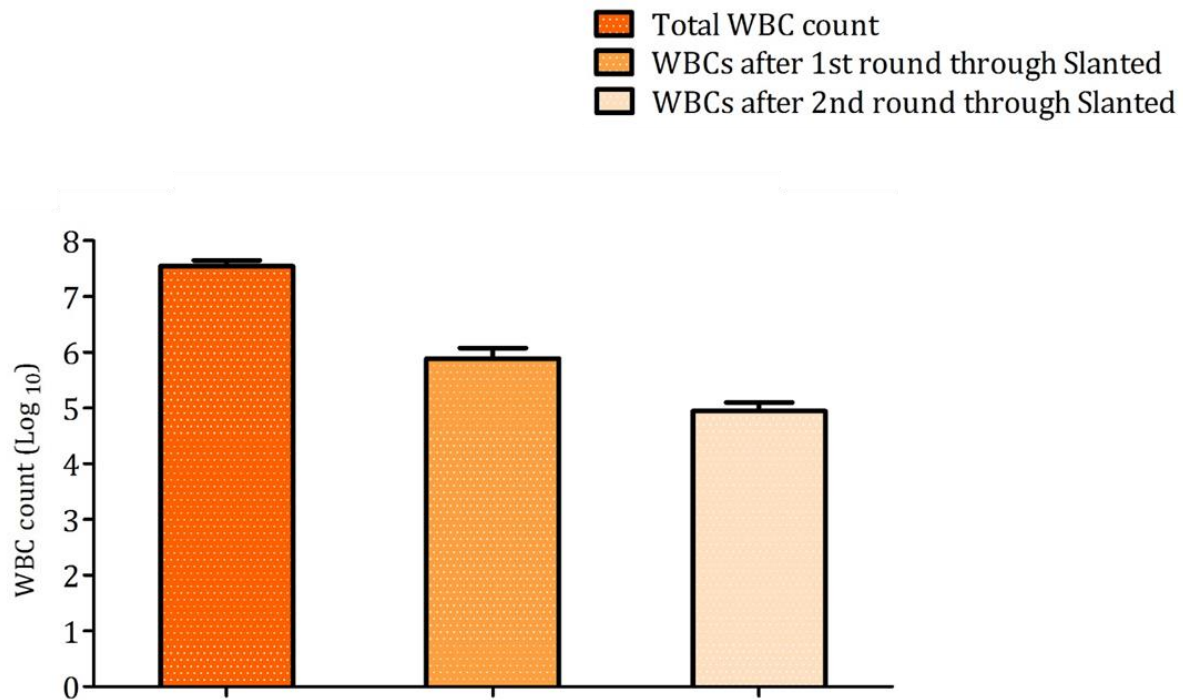
Figure 28. WBCs counts in five patients prior to and after 1 and 2 rounds through the Slanted microfluidic device. A second round of enrichment showed significant depletion of WBCs ($p < 0.0001$).

5.3 Aim 3. To test additional cellular markers that can be used in immunostaining assays for optimisation of detection and phenotypic characterisation of heterogeneous melanoma CTCs.

5.3.1 Optimisation of immunostaining assays

The low number of CTCs identified in patients with active metastatic disease, revealed the urgent need to test additional markers that can be used for detection of CTCs in samples processed through the Slanted microfluidic device. This is supported by previous observations that melanoma CTCs are heterogeneous and most commonly express cancer stem cells markers (ABCB5 and RANK) in addition to melanoma specific markers (gp100, Melan-A s100, and MCSP)[4, 170, 174]. Thus, it is possible that these stem cell-like melanoma CTCs were not detected in the patient samples isolated above, because these stem-like CTCs may not express the melanocytic markers included in our panel. Therefore, in this project, we established staining protocols for an additional 3 markers associated with cancer stem cell features: Vimentin[213], RANK[215], and ABCB5[222]. These markers have been detected previously in melanoma CTCs[170] and therefore their inclusion in this study could potentially improve melanoma CTC detection rates.

Firstly, the optimal dilutions of the antibodies used for their detection was determined by studying the immunocytochemical staining at different dilutions. Secondly, their expression in three melanoma cell lines (A2058, WM164, and SKMEL5) was analysed. Overall, the optimal immunostaining protocol for detection of expression of these markers in melanoma cells and the optimal antibody dilution was determined (see Table 7). Results from these experiments will inform future studies of the expression of these stem-like markers in CTCs from melanoma patients.

Each antibody was tested using three different dilutions as per the manufacturer´s recommendations. The optimal concentration of each antibody was assessed by determining the concentration that provided optimal immunocytochemical staining in melanoma cells whilst showing minimal background/ non-specific staining.
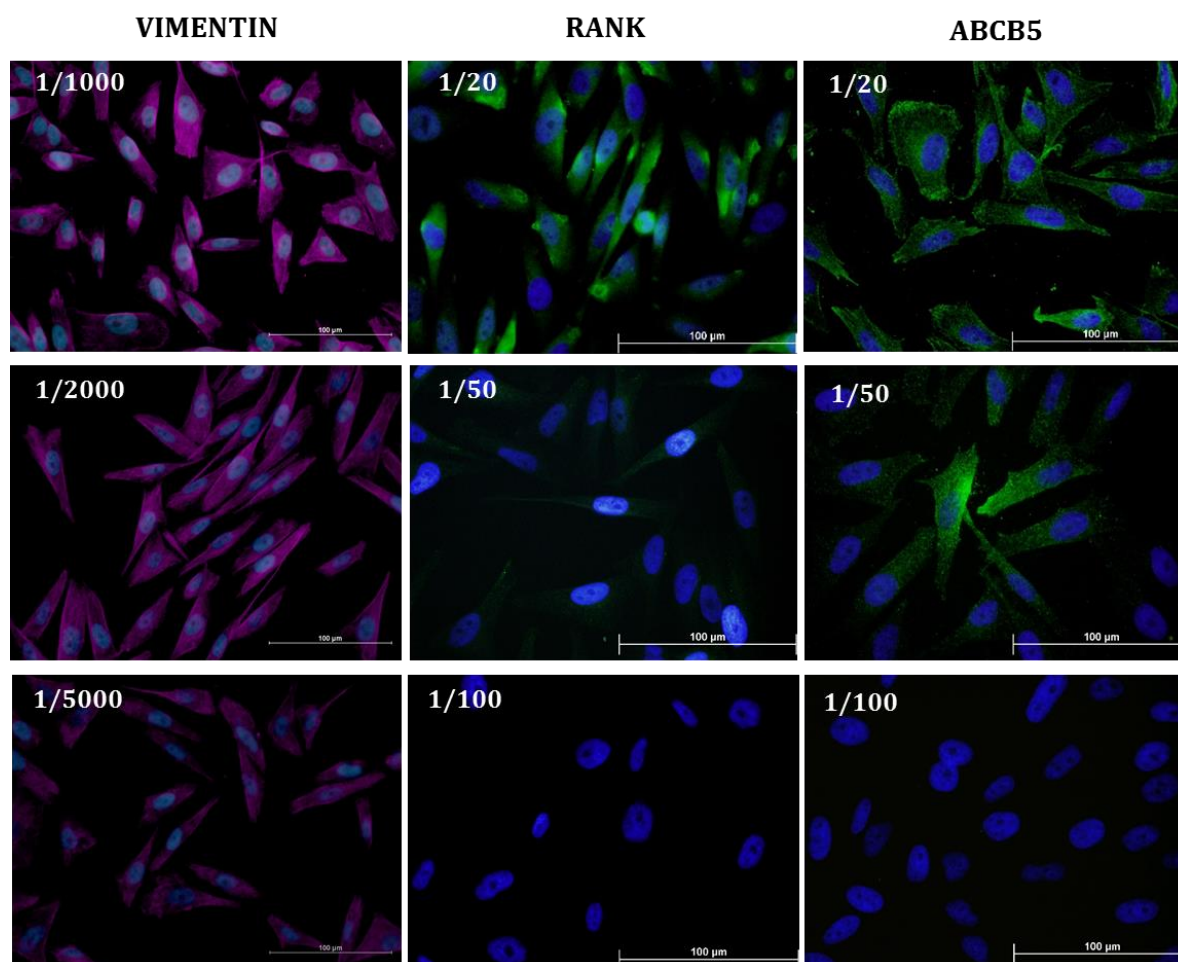
Figure 29. Antibody dilution optimisation. A2058 cells stained with different dilutions of Vimentin (AF647 -Cy5- Shown here as purple), RANK and ABCB5 (AF488 -FITC- Shown here as green). DAPI for nuclear recognition (UV- Shown here as blue). Negative controls were assessed for each marker (M488 for ABCB5 and RANK, and -647 ISO for Vimentin). Images at 40x magnification. Scale bar denotes 100 μm.

As shown in Figure 29, using an optimal concentration of 1/1000, anti-vimentin antibody stained the highest number of melanoma cells. A dilution of 1/20 for the anti-RANK antibody stained cells with minimal non-specific staining. Similarly, a dilution of 1/20 for the anti-ABCB5 antibody showed weak staining in a large number of cells.

5.3.2 Analysis of stem cell marker expression in melanoma cell lines

The optimal dilutions determined above for each marker were used to stain two additional melanoma cell lines: WM164, and SKMEL5 and the results were compared to those received for A2058 stained cells.

Table 8. Expression analysis of Vimentin, RANK and ABCB5 markers across three melanoma cell lines.

Marker	A2058	WM164	SKMEL5	Level of expression*
		Proportion of cells with positive staining (%)		
Vimentin	0-20	40-60	0-20	High
	20-40	20-40	20-40	Moderate
	20-40	0-20	20-40	Low
RANK	0	0	0	
	0-20	0-20	0	
	20-40	0-20	20-40	
ABCB5	0	0	0	
	0	0	0	
	40-60	0-20	0-20	

*Exemplified in Figure 29
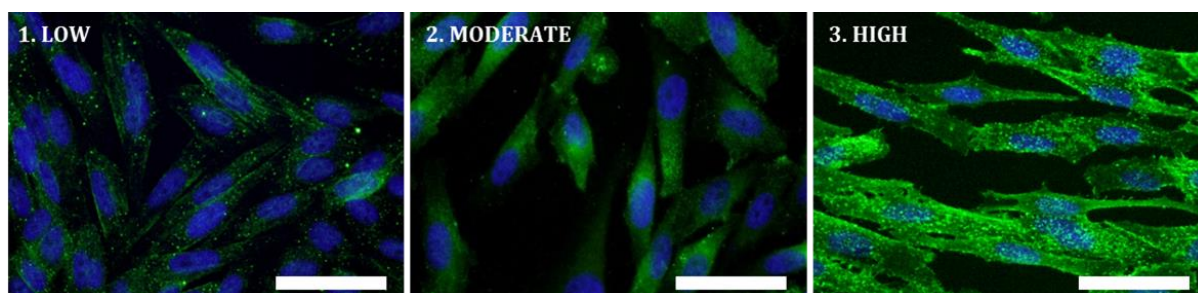
Figure 30. Differential staining to exemplify the level of expression of Vimentin, RANK, and ABCB5 across three melanoma cell lines. **1.** Low level of expression. **2.** Moderate level of expression. **3.** High level of expression. Scale bar denotes 40 μm.

The expression analysis revealed high Vimentin expression, predominantly by WM164 cells (60%). However, some A2058 and SKMEL5 cells also had also high Vimentin staining intensities. In addition, a greater proportion of cells expressed moderate Vimentin staining across all cell lines, with SKMEL5 and A2058 being the cell lines with more cells presenting low staining intensities (Table 8; Figure 31).

RANK was mainly expressed by the A2058 cell line at moderate to low levels of expression. WM164 also expressed this marker in less than half of the cells at moderate to low levels of expression. On the other hand, SKMEL5 showed low levels of RANK expression in approximately half of the cells (Table 8; Figure 31).

ABCB5 was the marker with the lowest expression across all cell lines. Low levels of expression were mainly observed in the majority of the A2058 cells. The other two cell lines, WM164 and SKMEL5 expressed this marker at low levels in only some cells and no positive staining for ABCB5 was present in most of the cells (Table 8; Figure 31).
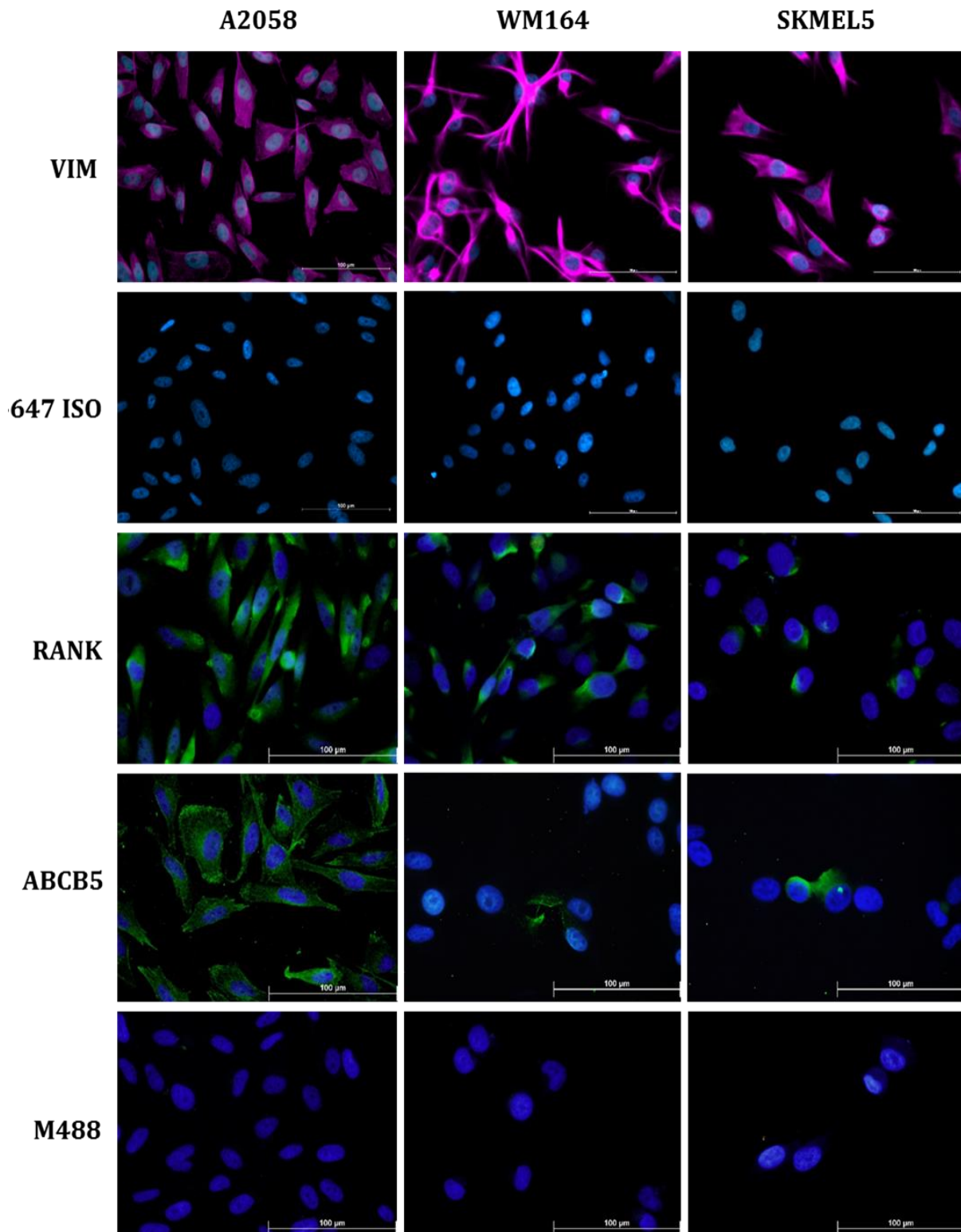
Figure 31. Expression pattern of the three additional markers across three melanoma cell lines (A2058, WM164 and SKMEL5). Intracellular markers Vimentin (AF647 -Cy5- Shown here as purple) and ABCB5 (AF488 -FITC- Shown here as green), and cell surface marker RANK (AF488 - FITC- Shown here as green). DAPI was used as a nuclear stain (UV- Shown here as blue). Negative controls were assessed for each marker in each cell line (647 ISO for Vimentin, and M488 for ABCB5 and RANK). Images at 40x magnification. Scale bar denotes 100 μm.

5.3.3 Analysis of the specificity

To determine the specificity of the markers in staining melanoma cells and not WBCs, A2058 cells were spiked into WBCs and transferred onto glass slides using the Cytospin then stained for each marker. In addition, negative control experiments were performed for each marker.

Vimentin

Vimentin showed different patterns of staining in spiked cells (Figure 32). Around 60% of cells had low expression of this marker and were slightly stained (i.e. Figure 32, CELL 1), whereas 30% of cells expressed higher amounts of Vimentin (i.e. Figure 32, CELL 2) and 10% cells were completely negative for this marker (i.e. Figure 32, CELL 3). Importantly, no WBCs were positively stained for Vimentin, showing the specificity of this marker in detecting melanoma cells.
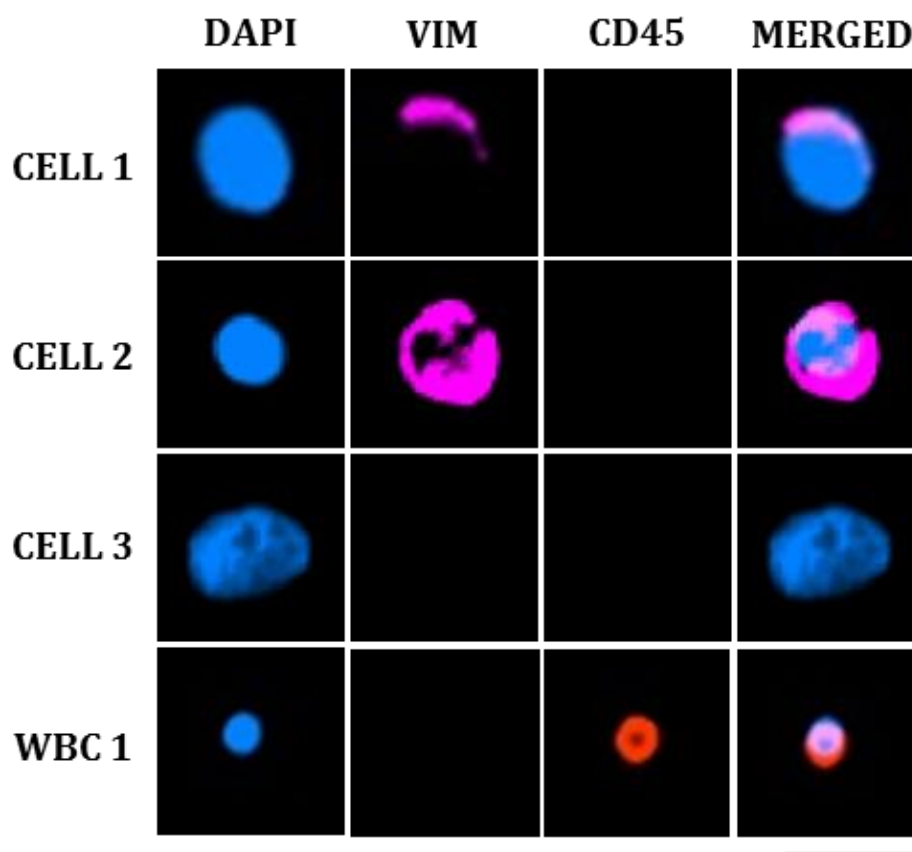
Figure 32. Microscopic images indicating the differential Vimentin expression intensities observed for A2058 melanoma cells spiked into WBCs. The immunostaining shows vimentin expression (AF647 -Cy5- Shown here as purple). DAPI (UV- Shown here as blue) was used as a nuclear stain and CD45 (PE -TRITC- Shown here as red) as a leukocyte-specific marker. Scale bar denotes 15 μm.

RANK

As observed in Figure 33, spiked A2058 cells did not express RANK over the background level. In addition, some WBCs showed positive signal for the marker. This findings are supported by the literature describing the expression of RANK in WBCs[215, 223].
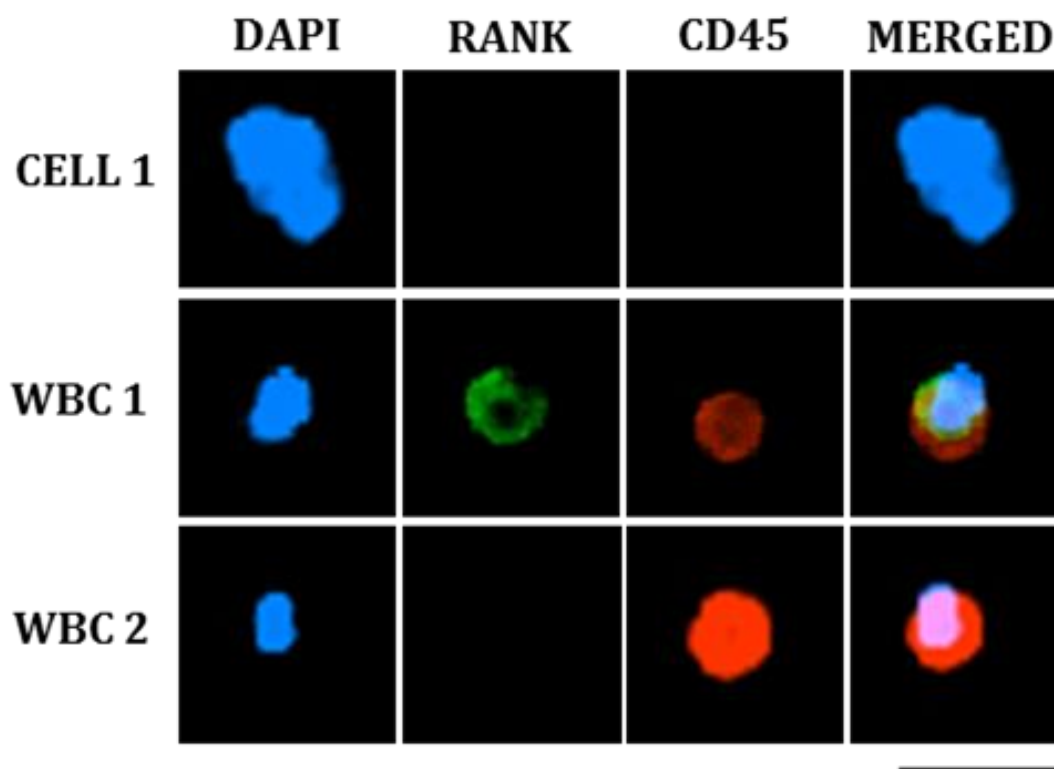
Figure 33. Microscopic images showing the RANK staining pattern in spiking experiments. The immunostaining uses an anti-RANK antibody (AF488 -FITC-Showed here as green). DAPI (UV-Shown here as blue) was used as a nuclear stain and CD45 (PE -TRITC- Shown here as red) as a leukocyte-specific marker. Scale bar denotes 15 µm.

ABCB5

As presented in Figure 34, ABCB5 staining was highly specific for melanoma cells, with no WBCs staining positive for this marker (i.e. Figure 34, WBC 1). However, the weak staining pattern present in A2058 spiked cells showed that this marker is expressed very weakly in melanoma cells. A few cells (10%) were stained only at the margins of the cell (i.e. Figure 34, CELL 1) and some cells (30%) were stained in a very speckled pattern, which makes it difficult to confidently identify them as ABCB5 positive cells (i.e. Figure 34, CELL 2). The majority of cells were negative for ABCB5 expression.
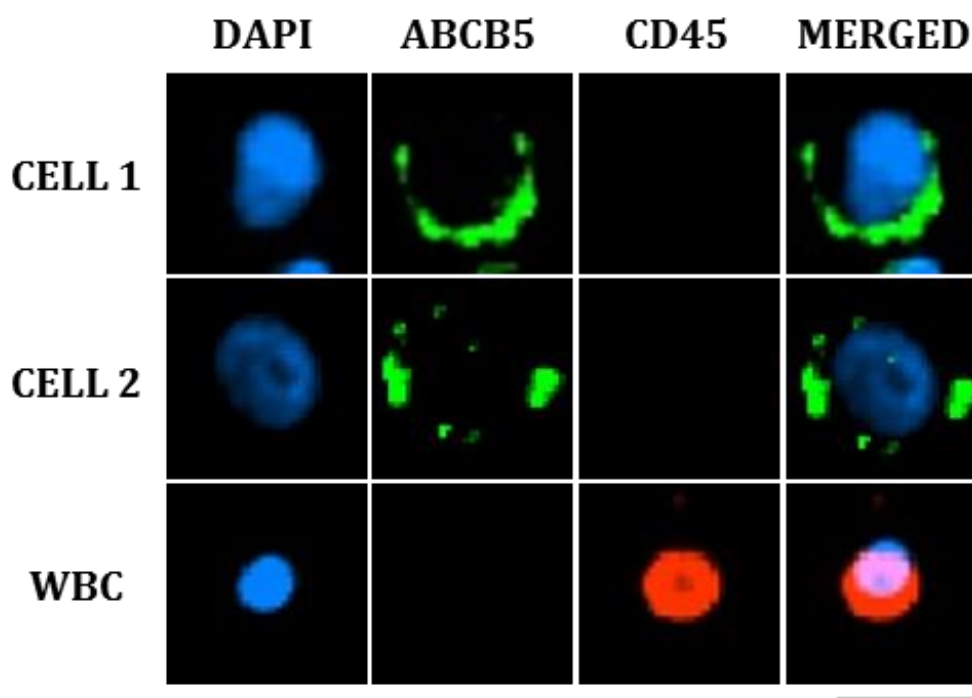
Figure 34. Microscopic images showing the ABCB5 staining pattern in spiked cells. The immunostaining uses an anti-ABCB5 antibody (R488 -FITC- Shown here as green). DAPI (UV-Shown here as blue) was used as a nuclear stain and CD45 (PE -TRITC- Shown here as red) as a leukocyte-specific marker. Scale bar denotes 15 μm.

5.3.4 Tyramide Signal Amplification in ABCB5 marker.

Tyramide Signal Amplification (TSA) is an enzyme-mediated detection method that utilises the catalytic activity of horseradish peroxidase (HRP) to generate a high-density labelled target protein thereby providing an intensified staining signal.

The above results show that A2058 cells express ABCB5 very weakly, complicating the detection and characterisation of these ABCB5 positive cells. Therefore, the TSA was trialled in order to discover if this method of immunostaining improves the signal shown by ABCB5 positive cells, therefore improving their detection.

Firstly, in order to test the ability of this method to increase and amplify the expression signal, MCSP, a marker known for being expressed by A2058[4], was tested as a positive control. When MCSP was tested using the TSA methodology and the same exposure and fluorescent intensities for both, standard and TSA immunocytochemistry methods, the level of signal observed for MCSP expression was higher (Figure 35.A2) than that of the signal obtained by staining with the standard immunocytochemistry protocol (Figure 35.A1).

Next, the ABCB5 expression was tested in order to verify the ability of this method to increase the signal produced by A2058 cells that express this marker in low amounts. For this, we utilised an antibody that recognises an epitope in a domain of ABCB5 that is situated on the external side of the cell membrane (Clone 1D12)[217]. Results show that, compared with the standard immunocytochemistry (ICC) protocol (Figure 35.B1), the TSA improved the level of intensity of the signal denoting ABCB5 expression (Figure 35.B2), allowing the detection of a higher number of ABCB5 positive cells (60%).
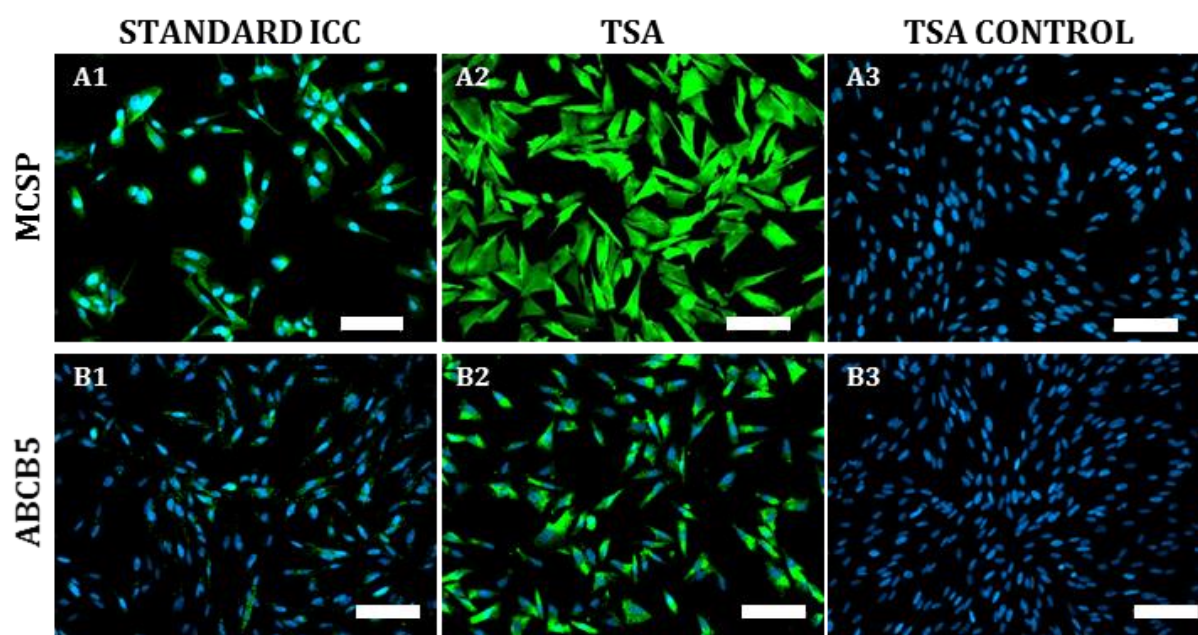
Figure 35. Differential signal shown by A2058 cells when comparing the TSA method with standard immunocytochemistry. Marker expression of A2058 cells stained with **(A1)** anti-MCSP antibodies (anti-mouse-AF488. Shown here as green), **(A2)** anti-MCSP antibodies (anti-mouse-HRP, fluorescein. Shown here as green), and **(A3)** negative control without primary antibody, treated with anti-mouse-HRP (fluorescein). **(B1)** Cells stained with anti-ABCB5 antibodies (anti-mouse-AF488. Shown here as green), **(B2)** anti-ABCB5 antibodies (anti-mouse-HRP, fluorescein. Shown here as green), and **(B3)** negative control without primary antibody, treated with anti-mouse-HRP (fluorescein). DAPI was used as a nuclear stain (UV- Shown here as blue). Scale bar denotes 100 μm.

Before applying this methodology in samples containing spiked A2058 cells and WBCs, the endogenous peroxidase activity of the WBCs was tested. For this, WBCs only were stained with isotype antibodies, anti-mouse secondary antibody labelled with HRP and then with the TSA Working Solution that contains fluorescein. CD45 antibody was used for leukocyte staining.

In this setting, the fluorescein present in the working solution is normally activated by the peroxidase activity of the HRP added to the experimental sample. However, in this

case, the presence of peroxidase activity in the WBCs activated the fluorescein, showing nonspecific signal in the WBCs (Figure 36.A). This nonspecific fluorescence present in WBCs is thought to be due to endogenous peroxidase activity present in the eosinophils[224].

In order to block this non-specific background signal and avoid the nonspecific staining, three different concentrations of a blocking agent, hydrogen peroxide (H_2O_2) were tested. Results show that by incubating the cells prior to staining with 0.3% H_2O_2 in PBS for 20 min, the endogenous peroxidase activity was blocked (Figure 36.B) as the fluorescein signal was not detected.
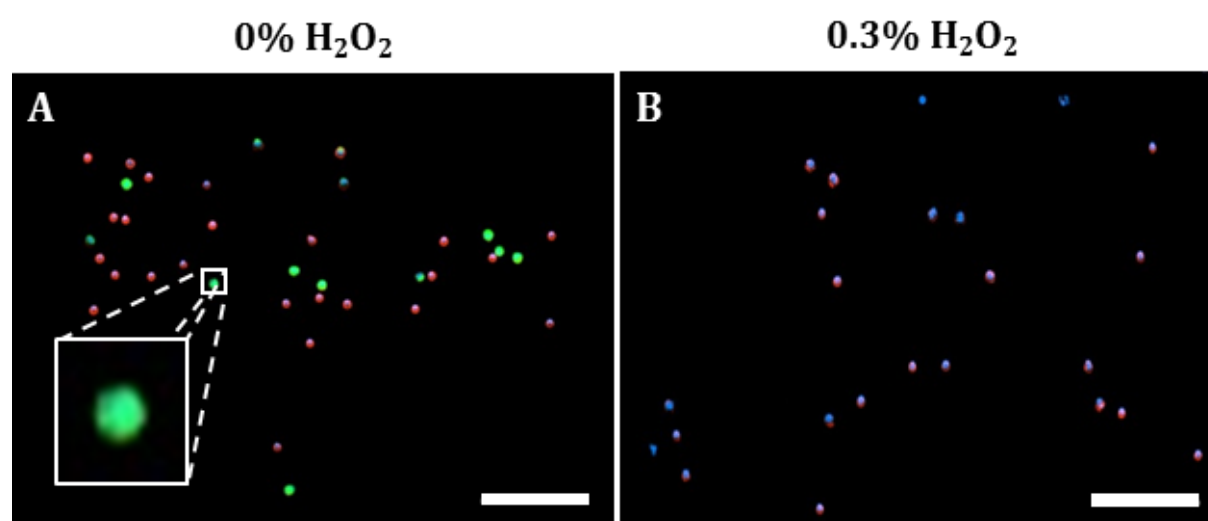
Figure 36. Differential expression pattern in WBCs treated or not with hydrogen peroxide. **(A)** WBCs stained with a mouse isotype control (negative control) and anti-mouse-HRP showing the endogenous peroxidase activity (-FITC-Shown here as green). **(B)** Nonspecific signal quenching after treating the sample with 0.3% H_2O_2. DAPI (UV- Shown here as blue) was used for nuclear staining and CD45 (PE -TRITC- Shown here as red) as a leukocyte-specific marker. Scale bar denotes 100 μm.

To study the specificity of this methodology for staining melanoma cells, A2058 cells spiked into WBCs were treated with 0.3% H_2O_2 peroxidase quenching solution and then tested for ABCB5 expression. Again, MCSP was used as a positive control, and an isotype negative control was also used to detect the background level of non-specific staining.

Results showed that the majority of A2058 cells (60%) presented with a higher signal intensity than that found in previous spiking experiments without TSA amplification (Figure 34).

The MCSP staining used as a positive control provided a high signal in all spiked A2058 cells after TSA amplification (Figure 37.B). By contrast, ABCB5 expression was mainly present on the periphery of the cells (Figure 37.A), with some cells showing low or no staining. This is as expected since ABCB5, a stem cell marker[225], is not expected to be present in all cells and confirms the specificity of the observed staining. Negative controls performed with an isotype antibody were used to define the background level of non-specific staining (Figure 37.C).
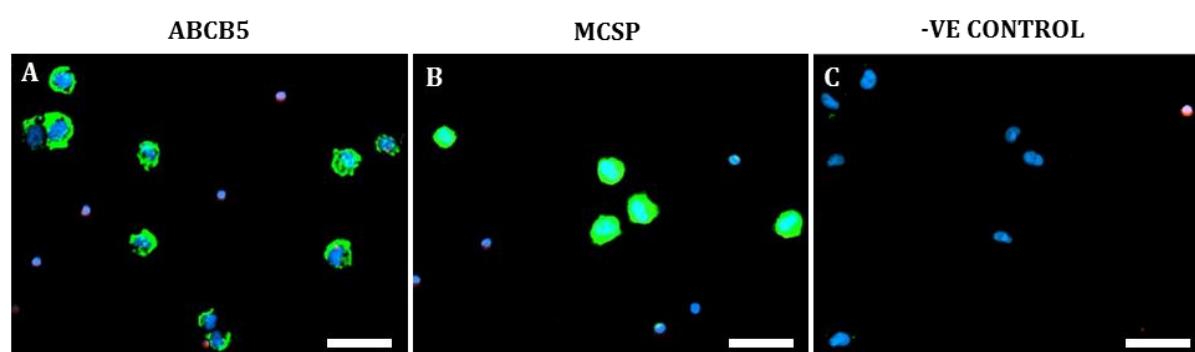
Figure 37. Marker expression of A2058 cells spiked in WBCs. Cells stained with **(A)** anti-ABCB5 antibodies at 20 μg/mL (anti-mouse-HRP, fluorescein -FITC- Shown here as green), **(B)** Positive control with anti-MCSP antibodies (anti-mouse-HRP, fluorescein; green), and **(C)** negative control with mouse isotype antibodies DAPI (UV- Shown here as blue) was used as a nuclear stain and CD45 (PE -TRITC- Shown here as red) as a leukocyte-specific marker. Scale bar denotes 50 μm.

In summary, TSA specifically enhanced immunostaining of these two melanoma markers. Most importantly, the staining signal of the weakly expressed stem cell marker, ABCB5, was significantly improved by TSA, allowing a more accurate detection of the expression of this marker in melanoma cells when immunostaining is used for their detection.

6. DISCUSSION

The isolation of CTCs is critical for the understanding of the role of these cells in the metastatic process and in determining their utility as biomarkers in the clinical management of cancer. The extreme heterogeneity of melanoma CTCs, also demands the implementation of better methods for the isolation and identification of the whole diversity of melanoma CTCs present in the blood of melanoma patients. Therefore, the application of methods that enable the isolation of viable CTCs and detection methods that allow the identification of these highly heterogeneous cells, is of high biological and clinical significance.

This project was aimed at developing an optimal procedure for the isolation and identification of CTCs in the blood of melanoma patients. The 2X Slanted microfluidic device was shown here, for the first time, to allow enrichment of CTCs from the blood of metastatic melanoma patients. This is of importance since only two microfluidic devices (CTC-iChip and Cluster-Chip) have been utilised previously for the isolation of CTCs from melanoma patients[178, 185]. The protocols required to successfully transfer the microfluidic enriched CTCs onto coverslips using the cytospin, and to detect the CTCs by immunofluorescence, were also developed. Here the detection of CTCs was achieved using a multimarker panel that combines four cellular markers involved in melanocytic function and melanomagenesis, commonly used in melanoma diagnosis. Since melanoma is a very heterogeneous cancer and melanoma CTCs have been shown to express different markers, the expression of three additional markers that can potentially improve the possibility of capturing heterogeneous CTCs, was evaluated in melanoma cell lines.

6.1 Microfluidic devices in melanoma CTC enrichment

Several methods have been developed to isolate melanoma CTCs from blood samples, predominantly using cell surface markers to capture and isolate the CTCs. However, due to the extraordinary marker heterogeneity found in melanoma, these methods bias the isolation to include only a proportion of CTCs. Thus, methods such as those based on the use of microfluidic devices, which isolate CTCs based on their physical properties relative to the other blood components, rather than surface marker expression, would improve CTC isolation and are thus of significant benefit in melanoma CTC research.

Recovery rates

The study and comparison of the recovery rates and the purity obtained by using different spiral microfluidic approaches, determined that the best recovery rate was offered by the 1X Slanted chip, which retrieves more than 80% of spiked melanoma cells. A similar result has been reported previously by Warkiani *et al.* for spiked breast and bladder cancer cell lines, where a recovery rate of ~85% was achieved[11]. By contrast, the A5 device, failed to capture more than half of the spiked melanoma cells, in contrast to previous reported results of >85% of recovery of breast cancer cells (MCF-7)[12].

Surprisingly, the SKMEL5 cells, previously characterised as larger than A2058 cells[226], showed a lower recovery rate when spiked and processed through the different spiral devices. This difference was amplified by the use of the A5 device that recovered, in the enriched fraction, only 10.6% of the 50 spiked SKMEL5 compared with 55.3% recovery observed when A2058 cells were spiked. It is possible that the A2058 and SKMEL5 cells may not only differ in size but also in other physical properties such as cell density or deformability, affecting their differential recoveries. Remarkably, previous experiments using the multiplexed version of the A5 chip[199], also showed a lower recovery rate (76.4%) when larger cell line (T24; ~30 μm) rather than a smaller cell line (MCF-7; ~20 μm) was used (87.6%).

Additionally, the recovery rates of melanoma cell lines using the A5 microfluidic device have not been reported previously. A2058 and SKMEL5 melanoma cell lines have a smaller average cell size (13.7 μm and 18.2 μm, respectively[226]) than the breast cancer cells used in A5 studies[12]. Taken together, the results support the idea that tumour cells from the same cancer type may have differential characteristics that may affect their recovery rates by microfluidics. Therefore, the use of multiple cancer cell lines is recommended when testing the recovery rates of microfluidic enrichment devices for CTC isolation.

Purity

Although melanoma CTCs have been detected and quantified previously by using label-dependent methodologies[4, 165, 168, 169], one of the most important advantages of using label-free isolation methods is the ability to enrich a viable and intact CTC population.

This method of isolation allows CTC downstream analyses of CTCs aimed at unveiling the genomic and transcriptomic profile of CTCs. Towards this end, achieving a highly purified enriched fraction is of vital importance for any type of downstream genomic analysis.

Given that the purity of the recovered fraction is a high priority for future applications, interrogation of the WBC background resulting from these different approaches was important and here it is shown for the first time that the enrichment through the A5 chip resulted in the highest WBC background when melanoma cells are isolated. Therefore, no further experiments were conducted using this spiral device. Although the 1X Slanted resulted in a more than 2 log fold reduction of WBC background from the blood of healthy donors and patients, this chip showed a higher leukocytic background than previously reported of 5 x 10^3 WBCs per 8 mL[11]. For this reason, the ability of the 2X Slanted to further deplete the WBC background while still providing significant recovery rates, was interrogated. The 2X Slanted spiral microfluidic device achieved close to a 3 log reduction of WBCs after a second round of Slanted enrichment without markedly affecting the enrichment efficiency (>60%).

However, despite the need to further improve the leukocytic background yielded by the slanted device in controls (18,000 WBCs per 8 mL of blood), these values are better than those reported for the only other microfluidic device used for melanoma CTCs, the CTC-iChip (32,000 WBCs per mL of control blood), which was previously used for isolation of melanoma CTCs[185].

Further strategies testing the application of additional WBC depletion methodologies to blood prior to enrichment through the 2X Slanted enrichment, such Ficoll density centrifugation, or negative leukocyte depletion of the enriched fraction after 2X Slanted[227], are strongly recommended. However, the potential of the Ficoll density centrifugation to deplete WBCs prior to microfluidic enrichment needs to be tested since these methods could affect physical properties of the cells and therefore affect the recovery rates. Another technique that can be used to obtain pure CTCs for downstream applications such as single cell sequencing are laser capture microdissection of the cells on the stained slide or picking of the cells after the staining. Although these processes may increase the purity of the enriched cells, is important to consider that the addition of

extra manipulation steps to the enrichment process, may increase cell damage and cell loss.

Ultimately, the combination of the purity and recovery rate of the 2X Slanted offered the best outcome amongst the three different spiral microfluidic approaches tested. Therefore, this approach was validated for the enrichment of CTCs from the blood of metastatic melanoma patients.

6.2 Detecting CTCs in metastatic melanoma patients

Detection and quantification of CTCs after enrichment through label-free approaches, such as microfluidic devices, is critical for the validation of these isolation techniques.

In this project, four melanocytic markers (gp100, Melan-A, s100 and MCSP), have been used to detect CTCs at a single cell level in the background of thousands of WBCs after microfluidic enrichment of patients' samples[226]. These markers have been reported to be over-expressed in melanoma tumours[210], a fact that has driven the extensive use of these markers in the capture and detection of CTCs from melanoma patients[165, 174, 203, 218, 228].

Previous studies have detected melanoma CTCs in 40%[168], 57%[174], 52%[170], 79%[165], using CellSearch®, ISET platform, multimarker flow cytometry and the herringbone CTC-Chip, respectively. By using the 2X Slanted microfluidic enrichment method and a multimarker panel for immunostaining detection, CTCs were detected in 40% of the metastatic melanoma patients analysed. This finding validated, for the first time, the use of the 2X Slanted microfluidic device in enriching CTCs from the blood of metastatic melanoma patients. However, it is likely that differences in the CTC detection rates across all CTC studies may be attributed to the extraordinary heterogeneity of melanoma CTCs both within and between patients. Therefore, the ability of label-free methodologies, such as the proposed microfluidic approach, to capture a wider population of viable and intact CTCs may be beneficial for studies aiming at studying and characterising CTCs using phenotypic and single-cell genomic approaches, providing a significant advantage over label-dependant methods which do not allow downstream characterisation of detected CTCs.

Although MCSP is highly expressed in both primary and metastatic lesions[229], and different methods have detected MCSP positive CTCs[4, 98], the immunostaining approach used in this project did not detect MCSP positive CTCs in metastatic melanoma patients enriched using the 2X Slanted device. Ozkumur *et al.* have indicated a variability of melanoma CTCs in cell size after microfluidic isolation[185], but it is still unclear whether CTC subtypes do in fact vary in cell size and density. In addition, previous reports suggested that the population of CTCs expressing melanocytic markers is lower than the subpopulation of CTCs expressing cancer stem cell markers[170].

Based on previous studies[4, 170, 174], we expect that not all melanoma CTCs express the same markers. Therefore, it is possible that the current markers used in downstream approaches for CTC detection may constrain our ability to detect the vast majority of melanoma CTC subtypes. Thus, studies aimed at the detection and study of the whole range of melanoma CTCs to identify the real diversity of these cells are urgently needed in order to pinpoint better markers that minimise false negative results.

Methods utilised to detect CTCs to date, are derived from our limited available knowledge of the whole spectrum of the diversity of melanoma CTCs. Studies are needed therefore to investigate melanoma CTC phenotypes and their role in melanoma biology and prognosis. Gray *et al.* found that the proportion of CTCs expressing RANK were significantly increased after therapy initiation compared with baseline (p=0.0039) in patients treated with BRAF inhibitors (n=16)[170]. Similarly, CTCs expressing PD-L1 were found to be specific biomarkers of response to anti-PD1 blockade[171]. Thus, prognostic utility was found not by using total CTCs counts but by studying subpopulations. Additionally, the pharmacodynamics responses of the different subpopulations of CTCs to therapy require additional studies to more clearly define the differential relationship of these subpopulations with response to drugs[170].

Importantly, the study of different marker subpopulations is of crucial importance in melanoma in order to improve our understanding of the role of CTC subpopulations in melanoma biology. Previous studies comparing melanoma cell subpopulations between patient-matched blood and metastatic tumours, revealed that cell populations expressing melanoma initiating markers, such as ABCB5 and RANK, are more common amongst CTCs

than in the matching tumour, suggesting a preferential selection for certain tumour cell subtypes in the blood[170].

In addition, examining CTC subpopulations and their markers will reveal whether specific subsets of CTCs are responsible for metastatic initiation and development, thus aiding in a better classification of high-risk patients or patients in need for adjuvant therapies. In addition, another important clinical question that could be addressed by characterisation of CTC subtypes is the identification of differential response or resistance to metastatic melanoma treatments, providing important information that will impact drug design and personalised treatment regimes. Such studies will dramatically advance the use of CTCs in the clinic. Moreover, optimal isolation of melanoma CTCs paves the way for dissection of their real heterogeneity and the mechanisms underlying their role in melanoma spreading.

6.3 Additional markers to detect melanoma CTCs

Even though great advances have been made in melanoma CTC isolation techniques, quantification of melanoma CTCs remains challenging given the low numbers of CTCs identified even when multimarker assays are used to detect these cells. This exemplified by our results and by other studies[165]. The high heterogeneity present in melanoma CTCs and the low rate of detection of these cells, has highlighted the need to increase the marker spectrum applied in detecting CTCs.

The immunocytochemistry staining protocol used in patients, identified CTCs expressing melanocytic markers in 40% of metastatic melanoma patients. However, this method would miss cells expressing melanoma-initiating markers, which have been shown to be expressed in a great proportion of CTCs[170, 215]. Here we optimised immunostaining of potential markers expressed in melanoma CTCs, including stem-like CTCs in order to increase CTC detection rates.

Vimentin

Vimentin is an intermediate filaments (IFs) found in the cytoplasm of mesenchymal cells, maintaining the structure of the cell and the integrity of the tissue[230]. The presence of Vimentin in melanoma has been defined as a melanoma diagnostic marker[213]. The

detection of this marker in primary tumours has been associated with metastatic progression, and therefore with worse outcome[212, 231, 232].

This study tested the expression of Vimentin in 3 melanoma cell lines. Interestingly, this marker was expressed by all three cell lines at moderately to high levels. Importantly, WBCs do not express this marker, as observed in our spiking experiments. Therefore, this marker is now ready to be used together with the multimarker panel in detecting melanoma CTCs, Given its high expression in the melanoma cell lines used, it has the potential to improve the detection of melanoma CTCs.

It has been reported previously that only a proportion of CTCs present in the bloodstream will ultimately initiate development of a metastatic tumour[9]. Further studies are needed to determine whether Vimentin is a marker of aggressive features in CTCs, which can aid in stratifying patients that require more aggressive treatment.

RANK

Recently, a flow-cytometry multimarker approach was developed, to detect and analyse CTCs for the presence of melanoma-associated markers, such as MCSP and MCAM, in combination with melanoma stem cell markers, such as RANK (receptor activator of NF-κβ), ABCB5 and CD271[170]. The evidence provided by Gray *et al.* that the vast majority of melanoma CTCs express "stem cell" markers RANK and ABCB5, argues for inclusion of such markers in CTC detection by immunocytochemistry.

In melanoma, RANK has been described as a tumour-initiating cell marker[215]. In addition, Gray *et al.* found significant association between high numbers of CTCs expressing RANK and shorter PFS rates in patients treated with MAPK inhibitors. Therefore, the study of this marker expression in melanoma CTCs serves as a prognostic marker for patients treated with MAPK inhibitors.

When studying RANK expression across three melanoma cell lines, cells expressing RANK were observed at moderate to low levels. However, when A2058 cells spiked into WBCs were assessed, no spiked cells were found positive for RANK. One possible explanation for this loss of signal in spiked cells, can be the fact that attached cells express RANK on their cell surface. In contrast, spiked cells that have been subjected to important changes

in their conditions during spiking, may internalise RANK. In fact, differential staining was observed between cells grown on coverslips and those spiked into WBCs for all markers tested, supporting the hypothesis that cells stained in spikes suffer loss of cell surface markers.

ABCB5

The expression of ABCB5, a tumour initiating or 'stem cell' marker known to be involved in tumour resistance to therapy, was tested in melanoma cell lines and in spiked cells. ABCB5 identifies a subset of slow-cycling tumour cells with increased potential to initiate metastases[217, 233].

The identification of this marker in melanoma CTCs is of great clinical significance, as it is present in increased proportion of CTCs in patients resistant to targeted therapies[233]. Thus, the presence of ABCB5 positive CTCs, may serve as a predictor of poor responses to the targeted therapy. Using the staining protocol developed here, we now could explore this important question in future studies.

The study of ABCB5 expression in spiked cells, did not allow confident recognition of ABCB5 positive cells. The staining of this marker showed low expression signal in all three melanoma cell lines even when stained on coverslips. The TSA system is reported to increase the detection of poorly expressed proteins by 100-fold[234]. By applying this methodology to the ABCB5 staining, an increased signal was observed compared with standard immunocytochemistry. Now, the ability to detect ABCB5 in the microfluidic enriched fraction of metastatic melanoma patients needs to be tested.

In summary, while previous studies have been able to identify CTCs by using flow cytometry, there is an increasing need to unveil the genomic, transcriptomic and proteomic signature of CTCs. In order to perform such analyses, label-free approaches, such as microfluidics devices, are required. In future studies, microfluidic technology will dramatically assist with single-cell genomic downstream analyses. Although this methodology requires a high level of optimisation, the addition of multiple markers including rare CTC markers, can be a beneficial step towards unveiling the real heterogeneity of melanoma CTC subpopulations.

6.4 Limitations of the study

Our study of the isolation of melanoma CTCs has several limitations. One such limitation is that there is no knowledge of the ability to detect CTCs in patients with low disease burden, even those with metastatic disease, especially when only 8 mL of blood are analysed. The analysis of larger amounts of blood would increase the chances of detecting CTCs, however, this is not feasible in a clinical setting where patients are required to provide several blood samples for other clinical measures. Another limitation is that cell lines used here for optimisation of protocols are unlikely to have the same characteristics as CTCs. Despite melanoma cell lines being critically useful in understanding melanoma biology, the culture conditions of these cell lines might cause some changes to cell morphology, biology, and cell surface markers, in particular, when compared to CTCs derived from melanoma tumours. Thus, it is possible that cell line cultures derived from melanoma tumours may differ in shape or size from the CTCs present in patients. Changes in cell size or shape of melanoma CTCs and melanoma cell line cells may induce a different interaction with the Dean forces generated inside the micro-channels of these biochips. Consequently, changes in the recovery rates of melanoma cell lines compared to CTCs derived from patients are likely.

An additional limitation is the high marker heterogeneity present in CTC populations. Although in this project different markers have been utilised to improve the detection of CTCs by immunostaining approaches, cell culture conditions may alter the expression of certain markers and cell lines may not express the same markers or the same level of markers as those found in CTCs.

On the other hand, the method of enrichment and detection had several steps that could have affected the integrity of the cells, interfering with marker expression or cell integrity. Also, the processing timeframe of 24 hours could be too long and cause damage to the cells, hampering their isolation. To confirm this, studies that investigate marker expression on CTCs at several steps along the pathway and processing samples within 4 hours of collection need to be performed.

6.5 Future directions

Challenges in the isolation and detection of CTCs, particularly in melanoma, have hindered studies aimed at unveiling the molecular mechanisms underlying melanoma CTC biology and metastasis.

Moreover, use of the 2X Slanted microfluidic device to isolate viable and label-free melanoma CTCs, will pave the way for studies aimed at dissecting their real heterogeneity and subsequently the mechanisms underlying their role in melanoma metastasis.

Although challenging, studying the marker expression, gene expression and mutational landscape of single melanoma CTCs, their relationship with tumour tissue cells and their connection with treatment response and resistance will significantly increase the clinical value of CTCs as a biomarker and dramatically advance CTC use in the clinic.

6.6 Conclusion

This project developed and validated the use of a double round of enrichment using the Slanted microfluidic device in capturing CTCs from the blood of metastatic melanoma patients. A multimarker assay including four common melanoma markers was used in order to detect CTCs present in the enriched fraction. This method of enrichment and detection identified CTCs in 40 % of the ten metastatic melanoma patients examined.

Two additional stem cell markers, Vimentin, and ABCB5, have been identified as potential markers that can be used in detecting a higher number of melanoma CTCs after spiral microfluidic enrichment. The use of TSA in detecting markers that are not highly expressed in CTCs but are of great importance in melanoma management will facilitate the detection of a broader spectrum of heterogeneous CTCs.

Ultimately, the isolation of viable, label-free heterogeneous populations of melanoma CTCs using this slanted enrichment device will facilitate future studies aimed at unveiling the molecular mechanisms and biology of melanoma CTCs and their role in melanoma metastasis and response to therapy.

7. REFERENCES

1.   Siegel, R., J. Ma, Z. Zou, and A. Jemal, *Cancer statistics, 2014.* CA Cancer J Clin, 2014. **64**(1): p. 9-29.

2.   Miller, A.J. and M.C. Mihm, Jr., *Melanoma.* N Engl J Med, 2006. **355**(1): p. 51-65.

3.   Homet, B. and A. Ribas, *New drug targets in metastatic melanoma.* J Pathol, 2014. **232**(2): p. 134-41.

4.   Freeman, J.B., E.S. Gray, M. Millward, R. Pearce, and M. Ziman, *Evaluation of a multi-marker immunomagnetic enrichment assay for the quantification of circulating melanoma cells.* J Transl Med, 2012. **10**: p. 192.

5.   Vishnoi, M., S. Peddibhotla, W. Yin, T.S. A, G.C. George, D.S. Hong, and D. Marchetti, *The isolation and characterization of CTC subsets related to breast cancer dormancy.* Sci Rep, 2015. **5**: p. 17533.

6.   Olmos, D., H.T. Arkenau, J.E. Ang, I. Ledaki, G. Attard, C.P. Carden, A.H. Reid, R. A'Hern, P.C. Fong, N.B. Oomen, R. Molife, D. Dearnaley, C. Parker, L.W. Terstappen, and J.S. de Bono, *Circulating tumour cell (CTC) counts as intermediate end points in castration-resistant prostate cancer (CRPC): a single-centre experience.* Ann Oncol, 2009. **20**(1): p. 27-33.

7.   Cristofanilli, M., D.F. Hayes, G.T. Budd, M.J. Ellis, A. Stopeck, J.M. Reuben, G.V. Doyle, J. Matera, W.J. Allard, M.C. Miller, H.A. Fritsche, G.N. Hortobagyi, and L.W. Terstappen, *Circulating tumor cells: a novel prognostic factor for newly diagnosed metastatic breast cancer.* J Clin Oncol, 2005. **23**(7): p. 1420-30.

8.   de Bono, J.S., H.I. Scher, R.B. Montgomery, C. Parker, M.C. Miller, H. Tissing, G.V. Doyle, L.W. Terstappen, K.J. Pienta, and D. Raghavan, *Circulating tumor cells predict survival benefit from treatment in metastatic castration-resistant prostate cancer.* Clin Cancer Res, 2008. **14**(19): p. 6302-9.

9.   Cohen, S.J., C.J. Punt, N. Iannotti, B.H. Saidman, K.D. Sabbath, N.Y. Gabrail, J. Picus, M. Morse, E. Mitchell, M.C. Miller, G.V. Doyle, H. Tissing, L.W. Terstappen, and N.J. Meropol, *Relationship of circulating tumor cells to tumor response, progression-free survival, and overall survival in patients with metastatic colorectal cancer.* J Clin Oncol, 2008. **26**(19): p. 3213-21.

10.   Alix-Panabieres, C. and K. Pantel, *Challenges in circulating tumour cell research.* Nat Rev Cancer, 2014. **14**(9): p. 623-31.

11.   Warkiani, M.E., G. Guan, K.B. Luan, W.C. Lee, A.A. Bhagat, P.K. Chaudhuri, D.S. Tan, W.T. Lim, S.C. Lee, P.C. Chen, C.T. Lim, and J. Han, *Slanted spiral microfluidics for the ultra-fast, label-free isolation of circulating tumor cells.* Lab Chip, 2014. **14**(1): p. 128-37.

12.   Hou, H.W., M.E. Warkiani, B.L. Khoo, Z.R. Li, R.A. Soo, D.S. Tan, W.T. Lim, J. Han, A.A. Bhagat, and C.T. Lim, *Isolation and retrieval of circulating tumor cells using centrifugal forces.* Sci Rep, 2013. **3**: p. 1259.

13.   Tortora, G.J. and B. Derrickson, *Principles of anatomy and physiology*. 13th ed. 2012, Hoboken, N.J.: John Wiley & Sons. 1 v. (various pagings).

14.   Winslow, T., *Melanoma Anatomy*. 2008: National Cancer Institute.

15.   Bastian, B.C., *The molecular pathology of melanoma: an integrated taxonomy of melanocytic neoplasia.* Annu Rev Pathol, 2014. **9**: p. 239-71.

16.   Nezos, A., P. Msaouel, N. Pissimissis, P. Lembessis, A. Sourla, A. Armakolas, H. Gogas, A.J. Stratigos, A.D. Katsambas, and M. Koutsilieris, *Methods of detection of circulating melanoma cells: a comparative overview.* Cancer Treat Rev, 2011. **37**(4): p. 284-90.

17. Sneyd, M.J. and B. Cox, *A comparison of trends in melanoma mortality in New Zealand and Australia: the two countries with the highest melanoma incidence and mortality in the world.* BMC Cancer, 2013. **13**: p. 372.

18. AIHW, *Cancer in Australia: An overview 2014.* Cancer Series. Vol. 90. 2014, Canberra: Australian Institute of Health and Welfare. 202.

19. Marks, R., *The changing incidence and mortality of melanoma in Australia.* Recent Results Cancer Res, 2002. **160**: p. 113-21.

20. Nikolaou, V. and A.J. Stratigos, *Emerging trends in the epidemiology of melanoma.* Br J Dermatol, 2014. **170**(1): p. 11-9.

21. Globocan. *Estimated Cancer Incidence, Mortality and Prevalence Worlwide in 2012.* 2012 [cited 2015; Available from: http://globocan.iarc.fr/Pages/Map.aspx.

22. Lancaster, H.O., *Some geographical aspects of the mortality from melanoma in Europeans.* Med J Aust, 1956. **43**(26): p. 1082-7.

23. Gandini, S., F. Sera, M.S. Cattaruzza, P. Pasquini, O. Picconi, P. Boyle, and C.F. Melchi, *Meta-analysis of risk factors for cutaneous melanoma: II. Sun exposure.* Eur J Cancer, 2005. **41**(1): p. 45-60.

24. Jhappan, C., F.P. Noonan, and G. Merlino, *Ultraviolet radiation and cutaneous malignant melanoma.* Oncogene, 2003. **22**(20): p. 3099-112.

25. Bald, T., T. Quast, J. Landsberg, M. Rogava, N. Glodde, D. Lopez-Ramos, J. Kohlmeyer, S. Riesenberg, D. van den Boorn-Konijnenberg, C. Homig-Holzel, R. Reuten, B. Schadow, H. Weighardt, D. Wenzel, I. Helfrich, D. Schadendorf, W. Bloch, M.E. Bianchi, C. Lugassy, R.L. Barnhill, M. Koch, B.K. Fleischmann, I. Forster, W. Kastenmuller, W. Kolanus, M. Holzel, E. Gaffal, and T. Tuting, *Ultraviolet-radiation-induced inflammation promotes angiotropism and metastasis in melanoma.* Nature, 2014. **507**(7490): p. 109-13.

26. Boniol, M., P. Autier, P. Boyle, and S. Gandini, *Cutaneous melanoma attributable to sunbed use: systematic review and meta-analysis.* BMJ, 2012. **345**: p. e4757.

27. Alexandrov, L.B., S. Nik-Zainal, D.C. Wedge, S.A. Aparicio, S. Behjati, A.V. Biankin, G.R. Bignell, N. Bolli, A. Borg, A.L. Borresen-Dale, S. Boyault, B. Burkhardt, A.P. Butler, C. Caldas, H.R. Davies, C. Desmedt, R. Eils, J.E. Eyfjord, J.A. Foekens, M. Greaves, F. Hosoda, B. Hutter, T. Ilicic, S. Imbeaud, M. Imielinski, N. Jager, D.T. Jones, D. Jones, S. Knappskog, M. Kool, S.R. Lakhani, C. Lopez-Otin, S. Martin, N.C. Munshi, H. Nakamura, P.A. Northcott, M. Pajic, E. Papaemmanuil, A. Paradiso, J.V. Pearson, X.S. Puente, K. Raine, M. Ramakrishna, A.L. Richardson, J. Richter, P. Rosenstiel, M. Schlesner, T.N. Schumacher, P.N. Span, J.W. Teague, Y. Totoki, A.N. Tutt, R. Valdes-Mas, M.M. van Buuren, L. van 't Veer, A. Vincent-Salomon, N. Waddell, L.R. Yates, I. Australian Pancreatic Cancer Genome, I.B.C. Consortium, I.M.-S. Consortium, I. PedBrain, J. Zucman-Rossi, P.A. Futreal, U. McDermott, P. Lichter, M. Meyerson, S.M. Grimmond, R. Siebert, E. Campo, T. Shibata, S.M. Pfister, P.J. Campbell, and M.R. Stratton, *Signatures of mutational processes in human cancer.* Nature, 2013. **500**(7463): p. 415-21.

28. American Cancer Society. *What are the risk factors for melanoma skin cancer?* 2015; Available from: http://www.cancer.org/cancer/skincancer-melanoma/detailedguide/melanoma-skin-cancer-risk-factors.

29. Gandini, S., F. Sera, M.S. Cattaruzza, P. Pasquini, R. Zanetti, C. Masini, P. Boyle, and C.F. Melchi, *Meta-analysis of risk factors for cutaneous melanoma: III. Family history, actinic damage and phenotypic factors.* Eur J Cancer, 2005. **41**(14): p. 2040-59.

30. Bliss, J.M., D. Ford, A.J. Swerdlow, B.K. Armstrong, M. Cristofolini, J.M. Elwood, A. Green, E.A. Holly, T. Mack, R.M. MacKie, and et al., *Risk of cutaneous melanoma associated with*

pigmentation characteristics and freckling: systematic overview of 10 case-control studies. The International Melanoma Analysis Group (IMAGE). Int J Cancer, 1995. **62**(4): p. 367-76.

31.   Gandini, S., F. Sera, M.S. Cattaruzza, P. Pasquini, D. Abeni, P. Boyle, and C.F. Melchi, *Meta-analysis of risk factors for cutaneous melanoma: I. Common and atypical naevi.* Eur J Cancer, 2005. **41**(1): p. 28-44.

32.   Abern, M.R., M. Tsivian, C.L. Coogan, H.L. Kaufman, and T.J. Polascik, *Characteristics of patients diagnosed with both melanoma and renal cell cancer.* Cancer Causes Control, 2013. **24**(11): p. 1925-33.

33.   Pappo, A.S., G.T. Armstrong, W. Liu, D.K. Srivastava, A. McDonald, W.M. Leisenring, S. Hammond, M. Stovall, J.P. Neglia, and L.L. Robison, *Melanoma as a subsequent neoplasm in adult survivors of childhood cancer: a report from the childhood cancer survivor study.* Pediatr Blood Cancer, 2013. **60**(3): p. 461-6.

34.   Lindelöf, B., B. Sigurgeirsson, H. Gäbel, and R.S. Stern, *Incidence of skin cancer in 5356 patients following organ transplantation.* British Journal of Dermatology, 2000. **143**(3): p. 513-519.

35.   Linos, E., S.M. Swetter, M.G. Cockburn, G.A. Colditz, and C.A. Clarke, *Increasing Burden of Melanoma in the United States.* J Invest Dermatol, 2009. **129**(7): p. 1666-1674.

36.   Norris, W., *Eight Cases of Melanosis with Pathological and Therapeutic Remarks on that Disease.*, ed. G. Brown, Roberts. 1857, London: Longman.

37.   Geller, A.C., D.R. Miller, G. Annas, M. Demierre, B.A. Gilchrest, and H.K. Koh, *Melanoma incidence and mortality among us whites, 1969-1999.* JAMA, 2002. **288**(14): p. 1719-1720.

38.   Meyle, K.D. and P. Guldberg, *Genetic risk factors for melanoma.* Hum Genet, 2009. **126**(4): p. 499-510.

39.   Goldstein, A.M., M. Chan, M. Harland, N.K. Hayward, F. Demenais, D.T. Bishop, E. Azizi, W. Bergman, G. Bianchi-Scarra, W. Bruno, D. Calista, L.A. Albright, V. Chaudru, A. Chompret, F. Cuellar, D.E. Elder, P. Ghiorzo, E.M. Gillanders, N.A. Gruis, J. Hansson, D. Hogg, E.A. Holland, P.A. Kanetsky, R.F. Kefford, M.T. Landi, J. Lang, S.A. Leachman, R.M. MacKie, V. Magnusson, G.J. Mann, J.N. Bishop, J.M. Palmer, S. Puig, J.A. Puig-Butille, M. Stark, H. Tsao, M.A. Tucker, L. Whitaker, E. Yakobson, G. Lund Melanoma Study, and C. Melanoma Genetics, *Features associated with germline CDKN2A mutations: a GenoMEL study of melanoma-prone families from three continents.* J Med Genet, 2007. **44**(2): p. 99-106.

40.   Ibarrola-Villava, M., H.H. Hu, M. Guedj, L.P. Fernandez, V. Descamps, N. Basset-Seguin, M. Bagot, A. Benssussan, P. Saiag, M.C. Fargnoli, K. Peris, J.A. Aviles, A. Lluch, G. Ribas, and N. Soufir, *MC1R, SLC45A2 and TYR genetic variants involved in melanoma susceptibility in southern European populations: results from a meta-analysis.* Eur J Cancer, 2012. **48**(14): p. 2183-91.

41.   Duffy, D.L., Z.Z. Zhao, R.A. Sturm, N.K. Hayward, N.G. Martin, and G.W. Montgomery, *Multiple pigmentation gene polymorphisms account for a substantial proportion of risk of cutaneous malignant melanoma.* J Invest Dermatol, 2010. **130**(2): p. 520-8.

42.   Gudbjartsson, D.F., P. Sulem, S.N. Stacey, A.M. Goldstein, T. Rafnar, B. Sigurgeirsson, K.R. Benediktsdottir, K. Thorisdottir, R. Ragnarsson, S.G. Sveinsdottir, V. Magnusson, A. Lindblom, K. Kostulas, R. Botella-Estrada, V. Soriano, P. Juberias, M. Grasa, B. Saez, R. Andres, D. Scherer, P. Rudnai, E. Gurzau, K. Koppova, L.A. Kiemeney, M. Jakobsdottir, S. Steinberg, A. Helgason, S. Gretarsdottir, M.A. Tucker, J.I. Mayordomo, E. Nagore, R. Kumar, J. Hansson, J.H. Olafsson, J. Gulcher, A. Kong, U. Thorsteinsdottir, and K. Stefansson, *ASIP and TYR pigmentation variants associate with cutaneous melanoma and basal cell carcinoma.* Nat Genet, 2008. **40**(7): p. 886-91.

43. Barrett, J.H., J.C. Taylor, C. Bright, M. Harland, A.M. Dunning, L.A. Akslen, P.A. Andresen, M.F. Avril, E. Azizi, G. Bianchi Scarra, M. Brossard, K.M. Brown, T. Debniak, D.E. Elder, E. Friedman, P. Ghiorzo, E.M. Gillanders, N.A. Gruis, J. Hansson, P. Helsing, M. Hocevar, V. Hoiom, C. Ingvar, M.T. Landi, J. Lang, G.M. Lathrop, J. Lubinski, R.M. Mackie, A. Molven, S. Novakovic, H. Olsson, S. Puig, J.A. Puig-Butille, N. van der Stoep, R. van Doorn, W. van Workum, A.M. Goldstein, P.A. Kanetsky, P.D. Pharoah, F. Demenais, N.K. Hayward, J.A. Newton Bishop, D.T. Bishop, M.M. Iles, and M.E.L.C. Geno, *Fine mapping of genetic susceptibility loci for melanoma reveals a mixture of single variant and multiple variant regions.* Int J Cancer, 2015. **136**(6): p. 1351-60.

44. Read, J., K.A. Wadt, and N.K. Hayward, *Melanoma genetics.* J Med Genet, 2015.

45. Hodis, E., I.R. Watson, G.V. Kryukov, S.T. Arold, M. Imielinski, J.P. Theurillat, E. Nickerson, D. Auclair, L. Li, C. Place, D. Dicara, A.H. Ramos, M.S. Lawrence, K. Cibulskis, A. Sivachenko, D. Voet, G. Saksena, N. Stransky, R.C. Onofrio, W. Winckler, K. Ardlie, N. Wagle, J. Wargo, K. Chong, D.L. Morton, K. Stemke-Hale, G. Chen, M. Noble, M. Meyerson, J.E. Ladbury, M.A. Davies, J.E. Gershenwald, S.N. Wagner, D.S. Hoon, D. Schadendorf, E.S. Lander, S.B. Gabriel, G. Getz, L.A. Garraway, and L. Chin, *A landscape of driver mutations in melanoma.* Cell, 2012. **150**(2): p. 251-63.

46. National Cancer Institute. *"Common Moles, Dysplastic Nevi, and Risk of Melanoma"*. Skin Cancer 2011 30 June 2015; Available from: http://www.cancer.gov/types/skin/moles-fact-sheet.

47. Longo, C., C. Rito, F. Beretti, A.M. Cesinaro, J. Piñeiro-Maceira, S. Seidenari, and G. Pellacani, *De novo melanoma and melanoma arising from pre-existing nevus: In vivo morphologic differences as evaluated by confocal microscopy.* Journal of the American Academy of Dermatology, 2011. **65**(3): p. 604-614.

48. National Cancer Institute. *Genetics of Skin Cancer* 2015 21 July 2015 - 9:40am.

49. Feit, N.E., S.W. Dusza, and A.A. Marghoob, *Melanomas detected with the aid of total cutaneous photography.* Br J Dermatol, 2004. **150**(4): p. 706-14.

50. Ascierto, P.A., R.A. Satriano, G. Palmieri, R. Parasole, L. Bosco, and G. Castello, *Epiluminescence microscopy as a useful approach in the early diagnosis of cutaneous malignant melanoma.* Melanoma Res, 1998. **8**(6): p. 529-37.

51. Gaynor, R., H.R. Herschman, R. Irie, P. Jones, D. Morton, and A. Cochran, *S100 protein: a marker for human malignant melanomas?* Lancet, 1981. **1**(8225): p. 869-71.

52. Chen, Y.T., E. Stockert, A. Jungbluth, S. Tsang, K.A. Coplan, M.J. Scanlan, and L.J. Old, *Serological analysis of Melan-A(MART-1), a melanocyte-specific protein homogeneously expressed in human melanomas.* Proc Natl Acad Sci U S A, 1996. **93**(12): p. 5915-9.

53. Wick, M.R., P.E. Swanson, and A. Rocamora, *Recognition of malignant melanoma by monoclonal antibody HMB-45. An immunohistochemical study of 200 paraffin-embedded cutaneous tumors.* J Cutan Pathol, 1988. **15**(4): p. 201-7.

54. Ordonez, N.G., X.L. Ji, and R.C. Hickey, *Comparison of HMB-45 monoclonal antibody and S-100 protein in the immunohistochemical diagnosis of melanoma.* Am J Clin Pathol, 1988. **90**(4): p. 385-90.

55. Willis, B.C., G. Johnson, J. Wang, and C. Cohen, *SOX10: a useful marker for identifying metastatic melanoma in sentinel lymph nodes.* Appl Immunohistochem Mol Morphol, 2015. **23**(2): p. 109-12.

56. Salazar-Onfray, F., M. Lopez, A. Lundqvist, A. Aguirre, A. Escobar, A. Serrano, C. Korenblit, M. Petersson, V. Chhajlani, O. Larsson, and R. Kiessling, *Tissue distribution and differential expression of melanocortin 1 receptor, a malignant melanoma marker.* Br J Cancer, 2002. **87**(4): p. 414-22.

57. Abbas, O., D.D. Miller, and J. Bhawan, *Cutaneous malignant melanoma: update on diagnostic and prognostic biomarkers.* Am J Dermatopathol, 2014. **36**(5): p. 363-79.

58. Balch, C.M., J.E. Gershenwald, S.J. Soong, J.F. Thompson, M.B. Atkins, D.R. Byrd, A.C. Buzaid, A.J. Cochran, D.G. Coit, S. Ding, A.M. Eggermont, K.T. Flaherty, P.A. Gimotty, J.M. Kirkwood, K.M. McMasters, M.C. Mihm, Jr., D.L. Morton, M.I. Ross, A.J. Sober, and V.K. Sondak, *Final version of 2009 AJCC melanoma staging and classification.* J Clin Oncol, 2009. **27**(36): p. 6199-206.

59. Balch, C.M., *Cutaneous melanoma.* 5th ed. 2009, St. Louis: Quality Medical Pub. xxix, 921 p.

60. Gershenwald, J.E., S.J. Soong, and C.M. Balch, *2010 TNM staging system for cutaneous melanoma...and beyond.* Ann Surg Oncol, 2010. **17**(6): p. 1475-7.

61. Breslow, A., *Thickness, cross-sectional areas and depth of invasion in the prognosis of cutaneous melanoma.* Ann Surg, 1970. **172**(5): p. 902-8.

62. Balch, C.M., A.C. Buzaid, S.J. Soong, M.B. Atkins, N. Cascinelli, D.G. Coit, I.D. Fleming, J.E. Gershenwald, A. Houghton, Jr., J.M. Kirkwood, K.M. McMasters, M.F. Mihm, D.L. Morton, D.S. Reintgen, M.I. Ross, A. Sober, J.A. Thompson, and J.F. Thompson, *Final version of the American Joint Committee on Cancer staging system for cutaneous melanoma.* J Clin Oncol, 2001. **19**(16): p. 3635-48.

63. Lens, M.B., M. Dawes, J.A. Newton-Bishop, and T. Goodacre, *Tumour thickness as a predictor of occult lymph node metastases in patients with stage I and II melanoma undergoing sentinel lymph node biopsy.* Br J Surg, 2002. **89**(10): p. 1223-7.

64. Sondak, V.K., J.M. Taylor, M.S. Sabel, Y. Wang, L. Lowe, A.C. Grover, A.E. Chang, A.M. Yahanda, J. Moon, and T.M. Johnson, *Mitotic rate and younger age are predictors of sentinel lymph node positivity: lessons learned from the generation of a probabilistic model.* Ann Surg Oncol, 2004. **11**(3): p. 247-58.

65. Clark, W.H., Jr., L. From, E.A. Bernardino, and M.C. Mihm, *The histogenesis and biologic behavior of primary human malignant melanomas of the skin.* Cancer Res, 1969. **29**(3): p. 705-27.

66. Deichmann, M., A. Benner, M. Bock, A. Jackel, K. Uhl, V. Waldmann, and H. Naher, *S100-Beta, melanoma-inhibiting activity, and lactate dehydrogenase discriminate progressive from nonprogressive American Joint Committee on Cancer stage IV melanoma.* J Clin Oncol, 1999. **17**(6): p. 1891-6.

67. McGovern, V.J., M.C. Mihm, Jr., C. Bailly, J.C. Booth, W.H. Clark, Jr., A.J. Cochran, E.G. Hardy, J.D. Hicks, A. Levene, M.G. Lewis, J.H. Little, and G.W. Milton, *The classification of malignant melanoma and its histologic reporting.* Cancer, 1973. **32**(6): p. 1446-57.

68. Clark, W.H., Jr., D.E. Elder, D.t. Guerry, M.N. Epstein, M.H. Greene, and M. Van Horn, *A study of tumor progression: the precursor lesions of superficial spreading and nodular melanoma.* Hum Pathol, 1984. **15**(12): p. 1147-65.

69. Hanahan, D. and R.A. Weinberg, *The hallmarks of cancer.* Cell, 2000. **100**(1): p. 57-70.

70. Davies, H., G.R. Bignell, C. Cox, P. Stephens, S. Edkins, S. Clegg, J. Teague, H. Woffendin, M.J. Garnett, W. Bottomley, N. Davis, E. Dicks, R. Ewing, Y. Floyd, K. Gray, S. Hall, R. Hawes, J. Hughes, V. Kosmidou, A. Menzies, C. Mould, A. Parker, C. Stevens, S. Watt, S. Hooper, R. Wilson, H. Jayatilake, B.A. Gusterson, C. Cooper, J. Shipley, D. Hargrave, K. Pritchard-Jones, N. Maitland, G. Chenevix-Trench, G.J. Riggins, D.D. Bigner, G. Palmieri, A. Cossu, A. Flanagan, A. Nicholson, J.W. Ho, S.Y. Leung, S.T. Yuen, B.L. Weber, H.F. Seigler, T.L. Darrow, H. Paterson, R. Marais, C.J. Marshall, R. Wooster, M.R. Stratton, and P.A. Futreal, *Mutations of the BRAF gene in human cancer.* Nature, 2002. **417**(6892): p. 949-54.

71.   Dhomen, N. and R. Marais, *BRAF signaling and targeted therapies in melanoma.* Hematol Oncol Clin North Am, 2009. **23**(3): p. 529-45, ix.

72.   Rubinstein, J.C., M. Sznol, A.C. Pavlick, S. Ariyan, E. Cheng, A. Bacchiocchi, H.M. Kluger, D. Narayan, and R. Halaban, *Incidence of the V600K mutation among melanoma patients with BRAF mutations, and potential therapeutic response to the specific BRAF inhibitor PLX4032.* J Transl Med, 2010. **8**: p. 67.

73.   Long, G.V., A.M. Menzies, A.M. Nagrial, L.E. Haydu, A.L. Hamilton, G.J. Mann, T.M. Hughes, J.F. Thompson, R.A. Scolyer, and R.F. Kefford, *Prognostic and clinicopathologic associations of oncogenic BRAF in metastatic melanoma.* J Clin Oncol, 2011. **29**(10): p. 1239-46.

74.   Pollock, P.M., U.L. Harper, K.S. Hansen, L.M. Yudt, M. Stark, C.M. Robbins, T.Y. Moses, G. Hostetter, U. Wagner, J. Kakareka, G. Salem, T. Pohida, P. Heenan, P. Duray, O. Kallioniemi, N.K. Hayward, J.M. Trent, and P.S. Meltzer, *High frequency of BRAF mutations in nevi.* Nat Genet, 2003. **33**(1): p. 19-20.

75.   Padua, R.A., N. Barrass, and G.A. Currie, *A novel transforming gene in a human malignant melanoma cell line.* Nature, 1984. **311**(5987): p. 671-3.

76.   Thomas, N.E., *BRAF somatic mutations in malignant melanoma and melanocytic naevi.* Melanoma Res, 2006. **16**(2): p. 97-103.

77.   Colombino, M., A. Lissia, M. Capone, V. De Giorgi, D. Massi, I. Stanganelli, E. Fonsatti, M. Maio, G. Botti, C. Caraco, N. Mozzillo, P.A. Ascierto, A. Cossu, and G. Palmieri, *Heterogeneous distribution of BRAF/NRAS mutations among Italian patients with advanced melanoma.* J Transl Med, 2013. **11**: p. 202.

78.   Hocker, T. and H. Tsao, *Ultraviolet radiation and melanoma: a systematic review and analysis of reported sequence variants.* Hum Mutat, 2007. **28**(6): p. 578-88.

79.   Goldinger, S.M., C. Murer, P. Stieger, and R. Dummer, *Targeted therapy in melanoma - the role of BRAF, RAS and KIT mutations.* EJC Suppl, 2013. **11**(2): p. 92-6.

80.   Karakousis, C.P., C.M. Balch, M.M. Urist, M.M. Ross, T.J. Smith, and A.A. Bartolucci, *Local recurrence in malignant melanoma: long-term results of the multiinstitutional randomized surgical trial.* Ann Surg Oncol, 1996. **3**(5): p. 446-52.

81.   Morton, D.L., J.F. Thompson, A.J. Cochran, N. Mozzillo, R. Elashoff, R. Essner, O.E. Nieweg, D.F. Roses, H.J. Hoekstra, C.P. Karakousis, D.S. Reintgen, B.J. Coventry, E.C. Glass, H.J. Wang, and M. Group, *Sentinel-node biopsy or nodal observation in melanoma.* N Engl J Med, 2006. **355**(13): p. 1307-17.

82.   Nguyen, D.X., P.D. Bos, and J. Massague, *Metastasis: from dissemination to organ-specific colonization.* Nat Rev Cancer, 2009. **9**(4): p. 274-84.

83.   Puzanov, I., R.K. Amaravadi, G.A. McArthur, K.T. Flaherty, P.B. Chapman, J.A. Sosman, A. Ribas, M. Shackleton, P. Hwu, B. Chmielowski, K.B. Nolop, P.S. Lin, and K.B. Kim, *Long-term outcome in BRAF(V600E) melanoma patients treated with vemurafenib: Patterns of disease progression and clinical management of limited progression.* Eur J Cancer, 2015. **51**(11): p. 1435-43.

84.   Schadendorf, D., F.S. Hodi, C. Robert, J.S. Weber, K. Margolin, O. Hamid, D. Patt, T.T. Chen, D.M. Berman, and J.D. Wolchok, *Pooled Analysis of Long-Term Survival Data From Phase II and Phase III Trials of Ipilimumab in Unresectable or Metastatic Melanoma.* J Clin Oncol, 2015. **33**(17): p. 1889-94.

85.   Haass, N.K., K.S. Smalley, L. Li, and M. Herlyn, *Adhesion, migration and communication in melanocytes and melanoma.* Pigment Cell Res, 2005. **18**(3): p. 150-9.

86.   Elder, D.E., *Pathology of melanoma.* Clin Cancer Res, 2006. **12**(7 Pt 2): p. 2308s-2311s.

87.   Li, G., K. Satyamoorthy, and M. Herlyn, *N-cadherin-mediated intercellular interactions promote survival and migration of melanoma cells.* Cancer Res, 2001. **61**(9): p. 3819-25.

88.   Hsu, M.Y., M.J. Wheelock, K.R. Johnson, and M. Herlyn, *Shifts in cadherin profiles between human normal melanocytes and melanomas.* J Investig Dermatol Symp Proc, 1996. **1**(2): p. 188-94.

89.   Chiang, A.C. and J. Massague, *Molecular basis of metastasis.* N Engl J Med, 2008. **359**(26): p. 2814-23.

90.   Sanz-Moreno, V., G. Gadea, J. Ahn, H. Paterson, P. Marra, S. Pinner, E. Sahai, and C.J. Marshall, *Rac activation and inactivation control plasticity of tumor cell movement.* Cell, 2008. **135**(3): p. 510-23.

91.   Egeblad, M. and Z. Werb, *New functions for the matrix metalloproteinases in cancer progression.* Nat Rev Cancer, 2002. **2**(3): p. 161-74.

92.   Holmgren, L., M.S. O'Reilly, and J. Folkman, *Dormancy of micrometastases: balanced proliferation and apoptosis in the presence of angiogenesis suppression.* Nat Med, 1995. **1**(2): p. 149-53.

93.   Paterlini-Brechot, P. and N.L. Benali, *Circulating tumor cells (CTC) detection: clinical impact and future directions.* Cancer Lett, 2007. **253**(2): p. 180-204.

94.   Fuertes, M.B., M.V. Girart, L.L. Molinero, C.I. Domaica, L.E. Rossi, M.M. Barrio, J. Mordoh, G.A. Rabinovich, and N.W. Zwirner, *Intracellular retention of the NKG2D ligand MHC class I chain-related gene A in human melanomas confers immune privilege and prevents NK cell-mediated cytotoxicity.* J Immunol, 2008. **180**(7): p. 4606-14.

95.   Lang, D., J.B. Mascarenhas, and C.R. Shea, *Melanocytes, melanocyte stem cells, and melanoma stem cells.* Clinics in dermatology, 2013. **31**(2): p. 166-178.

96.   Wan, L., K. Pantel, and Y. Kang, *Tumor metastasis: moving new biological insights into the clinic.* Nat Med, 2013. **19**(11): p. 1450-1464.

97.   Garraway, L.A., H.R. Widlund, M.A. Rubin, G. Getz, A.J. Berger, S. Ramaswamy, R. Beroukhim, D.A. Milner, S.R. Granter, J. Du, C. Lee, S.N. Wagner, C. Li, T.R. Golub, D.L. Rimm, M.L. Meyerson, D.E. Fisher, and W.R. Sellers, *Integrative genomic analyses identify MITF as a lineage survival oncogene amplified in malignant melanoma.* Nature, 2005. **436**(7047): p. 117-22.

98.   Klinac, D., E.S. Gray, J.B. Freeman, A. Reid, S. Bowyer, M. Millward, and M. Ziman, *Monitoring changes in circulating tumour cells as a prognostic indicator of overall survival and treatment response in patients with metastatic melanoma.* BMC Cancer, 2014. **14**: p. 423.

99.   Rahmathulla, G., S.A. Toms, and R.J. Weil, *The Molecular Biology of Brain Metastasis.* Journal of Oncology, 2012. **2012**: p. 16.

100.   Balch, C.M., M.M. Urist, C.P. Karakousis, T.J. Smith, W.J. Temple, K. Drzewiecki, W.R. Jewell, A.A. Bartolucci, M.C. Mihm, Jr., R. Barnhill, and et al., *Efficacy of 2-cm surgical margins for intermediate-thickness melanomas (1 to 4 mm). Results of a multi-institutional randomized surgical trial.* Ann Surg, 1993. **218**(3): p. 262-7; discussion 267-9.

101.   Balch, C.M., S.J. Soong, T. Smith, M.I. Ross, M.M. Urist, C.P. Karakousis, W.J. Temple, M.C. Mihm, R.L. Barnhill, W.R. Jewell, H.J. Wanebo, R. Desmond, and T. Investigators from the Intergroup Melanoma Surgical, *Long-term results of a prospective surgical trial comparing 2 cm vs. 4 cm excision margins for 740 patients with 1-4 mm melanomas.* Ann Surg Oncol, 2001. **8**(2): p. 101-8.

102. Serna-Macías, J.A., N.R. Sánchez-Casas, A.E. Morató-López, M.N. Reyes-García, and J.M. Isusi-Alcazar, *Melanoma maligno cutáneo. El rol del PET-CT.* Gaceta Mexicana de Oncología, 2012. **11**(02): p. 104-112.

103. Moore, D.A., G. Saldanha, A. Ehdode, M.Z. Mughal, L. Potter, L. Dyall, and J.H. Pringle, *Duplex Ratio Tests as Diagnostic Biomarkers in Malignant Melanoma.* J Mol Diagn, 2015. **17**(5): p. 616-22.

104. Weinstein, D., J. Leininger, C. Hamby, and B. Safai, *Diagnostic and Prognostic Biomarkers in Melanoma.* The Journal of Clinical and Aesthetic Dermatology, 2014. **7**(6): p. 13-24.

105. Robert, C., B. Karaszewska, J. Schachter, P. Rutkowski, A. Mackiewicz, D. Stroiakovski, M. Lichinitser, R. Dummer, F. Grange, L. Mortier, V. Chiarion-Sileni, K. Drucis, I. Krajsova, A. Hauschild, P. Lorigan, P. Wolter, G.V. Long, K. Flaherty, P. Nathan, A. Ribas, A.-M. Martin, P. Sun, W. Crist, J. Legos, S.D. Rubin, S.M. Little, and D. Schadendorf, *Improved Overall Survival in Melanoma with Combined Dabrafenib and Trametinib.* New England Journal of Medicine, 2015. **372**(1): p. 30-39.

106. Larkin, J., V. Chiarion-Sileni, R. Gonzalez, J.J. Grob, C.L. Cowey, C.D. Lao, D. Schadendorf, R. Dummer, M. Smylie, P. Rutkowski, P.F. Ferrucci, A. Hill, J. Wagstaff, M.S. Carlino, J.B. Haanen, M. Maio, I. Marquez-Rodas, G.A. McArthur, P.A. Ascierto, G.V. Long, M.K. Callahan, M.A. Postow, K. Grossmann, M. Sznol, B. Dreno, L. Bastholt, A. Yang, L.M. Rollin, C. Horak, F.S. Hodi, and J.D. Wolchok, *Combined Nivolumab and Ipilimumab or Monotherapy in Untreated Melanoma.* N Engl J Med, 2015. **373**(1): p. 23-34.

107. Luke, J.J., K.T. Flaherty, A. Ribas, and G.V. Long, *Targeted agents and immunotherapies: optimizing outcomes in melanoma.* Nat Rev Clin Oncol, 2017. **advance online publication**.

108. Carlino, M.S. and G.V. Long, *Is chemotherapy still an option in the treatment of melanoma?* Ann Oncol, 2015.

109. Chapman, P.B., A. Hauschild, C. Robert, J.B. Haanen, P. Ascierto, J. Larkin, R. Dummer, C. Garbe, A. Testori, M. Maio, D. Hogg, P. Lorigan, C. Lebbe, T. Jouary, D. Schadendorf, A. Ribas, S.J. O'Day, J.A. Sosman, J.M. Kirkwood, A.M. Eggermont, B. Dreno, K. Nolop, J. Li, B. Nelson, J. Hou, R.J. Lee, K.T. Flaherty, G.A. McArthur, and B.-S. Group, *Improved survival with vemurafenib in melanoma with BRAF V600E mutation.* N Engl J Med, 2011. **364**(26): p. 2507-16.

110. Gilmartin, A.G., M.R. Bleam, A. Groy, K.G. Moss, E.A. Minthorn, S.G. Kulkarni, C.M. Rominger, S. Erskine, K.E. Fisher, J. Yang, F. Zappacosta, R. Annan, D. Sutton, and S.G. Laquerre, *GSK1120212 (JTP-74057) is an inhibitor of MEK activity and activation with favorable pharmacokinetic properties for sustained in vivo pathway inhibition.* Clin Cancer Res, 2011. **17**(5): p. 989-1000.

111. Schindler, A.K. and M.A. Postow, *Current options and future directions in the systemic treatment of metastatic melanoma.* J Community Support Oncol, 2014. **12**(1): p. 20-6.

112. Green, J. and C. Ariyan, *Update on immunotherapy in melanoma.* Surg Oncol Clin N Am, 2015. **24**(2): p. 337-46.

113. Flaherty, K.T., I. Puzanov, K.B. Kim, A. Ribas, G.A. McArthur, J.A. Sosman, P.J. O'Dwyer, R.J. Lee, J.F. Grippo, K. Nolop, and P.B. Chapman, *Inhibition of mutated, activated BRAF in metastatic melanoma.* N Engl J Med, 2010. **363**(9): p. 809-19.

114. Claveau, J., V. Ho, and T. Petrella, *Metastatic melanoma: optimizing outcomes by managing dermatologic toxicities associated with novel therapies.* Skin Therapy Lett, 2014. **19**(2): p. 1-4.

115. Flaherty, K.T., J.R. Infante, A. Daud, R. Gonzalez, R.F. Kefford, J. Sosman, O. Hamid, L. Schuchter, J. Cebon, N. Ibrahim, R. Kudchadkar, H.A. Burris, 3rd, G. Falchook, A. Algazi, K.

Lewis, G.V. Long, I. Puzanov, P. Lebowitz, A. Singh, S. Little, P. Sun, A. Allred, D. Ouellet, K.B. Kim, K. Patel, and J. Weber, *Combined BRAF and MEK inhibition in melanoma with BRAF V600 mutations.* N Engl J Med, 2012. **367**(18): p. 1694-703.

116. Ascierto, P.A., M. Del Vecchio, C. Robert, A. Mackiewicz, V. Chiarion-Sileni, A.M.A. Fernandez, H. Schmidt, C. Lebbe, L. Bastholt, O. Hamid, P. Rutkowski, C. McNeil, C. Garbe, C. Loquai, B. Dreno, L. Thomas, J.J. Grob, D. Hennicken, A. Qureshi, and M. Maio, *Overall survival (OS) and safety results from a phase 3 trial of ipilimumab (IPI) at 3 mg/kg vs 10 mg/kg in patients with metastatic melanoma (MEL).* Annals of Oncology, 2016. **27**(suppl_6): p. 1106O-1106O.

117. Niezgoda, A., P. Niezgoda, and R. Czajkowski, *Novel Approaches to Treatment of Advanced Melanoma: A Review on Targeted Therapy and Immunotherapy.* Biomed Res Int, 2015. **2015**.

118. Khoja, L., M.O. Butler, S.P. Kang, S. Ebbinghaus, and A.M. Joshua, *Pembrolizumab.* J Immunother Cancer, 2015. **3**: p. 36.

119. Bayless, H. and S. Schneider, *Nivolumab: Immunotherapy in Malignant Melanoma.* Clin J Oncol Nurs, 2015. **19**(4): p. 430-2.

120. Robert, C., J. Schachter, G.V. Long, A. Arance, J.J. Grob, L. Mortier, A. Daud, M.S. Carlino, C. McNeil, M. Lotem, J. Larkin, P. Lorigan, B. Neyns, C.U. Blank, O. Hamid, C. Mateus, R. Shapira-Frommer, M. Kosh, H. Zhou, N. Ibrahim, S. Ebbinghaus, A. Ribas, and K.-. investigators, *Pembrolizumab versus Ipilimumab in Advanced Melanoma.* N Engl J Med, 2015. **372**(26): p. 2521-32.

121. Inozume, T., T. Yaguchi, J. Furuta, K. Harada, Y. Kawakami, and S. Shimada, *Melanoma Cells Control Anti-Melanoma CTL Responses via Interaction between TIGIT and CD155 in the Effector Phase.* J Invest Dermatol, 2015.

122. Rogiers, A., J.J. van den Oord, M. Garmyn, M. Stas, C. Kenis, H. Wildiers, J.C. Marine, and P. Wolter, *Novel Therapies for Metastatic Melanoma: An Update on Their Use in Older Patients.* Drugs Aging, 2015. **32**(10): p. 821-34.

123. Ito, A., S. Kondo, K. Tada, and S. Kitano, *Clinical Development of Immune Checkpoint Inhibitors.* Biomed Res Int, 2015. **2015**: p. 605478.

124. Sosman, J.A., K.B. Kim, L. Schuchter, R. Gonzalez, A.C. Pavlick, J.S. Weber, G.A. McArthur, T.E. Hutson, S.J. Moschos, K.T. Flaherty, P. Hersey, R. Kefford, D. Lawrence, I. Puzanov, K.D. Lewis, R.K. Amaravadi, B. Chmielowski, H.J. Lawrence, Y. Shyr, F. Ye, J. Li, K.B. Nolop, R.J. Lee, A.K. Joe, and A. Ribas, *Survival in BRAF V600-mutant advanced melanoma treated with vemurafenib.* N Engl J Med, 2012. **366**(8): p. 707-14.

125. Hodi, F.S., S.J. O'Day, D.F. McDermott, R.W. Weber, J.A. Sosman, J.B. Haanen, R. Gonzalez, C. Robert, D. Schadendorf, J.C. Hassel, W. Akerley, A.J. van den Eertwegh, J. Lutzky, P. Lorigan, J.M. Vaubel, G.P. Linette, D. Hogg, C.H. Ottensmeier, C. Lebbe, C. Peschel, I. Quirt, J.I. Clark, J.D. Wolchok, J.S. Weber, J. Tian, M.J. Yellin, G.M. Nichol, A. Hoos, and W.J. Urba, *Improved survival with ipilimumab in patients with metastatic melanoma.* N Engl J Med, 2010. **363**(8): p. 711-23.

126. Carlson, J.A., A. Slominski, G.P. Linette, M.C. Mihm, Jr., and J.S. Ross, *Biomarkers in melanoma: staging, prognosis and detection of early metastases.* Expert Rev Mol Diagn, 2003. **3**(3): p. 303-30.

127. Solassol, J., A. Du-Thanh, T. Maudelonde, and B. Guillot, *Serum proteomic profiling reveals potential biomarkers for cutaneous malignant melanoma.* Int J Biol Markers, 2011. **26**(2): p. 82-7.

128. Brochez, L. and J.M. Naeyaert, *Serological markers for melanoma.* Br J Dermatol, 2000. **143**(2): p. 256-68.

129. Quaglino, P., S. Osella-Abate, N. Cappello, M. Ortoncelli, T. Nardo, M.T. Fierro, F. Cavallo, P. Savoia, and M.G. Bernengo, *Prognostic relevance of baseline and sequential peripheral blood tyrosinase expression in 200 consecutive advanced metastatic melanoma patients.* Melanoma Res, 2007. **17**(2): p. 75-82.

130. Ugurel, S., G. Rappl, W. Tilgen, and U. Reinhold, *Increased serum concentration of angiogenic factors in malignant melanoma patients correlates with tumor progression and survival.* J Clin Oncol, 2001. **19**(2): p. 577-83.

131. Maier, T., R.P. Laubender, R.A. Sturm, A. Klingenstein, H.C. Korting, T. Ruzicka, and C. Berking, *Osteopontin expression in plasma of melanoma patients and in melanocytic tumours.* Journal of the European Academy of Dermatology and Venereology, 2012. **26**(9): p. 1084-1091.

132. Schmidt, H., J.S. Johansen, J. Gehl, P.F. Geertsen, K. Fode, and H. von der Maase, *Elevated serum level of YKL-40 is an independent prognostic factor for poor survival in patients with metastatic melanoma.* Cancer, 2006. **106**(5): p. 1130-1139.

133. Díaz-Lagares, A., E. Alegre, A. Arroyo, M. González-Cao, M. Zudaire, S. Viteri, S. Martín-Algarra, and A. González, *Evaluation of multiple serum markers in advanced melanoma.* Tumor Biology, 2011. **32**(6): p. 1155-1161.

134. Kruijff, S., E. Bastiaannet, A.C. Muller Kobold, R.J. van Ginkel, A.J.H. Suurmeijer, and H.J. Hoekstra, *S-100B Concentrations Predict Disease-Free Survival in Stage III Melanoma Patients.* Annals of Surgical Oncology, 2009. **16**(12): p. 3455-3462.

135. Sanmamed, M.F., O. Carranza-Rua, C. Alfaro, C. Oñate, S. Martín-Algarra, G. Perez, S.F. Landazuri, Á. Gonzalez, S. Gross, I. Rodriguez, C. Muñoz-Calleja, M. Rodríguez-Ruiz, B. Sangro, J.M. López-Picazo, M. Rizzo, G. Mazzolini, J.I. Pascual, M.P. Andueza, J.L. Perez-Gracia, and I. Melero, *Serum Interleukin-8 Reflects Tumor Burden and Treatment Response across Malignancies of Multiple Tissue Origins.* Clinical Cancer Research, 2014. **20**(22): p. 5697-5707.

136. Becker, M.R., M.D. Siegelin, R. Rompel, A.H. Enk, and T. Gaiser, *COX-2 expression in malignant melanoma: a novel prognostic marker?* Melanoma Res, 2009. **19**(1): p. 8-16.

137. Reynolds, S.R., I.J. Vergilis, M. Szarek, S. Ferrone, and J.C. Bystryn, *Cytoplasmic melanoma-associated antigen (CYT-MAA) serum level in patients with melanoma: a potential marker of response to immunotherapy?* Int J Cancer, 2006. **119**(1): p. 157-61.

138. Karagiannis, P., M. Fittall, and S.N. Karagiannis, *Evaluating biomarkers in melanoma.* Front Oncol, 2014. **4**: p. 383.

139. Ramskold, D., S. Luo, Y.C. Wang, R. Li, Q. Deng, O.R. Faridani, G.A. Daniels, I. Khrebtukova, J.F. Loring, L.C. Laurent, G.P. Schroth, and R. Sandberg, *Full-length mRNA-Seq from single-cell levels of RNA and individual circulating tumor cells.* Nat Biotechnol, 2012. **30**(8): p. 777-82.

140. Ashworth, T.R., *A case of cancer in which cells similar to those in the tumours were seen in the blood after death.* Med J Aust, 1869. **14**: p. 146-147.

141. Smith, B., P. Selby, J. Southgate, K. Pittman, C. Bradley, and G.E. Blair, *Detection of melanoma cells in peripheral blood by means of reverse transcriptase and polymerase chain reaction.* Lancet, 1991. **338**(8777): p. 1227-9.

142. Friedl, P. and S. Alexander, *Cancer invasion and the microenvironment: plasticity and reciprocity.* Cell, 2011. **147**(5): p. 992-1009.

143. Camara, O., A. Kavallaris, H. Noschel, M. Rengsberger, C. Jorke, and K. Pachmann, *Seeding of epithelial cells into circulation during surgery for breast cancer: the fate of malignant and benign mobilized cells.* World J Surg Oncol, 2006. **4**: p. 67.

144. Lawson, D.A., N.R. Bhakta, K. Kessenbrock, K.D. Prummel, Y. Yu, K. Takai, A. Zhou, H. Eyob, S. Balakrishnan, C.-Y. Wang, P. Yaswen, A. Goga, and Z. Werb, *Single-cell analysis reveals a stem-cell program in human metastatic breast cancer cells.* Nature, 2015. **advance online publication**.

145. Park, Y., T. Kitahara, T. Urita, Y. Yoshida, and R. Kato, *Expected clinical applications of circulating tumor cells in breast cancer.* World J Clin Oncol, 2011. **2**(8): p. 303-10.

146. Wikman, H., R. Vessella, and K. Pantel, *Cancer micrometastasis and tumour dormancy.* APMIS, 2008. **116**(7-8): p. 754-70.

147. Braun, S., K. Pantel, P. Muller, W. Janni, F. Hepp, C.R. Kentenich, S. Gastroph, A. Wischnik, T. Dimpfl, G. Kindermann, G. Riethmuller, and G. Schlimok, *Cytokeratin-positive cells in the bone marrow and survival of patients with stage I, II, or III breast cancer.* N Engl J Med, 2000. **342**(8): p. 525-33.

148. Jiang, W.G., T.A. Martin, and R.E. Mansel, *Molecular detection of micro-metastasis in breast cancer.* Crit Rev Oncol Hematol, 2002. **43**(1): p. 13-31.

149. Cotran, R.S., Kumar, V., Collins, T., *Robbins Pathologic Basis of Disease.* 1991, Philadelphia: W.B.Saunders, Co.

150. Cristofanilli, M., *Circulating tumor cells, disease progression, and survival in metastatic breast cancer.* Semin Oncol, 2006. **33**(3 Suppl 9): p. S9-14.

151. Zhang, L., S. Riethdorf, G. Wu, T. Wang, K. Yang, G. Peng, J. Liu, and K. Pantel, *Meta-analysis of the prognostic value of circulating tumor cells in breast cancer.* Clin Cancer Res, 2012. **18**(20): p. 5701-10.

152. Stathopoulou, A., I. Vlachonikolis, D. Mavroudis, M. Perraki, C. Kouroussis, S. Apostolaki, N. Malamos, S. Kakolyris, A. Kotsakis, N. Xenidis, D. Reppa, and V. Georgoulias, *Molecular detection of cytokeratin-19-positive cells in the peripheral blood of patients with operable breast cancer: evaluation of their prognostic significance.* J Clin Oncol, 2002. **20**(16): p. 3404-12.

153. Obermayr, E., D.C. Castillo-Tong, D. Pils, P. Speiser, I. Braicu, T. Van Gorp, S. Mahner, J. Sehouli, I. Vergote, and R. Zeillinger, *Molecular characterization of circulating tumor cells in patients with ovarian cancer improves their prognostic significance -- a study of the OVCAD consortium.* Gynecol Oncol, 2013. **128**(1): p. 15-21.

154. Obermayr, E., F. Sanchez-Cabo, M.K. Tea, C.F. Singer, M. Krainer, M.B. Fischer, J. Sehouli, A. Reinthaller, R. Horvat, G. Heinze, D. Tong, and R. Zeillinger, *Assessment of a six gene panel for the molecular detection of circulating tumor cells in the blood of female cancer patients.* BMC Cancer, 2010. **10**: p. 666.

155. Poveda, A., S.B. Kaye, R. McCormack, S. Wang, T. Parekh, D. Ricci, C.A. Lebedinsky, J.C. Tercero, P. Zintl, and B.J. Monk, *Circulating tumor cells predict progression free survival and overall survival in patients with relapsed/recurrent advanced ovarian cancer.* Gynecol Oncol, 2011. **122**(3): p. 567-72.

156. Maheswaran, S., L.V. Sequist, S. Nagrath, L. Ulkus, B. Brannigan, C.V. Collura, E. Inserra, S. Diederichs, A.J. Iafrate, D.W. Bell, S. Digumarthy, A. Muzikansky, D. Irimia, J. Settleman, R.G. Tompkins, T.J. Lynch, M. Toner, and D.A. Haber, *Detection of mutations in EGFR in circulating lung-cancer cells.* N Engl J Med, 2008. **359**(4): p. 366-77.

157. Groot Koerkamp, B., N.N. Rahbari, M.W. Buchler, M. Koch, and J. Weitz, *Circulating tumor cells and prognosis of patients with resectable colorectal liver metastases or widespread metastatic colorectal cancer: a meta-analysis.* Ann Surg Oncol, 2013. **20**(7): p. 2156-65.

158. Sun, Y.F., Y. Xu, X.R. Yang, W. Guo, X. Zhang, S.J. Qiu, R.Y. Shi, B. Hu, J. Zhou, and J. Fan, *Circulating stem cell-like epithelial cell adhesion molecule-positive tumor cells indicate poor*

prognosis of hepatocellular carcinoma after curative resection. Hepatology, 2013. **57**(4): p. 1458-68.

159.   Schilling, D., T. Todenhofer, J. Hennenlotter, C. Schwentner, T. Fehm, and A. Stenzl, *Isolated, disseminated and circulating tumour cells in prostate cancer.* Nat Rev Urol, 2012. **9**(8): p. 448-63.

160.   Miller, M.C., G.V. Doyle, and L.W. Terstappen, *Significance of Circulating Tumor Cells Detected by the CellSearch System in Patients with Metastatic Breast Colorectal and Prostate Cancer.* J Oncol, 2010. **2010**: p. 617421.

161.   Riethdorf, S., H. Fritsche, V. Muller, T. Rau, C. Schindlbeck, B. Rack, W. Janni, C. Coith, K. Beck, F. Janicke, S. Jackson, T. Gornet, M. Cristofanilli, and K. Pantel, *Detection of circulating tumor cells in peripheral blood of patients with metastatic breast cancer: a validation study of the CellSearch system.* Clin Cancer Res, 2007. **13**(3): p. 920-8.

162.   Reid, A.L., M. Millward, R. Pearce, M. Lee, M.H. Frank, A. Ireland, L. Monshizadeh, T. Rai, P. Heenan, S. Medic, P. Kumarasinghe, and M. Ziman, *Markers of circulating tumour cells in the peripheral blood of patients with melanoma correlate with disease recurrence and progression.* Br J Dermatol, 2013. **168**(1): p. 85-92.

163.   Koyanagi, K., C. Kuo, T. Nakagawa, T. Mori, H. Ueno, A.R. Lorico, Jr., H.J. Wang, E. Hseuh, S.J. O'Day, and D.S. Hoon, *Multimarker quantitative real-time PCR detection of circulating melanoma cells in peripheral blood: relation to disease stage in melanoma patients.* Clin Chem, 2005. **51**(6): p. 981-8.

164.   Hoshimoto, S., M.B. Faries, D.L. Morton, T. Shingai, C. Kuo, H.J. Wang, R. Elashoff, N. Mozzillo, M.C. Kelley, J.F. Thompson, J.E. Lee, and D.S. Hoon, *Assessment of prognostic circulating tumor cells in a phase III trial of adjuvant immunotherapy after complete resection of stage IV melanoma.* Ann Surg, 2012. **255**(2): p. 357-62.

165.   Luo, X., D. Mitra, R.J. Sullivan, B.S. Wittner, A.M. Kimura, S.W. Pan, M.P. Hoang, B.W. Brannigan, D.P. Lawrence, K.T. Flaherty, L.V. Sequist, M. McMahon, M.W. Bosenberg, S.L. Stott, D.T. Ting, S. Ramaswamy, M. Toner, D.E. Fisher, S. Maheswaran, and D.A. Haber, *Isolation and Molecular Characterization of Circulating Melanoma Cells.* Cell Reports, 2014. **7**(3): p. 645-653.

166.   De Giorgi, V., P. Pinzani, F. Salvianti, J. Panelos, M. Paglierani, A. Janowska, M. Grazzini, J. Wechsler, C. Orlando, M. Santucci, T. Lotti, M. Pazzagli, and D. Massi, *Application of a filtration- and isolation-by-size technique for the detection of circulating tumor cells in cutaneous melanoma.* J Invest Dermatol, 2010. **130**(10): p. 2440-7.

167.   Xu, X. and J.F. Zhong, *Circulating tumor cells and melanoma progression.* J Invest Dermatol, 2010. **130**(10): p. 2349-51.

168.   Khoja, L., P. Lorigan, C. Zhou, M. Lancashire, J. Booth, J. Cummings, R. Califano, G. Clack, A. Hughes, and C. Dive, *Biomarker utility of circulating tumor cells in metastatic cutaneous melanoma.* J Invest Dermatol, 2013. **133**(6): p. 1582-90.

169.   Rao, C., T. Bui, M. Connelly, G. Doyle, I. Karydis, M.R. Middleton, G. Clack, M. Malone, F.A. Coumans, and L.W. Terstappen, *Circulating melanoma cells and survival in metastatic melanoma.* Int J Oncol, 2011. **38**(3): p. 755-60.

170.   Gray, E.S., A.L. Reid, S. Bowyer, L. Calapre, K. Siew, R. Pearce, L. Cowell, M.H. Frank, M. Millward, and M. Ziman, *Circulating Melanoma Cell Subpopulations: Their Heterogeneity and Differential Responses to Treatment.* J Invest Dermatol, 2015. **135**(8): p. 2040-8.

171.   Khattak, M.A., E. Gray, J. Freeman, M. Pereira, T.Meniawy, K. Siew, M. Millward, and M. Ziman;, *PD-L1 expression on Circulating Melanoma Cells is predictive of response to Pembrolizumab.* Pigment Cell & Melanoma Research, 2017. **30**(1): p. 101.

172. Girotti, M.R., G. Gremel, R. Lee, E. Galvani, D. Rothwell, A. Viros, A.K. Mandal, K.H. Lim, G. Saturno, S.J. Furney, F. Baenke, M. Pedersen, J. Rogan, J. Swan, M. Smith, A. Fusi, D. Oudit, N. Dhomen, G. Brady, P. Lorigan, C. Dive, and R. Marais, *Application of Sequencing, Liquid Biopsies, and Patient-Derived Xenografts for Personalized Medicine in Melanoma.* Cancer Discov, 2016. **6**(3): p. 286-99.

173. Dupin, E. and N. Le Douarin, *Development of melanocyte precursors from the vertebrate neural crest.* Oncogene, 2003. **22**(20): p. 3016-3023.

174. Khoja, L., P. Shenjere, C. Hodgson, J. Hodgetts, G. Clack, A. Hughes, P. Lorigan, and C. Dive, *Prevalence and heterogeneity of circulating tumour cells in metastatic cutaneous melanoma.* Melanoma Res, 2014. **24**(1): p. 40-6.

175. Rodic, S., C. Mihalcioiu, and R.R. Saleh, *Detection methods of circulating tumor cells in cutaneous melanoma: a systematic review.* Crit Rev Oncol Hematol, 2014. **91**(1): p. 74-92.

176. Yu, M., S. Stott, M. Toner, S. Maheswaran, and D.A. Haber, *Circulating tumor cells: approaches to isolation and characterization.* J Cell Biol, 2011. **192**(3): p. 373-82.

177. Joosse, S.A., T.M. Gorges, and K. Pantel, *Biology, detection, and clinical implications of circulating tumor cells.* EMBO Mol Med, 2015. **7**(1): p. 1-11.

178. Sarioglu, A.F., N. Aceto, N. Kojic, M.C. Donaldson, M. Zeinali, B. Hamza, A. Engstrom, H. Zhu, T.K. Sundaresan, D.T. Miyamoto, X. Luo, A. Bardia, B.S. Wittner, S. Ramaswamy, T. Shioda, D.T. Ting, S.L. Stott, R. Kapur, S. Maheswaran, D.A. Haber, and M. Toner, *A microfluidic device for label-free, physical capture of circulating tumor cell clusters.* Nat Methods, 2015. **12**(7): p. 685-91.

179. Liu, Z., A. Fusi, E. Klopocki, A. Schmittel, I. Tinhofer, A. Nonnenmacher, and U. Keilholz, *Negative enrichment by immunomagnetic nanobeads for unbiased characterization of circulating tumor cells from peripheral blood of cancer patients.* J Transl Med, 2011. **9**: p. 70.

180. Sakaizawa, K., Y. Goto, Y. Kiniwa, A. Uchiyama, K. Harada, S. Shimada, T. Saida, S. Ferrone, M. Takata, H. Uhara, and R. Okuyama, *Mutation analysis of BRAF and KIT in circulating melanoma cells at the single cell level.* Br J Cancer, 2012. **106**(5): p. 939-46.

181. Allard, W.J., J. Matera, M.C. Miller, M. Repollet, M.C. Connelly, C. Rao, A.G. Tibbe, J.W. Uhr, and L.W. Terstappen, *Tumor cells circulate in the peripheral blood of all major carcinomas but not in healthy subjects or patients with nonmalignant diseases.* Clin Cancer Res, 2004. **10**(20): p. 6897-904.

182. Danila, D.C., G. Heller, G.A. Gignac, R. Gonzalez-Espinoza, A. Anand, E. Tanaka, H. Lilja, L. Schwartz, S. Larson, M. Fleisher, and H.I. Scher, *Circulating tumor cell number and prognosis in progressive castration-resistant prostate cancer.* Clin Cancer Res, 2007. **13**(23): p. 7053-8.

183. Cohen, S.J., R.K. Alpaugh, S. Gross, S.M. O'Hara, D.A. Smirnov, L.W. Terstappen, W.J. Allard, M. Bilbee, J.D. Cheng, J.P. Hoffman, N.L. Lewis, A. Pellegrino, A. Rogatko, E. Sigurdson, H. Wang, J.C. Watson, L.M. Weiner, and N.J. Meropol, *Isolation and characterization of circulating tumor cells in patients with metastatic colorectal cancer.* Clin Colorectal Cancer, 2006. **6**(2): p. 125-32.

184. Fusi, A., U. Reichelt, A. Busse, S. Ochsenreither, A. Rietz, M. Maisel, and U. Keilholz, *Expression of the Stem Cell Markers Nestin and CD133 on Circulating Melanoma Cells.* Journal of Investigative Dermatology, 2011. **131**(2): p. 487-494.

185. Ozkumur, E., A.M. Shah, J.C. Ciciliano, B.L. Emmink, D.T. Miyamoto, E. Brachtel, M. Yu, P.I. Chen, B. Morgan, J. Trautwein, A. Kimura, S. Sengupta, S.L. Stott, N.M. Karabacak, T.A. Barber, J.R. Walsh, K. Smith, P.S. Spuhler, J.P. Sullivan, R.J. Lee, D.T. Ting, X. Luo, A.T. Shaw, A. Bardia, L.V. Sequist, D.N. Louis, S. Maheswaran, R. Kapur, D.A. Haber, and M. Toner,

Inertial focusing for tumor antigen-dependent and -independent sorting of rare circulating tumor cells. Sci Transl Med, 2013. **5**(179): p. 179ra47.

186.   Gupta, V., I. Jafferji, M. Garza, V.O. Melnikova, D.K. Hasegawa, R. Pethig, and D.W. Davis, *ApoStream(), a new dielectrophoretic device for antibody independent isolation and recovery of viable cancer cells from blood.* Biomicrofluidics, 2012. **6**(2): p. 24133.

187.   Vona, G., A. Sabile, M. Louha, V. Sitruk, S. Romana, K. Schutze, F. Capron, D. Franco, M. Pazzagli, M. Vekemans, B. Lacour, C. Brechot, and P. Paterlini-Brechot, *Isolation by size of epithelial tumor cells : a new method for the immunomorphological and molecular characterization of circulating tumor cells.* Am J Pathol, 2000. **156**(1): p. 57-63.

188.   De Giorgi, V., D. Massi, M. Grazzini, P. Pinzani, and T. Lotti, *Application of a filtration and isolation by size technique for the detection of circulating tumor cells in cutaneous melanoma.* Journal of the American Academy of Dermatology, 2011. **64**(2): p. AB9-AB9.

189.   De Giorgi, V., P. Pinzani, F. Salvianti, and et al., *Circulating benign nevus cells detected by ISET technique: Warning for melanoma molecular diagnosis.* Archives of Dermatology, 2010. **146**(10): p. 1120-1124.

190.   Rosenberg, R., R. Gertler, J. Friederichs, K. Fuehrer, M. Dahm, R. Phelps, S. Thorban, H. Nekarda, and J.R. Siewert, *Comparison of two density gradient centrifugation systems for the enrichment of disseminated tumor cells in blood.* Cytometry, 2002. **49**(4): p. 150-8.

191.   Clawson, G.A., E. Kimchi, S.D. Patrick, P. Xin, R. Harouaka, S. Zheng, A. Berg, T. Schell, K.F. Staveley-O'Carroll, R.I. Neves, P.J. Mosca, and D. Thiboutot, *Circulating Tumor Cells in Melanoma Patients.* PLoS One, 2012. **7**(7): p. e41052.

192.   Squires, T.M. and S.R. Quake, *Microfluidics: Fluid physics at the nanoliter scale.* Reviews of Modern Physics, 2005. **77**(3): p. 977-1026.

193.   Whitesides, G.M., *The origins and the future of microfluidics.* Nature, 2006. **442**(7101): p. 368-73.

194.   Quake, S.R. and A. Scherer, *From micro- to nanofabrication with soft materials.* Science, 2000. **290**(5496): p. 1536-40.

195.   Hong, J.W. and S.R. Quake, *Integrated nanoliter systems.* Nat Biotechnol, 2003. **21**(10): p. 1179-83.

196.   Hansen, C. and S.R. Quake, *Microfluidics in structural biology: smaller, faster em leader better.* Curr Opin Struct Biol, 2003. **13**(5): p. 538-44.

197.   Lu, Y., H. Liang, T. Yu, J. Xie, S. Chen, H. Dong, P.J. Sinko, S. Lian, J. Xu, J. Wang, S. Yu, J. Shao, B. Yuan, L. Wang, and L. Jia, *Isolation and characterization of living circulating tumor cells in patients by immunomagnetic negative enrichment coupled with flow cytometry.* Cancer, 2015. **121**(17): p. 3036-45.

198.   Bhagat, A.A.S., S.S. Kuntaegowdanahalli, and I. Papautsky, *Continuous particle separation in spiral microchannels using dean flows and differential migration.* Lab on a Chip, 2008. **8**(11): p. 1906-1914.

199.   Warkiani, M.E., B.L. Khoo, D.S. Tan, A.A. Bhagat, W.T. Lim, Y.S. Yap, S.C. Lee, R.A. Soo, J. Han, and C.T. Lim, *An ultra-high-throughput spiral microfluidic biochip for the enrichment of circulating tumor cells.* Analyst, 2014. **139**(13): p. 3245-55.

200.   Guan, G., L. Wu, A.A. Bhagat, Z. Li, P.C. Chen, S. Chao, C.J. Ong, and J. Han, *Spiral microchannel with rectangular and trapezoidal cross-sections for size based particle separation.* Sci Rep, 2013. **3**: p. 1475.

201.   Khoo, B.L., M.E. Warkiani, D.S. Tan, A.A. Bhagat, D. Irwin, D.P. Lau, A.S. Lim, K.H. Lim, S.S. Krisna, W.T. Lim, Y.S. Yap, S.C. Lee, R.A. Soo, J. Han, and C.T. Lim, *Clinical validation of an*

ultra high-throughput spiral microfluidics for the detection and enrichment of viable circulating tumor cells. PLoS One, 2014. **9**(7): p. e99409.

202. Ruiz, C., J. Li, M.S. Luttgen, A. Kolatkar, J.T. Kendall, E. Flores, Z. Topp, W.E. Samlowski, E. McClay, K. Bethel, S. Ferrone, J. Hicks, and P. Kuhn, *Limited genomic heterogeneity of circulating melanoma cells in advanced stage patients.* Phys Biol, 2015. **12**(1): p. 016008.

203. Kitago, M., K. Koyanagi, T. Nakamura, Y. Goto, M. Faries, S.J. O'Day, D.L. Morton, S. Ferrone, and D.S. Hoon, *mRNA expression and BRAF mutation in circulating melanoma cells isolated from peripheral blood with high molecular weight melanoma-associated antigen-specific monoclonal antibody beads.* Clin Chem, 2009. **55**(4): p. 757-64.

204. Steen, S., J. Nemunaitis, T. Fisher, and J. Kuhn, *Circulating tumor cells in melanoma: a review of the literature and description of a novel technique.* Proc (Bayl Univ Med Cent), 2008. **21**(2): p. 127-32.

205. Nezos, A., P. Lembessis, A. Sourla, N. Pissimissis, H. Gogas, and M. Koutsilieris, *Molecular markers detecting circulating melanoma cells by reverse transcription polymerase chain reaction: methodological pitfalls and clinical relevance.* Clinical Chemistry and Laboratory Medicine, 2009. **47**(1): p. 1-11.

206. Reid, A.L., J.B. Freeman, M. Millward, M. Ziman, and E.S. Gray, *Detection of BRAF-V600E and V600K in melanoma circulating tumour cells by droplet digital PCR.* Clin Biochem, 2015. **48**(15): p. 999-1002.

207. Xu, M.J., M. Cooke, D. Steinmetz, G. Karakousis, D. Saxena, E. Bartlett, X. Xu, S.M. Hahn, J.F. Dorsey, and G.D. Kao, *A novel approach for the detection and genetic analysis of live melanoma circulating tumor cells.* PLoS One, 2015. **10**(3): p. e0123376.

208. Rothberg, B.E., C.B. Moeder, H. Kluger, R. Halaban, D.E. Elder, G.F. Murphy, A. Lazar, V. Prieto, L.M. Duncan, and D.L. Rimm, *Nuclear to non-nuclear Pmel17/gp100 expression (HMB45 staining) as a discriminator between benign and malignant melanocytic lesions.* Mod Pathol, 2008. **21**(9): p. 1121-9.

209. Xu, X., A.Y. Chu, T.L. Pasha, D.E. Elder, and P.J. Zhang, *Immunoprofile of MITF, tyrosinase, melan-A, and MAGE-1 in HMB45-negative melanomas.* Am J Surg Pathol, 2002. **26**(1): p. 82-7.

210. Viray, H., W.R. Bradley, K.A. Schalper, D.L. Rimm, and B.E. Gould Rothberg, *Marginal and joint distributions of S100, HMB-45, and Melan-A across a large series of cutaneous melanomas.* Arch Pathol Lab Med, 2013. **137**(8): p. 1063-73.

211. Ulmer, A., O. Schmidt-Kittler, J. Fischer, U. Ellwanger, G. Rassner, G. Riethmuller, G. Fierlbeck, and C.A. Klein, *Immunomagnetic enrichment, genomic characterization, and prognostic impact of circulating melanoma cells.* Clin Cancer Res, 2004. **10**(2): p. 531-7.

212. Caselitz, J., M. Jänner, E. Breitbart, K. Weber, and M. Osborn, *Malignant melanomas contain only the vimentin type of intermediate filaments.* Virchows Archiv A, 1983. **400**(1): p. 43-51.

213. Li, M., B. Zhang, B. Sun, X. Wang, X. Ban, T. Sun, Z. Liu, and X. Zhao, *A novel function for vimentin: the potential biomarker for predicting melanoma hematogenous metastasis.* J Exp Clin Cancer Res, 2010. **29**(1): p. 109.

214. Rodríguez, M.I., A. Peralta-Leal, F. O'Valle, J.M. Rodriguez-Vargas, A. Gonzalez-Flores, J. Majuelos-Melguizo, L. López, S. Serrano, A.G. de Herreros, J.C. Rodríguez-Manzaneque, R. Fernández, R.G. del Moral, J.M. de Almodóvar, and F.J. Oliver, *PARP-1 Regulates Metastatic Melanoma through Modulation of Vimentin-induced Malignant Transformation.* PLOS Genetics, 2013. **9**(6): p. e1003531.

215. Kupas, V., C. Weishaupt, D. Siepmann, M.L. Kaserer, M. Eickelmann, D. Metze, T.A. Luger, S. Beissert, and K. Loser, *RANK is expressed in metastatic melanoma and highly upregulated on melanoma-initiating cells.* J Invest Dermatol, 2011. **131**(4): p. 944-55.

216. Schatton, T., G.F. Murphy, N.Y. Frank, K. Yamaura, A.M. Waaga-Gasser, M. Gasser, Q. Zhan, S. Jordan, L.M. Duncan, C. Weishaupt, R.C. Fuhlbrigge, T.S. Kupper, M.H. Sayegh, and M.H. Frank, *Identification of cells initiating human melanomas.* Nature, 2008. **451**(7176): p. 345-9.

217. Frank, N.Y., S.S. Pendse, P.H. Lapchak, A. Margaryan, D. Shlain, C. Doeing, M.H. Sayegh, and M.H. Frank, *Regulation of progenitor cell fusion by ABCB5 P-glycoprotein, a novel human ATP-binding cassette transporter.* J Biol Chem, 2003. **278**(47): p. 47156-65.

218. Khoja, L., P. Lorigan, C. Dive, U. Keilholz, and A. Fusi, *Circulating tumour cells as tumour biomarkers in melanoma: detection methods and clinical relevance.* Ann Oncol, 2015. **26**(1): p. 33-9.

219. Maheswaran, S. and D.A. Haber, *Ex Vivo Culture of CTCs: An Emerging Resource to Guide Cancer Therapy.* Cancer Res, 2015. **75**(12): p. 2411-5.

220. Luo, X., D. Mitra, R.J. Sullivan, B.S. Wittner, A.M. Kimura, S. Pan, M.P. Hoang, B.W. Brannigan, D.P. Lawrence, K.T. Flaherty, L.V. Sequist, M. McMahon, M.W. Bosenberg, S.L. Stott, D.T. Ting, S. Ramaswamy, M. Toner, D.E. Fisher, S. Maheswaran, and D.A. Haber, *Isolation and molecular characterization of circulating melanoma cells.* Cell Rep, 2014. **7**(3): p. 645-53.

221. Warkiani, M.E., B.L. Khoo, L. Wu, A.K.P. Tay, A.A.S. Bhagat, J. Han, and C.T. Lim, *Ultra-fast, label-free isolation of circulating tumor cells from blood using spiral microfluidics.* Nat. Protocols, 2016. **11**(1): p. 134-148.

222. Schatton, T. and M.H. Frank, *Cancer stem cells and human malignant melanoma.* Pigment cell & melanoma research, 2008. **21**(1): p. 39-55.

223. Walsh, M.C. and Y. Choi, *Biology of the TRANCE axis.* Cytokine Growth Factor Rev, 2003. **14**(3-4): p. 251-63.

224. Khan, A.A., A.H. Rahmani, Y.H. Aldebasi, and S.M. Aly, *Biochemical and Pathological Studies on Peroxidases –An Updated Review.* Global Journal of Health Science, 2014. **6**(5): p. 87-98.

225. Schatton, T., N.Y. Frank, and M.H. Frank, *Identification and targeting of cancer stem cells.* BioEssays : news and reviews in molecular, cellular and developmental biology, 2009. **31**(10): p. 1038-1049.

226. Aya-Bonilla, C.A., G. Marsavela, J.B. Freeman, C. Lomma, M.H. Frank, M.A. Khattak, T.M. Meniawy, M. Millward, M.E. Warkiani, E.S. Gray, and M. Ziman, *Isolation and detection of circulating tumour cells from metastatic melanoma patients using a slanted spiral microfluidic device.* Oncotarget, 2017.

227. Karabacak, N.M., P.S. Spuhler, F. Fachin, E.J. Lim, V. Pai, E. Ozkumur, J.M. Martel, N. Kojic, K. Smith, P.I. Chen, J. Yang, H. Hwang, B. Morgan, J. Trautwein, T.A. Barber, S.L. Stott, S. Maheswaran, R. Kapur, D.A. Haber, and M. Toner, *Microfluidic, marker-free isolation of circulating tumor cells from blood samples.* Nat Protoc, 2014. **9**(3): p. 694-710.

228. Joshi, P., B. Jacobs, A. Derakhshan, L.R. Moore, P. Elson, P.L. Triozzi, E. Borden, and M. Zborowski, *Enrichment of circulating melanoma cells (CMCs) using negative selection from patients with metastatic melanoma.* Oncotarget, 2014. **5**(9): p. 2450-61.

229. Ferrone, S., M. Temponi, D. Gargiulo, G.A. Scassellati, R. Cavaliere, and P.G. Natali, *Selection and Utilization of Monoclonal Antibody Defined Melanoma Associated Antigens for Immunoscintigraphy in Patients with Melanoma*, in *Radiolabeled Monoclonal Antibodies for Imaging and Therapy*, S.C. Srivastava, Editor. 1988, Springer US: Boston, MA. p. 55-73.

230. Franke, W.W., C. Grund, C. Kuhn, B.W. Jackson, and K. Illmensee, *Formation of cytoskeletal elements during mouse embryogenesis. III. Primary mesenchymal cells and the first appearance of vimentin filaments.* Differentiation, 1982. **23**(1): p. 43-59.

231. Ben-Ze'ev, A. and A. Raz, *Relationship between the organization and synthesis of vimentin and the metastatic capability of B16 melanoma cells.* Cancer Res, 1985. **45**(6): p. 2632-41.

232. Hendrix, M.J., E.A. Seftor, Y.W. Chu, R.E. Seftor, R.B. Nagle, K.M. McDaniel, S.P. Leong, K.H. Yohem, A.M. Leibovitz, F.L. Meyskens, Jr., and et al., *Coexpression of vimentin and keratins by human melanoma tumor cells: correlation with invasive and metastatic potential.* J Natl Cancer Inst, 1992. **84**(3): p. 165-74.

233. Chartrain, M., J. Riond, A. Stennevin, I. Vandenberghe, B. Gomes, L. Lamant, N. Meyer, J.E. Gairin, N. Guilbaud, and J.P. Annereau, *Melanoma chemotherapy leads to the selection of ABCB5-expressing cells.* PLoS One, 2012. **7**(5): p. e36762.

234. Litt, G.J. and M.N. Bobrow, *Tyramide Signal Amplification*, in *Rapid Detection of Infectious Agents*, S. Specter, M. Bendinelli, and H. Friedman, Editors. 2002, Springer US: Boston, MA. p. 159-173.

235. Palmieri, G., M. Ombra, M. Colombino, M. Casula, M. Sini, A. Manca, P. Paliogiannis, P.A. Ascierto, and A. Cossu, *Multiple Molecular Pathways in Melanomagenesis: Characterization of Therapeutic Targets.* Front Oncol, 2015. **5**: p. 183.

8. APPENDICES

8.1 Supplementary Tables and Figures

Table S1. Important genes in melanomagenesis[2].

Pathway	Gene or Protein*	Function	Changes in Melanoma
RAS and MAPK			
	N-RAS	Oncogene	Sporadic activating mutation at G13R
	BRAF	Oncogene	Sporadic activating mutation at codon V600E in nevi and melanoma
	Mitogen-activated protein kinase–extracellular-related kinase (MEK)	Signal transduction	Up-regulated in radial-growth and vertical-growth phases
	Extracellular-related kinase 1 or 2 (ERK1 or ERK2) or mitogen-activated protein kinase (MAPK)	Signal transduction	Increased activity
INK4A, CDK, and Rb			
	Cyclin-dependent kinase inhibitor 2A or inhibitor of kinase 4A (CDKN2A or INK4A)	Tumor suppressor–negative regulator of cell proliferation	Germ-line mutations in some familial melanomas; sporadic deletions, promoter inactivation, loss of heterozygosity in many melanomas
	Cyclin-dependent kinase 4 (CDK4)	Promoter of cell proliferation	Protein insensitive to inhibition by INK4A due to rare familial germ-line mutations at R24C
	Cyclin D1 (CCND1)	Promoter of cell proliferation	Sporadic amplification in acral melanoma
	Retinoblastoma (Rb)	Tumor suppressor–negative regulator of cell proliferation	Phosphorylation leads to progression from G1 to S
ARF and p53			
	Alternate reading frame (ARF)	Tumor suppressor, degrades MDM2	Germ-line mutations in some familial melanomas; sporadic deletions, promoter inactivation, in many melanomas
	Tumor protein 53 (p53)	Tumor suppressor that induces apoptosis and suppressed proliferation after DNA damage	Expression usually present in melanoma
	Mouse double minute 2 (MDM2)	Targeter of p53 for ubiquination and destruction	Up-regulated in presence of ARF mutation
	BCL-2–associated X protein (BAX)	Inducer of cell death	Variable but usually down-regulated
PTEN and AKT			
	Phosphatase and tensin homologue (PTEN)	Tumor suppressor, represses PI3K	Sporadic deletion of chromosomal region
	Phosphatidylinositol 3 kinase (PI3K)	Signaling molecule for many growth factors	Active in presence of PTEN mutation
	Protein kinase B (AKT or PKB)	Oncogene that is activated by PI3K, leading to increased cell survival	Amplified in some melanomas
	BCL-2 antagonist of cell death (BAD)	Inducer of cell death	Variable but often down-regulated
	Forkhead receptor (FKHR)	Growth supression	Activated in response to PI3 pathway
MSH and MITF			
	Pro-opiomelanocortin or α-melanocyte–stimulating hormone (POMC or α-MSH)	Signaling molecule important in pigmentation	Increased melanoma vertical-growth phase
	Melanocortin receptor 1 (MC1R)	Receptor for α-MSH	Polymorphic gene affecting hair and skin color and response to ultraviolet radiation
	Adenylate cyclase (AC)	Producer of cyclic AMP	Up-regulated
	cAMP response element–binding protein (CREB)	Transcription factor	Up-regulated; affects MITF and melanocyte differentiation
	Microphthalmia-associated transcription factor (MITF)	Transcription factor	Sporadic amplification of chromosomal region
	Tyrosinase (TYR)	Pigment synthesis	Decreased expression
	Tyrosinase-related protein 1 (TYRP1)	Pigment synthesis	Decreased expression
	Dopachrome tautomerase (DCT)	Pigment synthesis	Decreased expression
	Melan-A (MLANA)	Antigen recognized by melan-A and melanoma antigen recognized by T-cells 1 (MART1) antibodies	Decreased expression
	Silver homologue (SILV)	Antigen recognized by HMB-45 antibody	Decreased expression
	Melastatin 1 (TRPM1)	Unknown	Decreased expression in metastatic melanoma
	BCL-2	Cell survival	Variable up-regulation in various phases of melanoma
Cell adhesion			
	Wingless-type mammary tumor virus integration-site family (WNT)	Protooncogene, secreted growth factor that inactivates GSK3-B	Pathway up-regulated
	Glycogen synthase kinase 3β (GSK3β)	Serine–threonine kinase that targets β-catenin for degradation	Variable; affected by WNT pathway
	β-Catenin	Adherens junction protein, transcriptional co-activator	Sporadic stabilizing mutations
	T-cell factor–lymphoid-enhancing factor (TCF–LEF)	Transcription factor	Up-regulated
	E-cadherin	Cell-adhesion molecule	Decreased expression in vertical-growth phase
	N-cadherin	Cell-adhesion molecule	Aberrant expression in vertical-growth phase
	αVβ 3integrin	Dimer that forms cell-adhesion molecule	Aberrant expression in vertical-growth phase

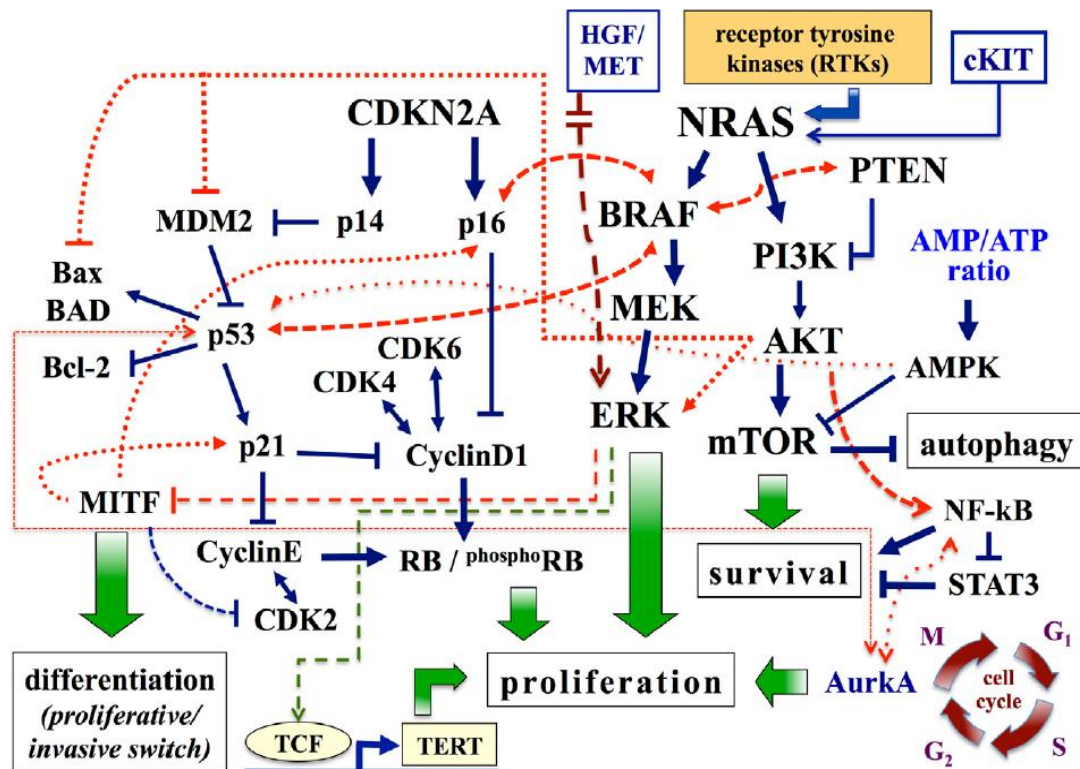*Abbreviated forms of the gene are given in parentheses.

Figure S1. Major pathways involved in melanoma. Pathways associated with cell proliferation, survival, and differentiations are schematically presented. Arrows, activating signals; interrupted lines, inhibiting signals. AMPK, AMP-activated protein kinase; Aurk, Aurora kinase; BAD, BCL-2 antagonist of cell death; CDK4, cyclin-dependent kinase 4; CDKN2A, cyclin-dependent kinase inhibitor of kinase 2A; ERK, extracellular-related kinase; HGF, hepatocyte growth factor; MITF, microphthalmia-associated transcription factor; MEK, mitogen-activated protein kinase-extracellular-related kinase; PI3K, phosphatidylinositol 3 kinase; PTEN, phosphatase and tensin homolog; RB, retinoblastoma protein; TERT, telomerase reverse transcriptase[235].